

# **Characterization and quantification of extracellular vesicles during the production of lentiviral vectors**

Aline Do Minh

Biological and Biomedical Engineering  
McGill University, Montreal

December 2022

*A thesis submitted to McGill University in partial fulfillment of the requirements of the  
degree of Doctor of Philosophy*

## Table of Contents

Table of Contents.....	1
Abstract.....	6
Résumé.....	8
Acknowledgements.....	10
Contribution to Original Knowledge .....	12
Contribution of Authors.....	14
List of Figures .....	16
List of Tables .....	17
List of Acronyms .....	18
Introduction .....	19
Objectives .....	20
Chapter 1 .....	21
Abstract.....	22
Keywords .....	22
1. Introduction .....	23
2. Viral Purification Processes.....	30
2.1. Harvest and Clarification .....	31
2.2. Concentration and Intermediate Purification .....	33

2.3. Polishing.....	40
3. Analytical Tools in Virus Production.....	41
3.1. Identity and Purity .....	43
3.2. Quantity and Potency .....	44
4. Conclusions .....	48
Funding.....	49
References.....	49
Preface to Chapter 2.....	63
Chapter 2 .....	64
Abstract.....	66
Keywords .....	67
1. Introduction .....	67
2. Materials and Methods.....	71
2.1. Cell Culture of HEK293SF Cells in Suspension.....	71
2.2. Production of Conditioned Medium Containing EVs .....	72
2.3. EV Isolation.....	72
2.4. Nomenclature.....	74
2.5. Quantification of Functional Viral Titer by Gene Transfer Assay (GTA) .....	74

2.6. Quantification of Total Particles by Digital Drop Polymerase Chain Reaction (ddPCR) .....	75
2.7. Quantification of Total Particles by Flow Virometry .....	76
2.8. Imaging of EVs by Transmission Electron Microscopy (TEM).....	77
2.9. Immunoblot Analysis.....	77
2.10. Protein and Nucleic Acid Quantification.....	78
2.11. EV Identification .....	78
2.12. Proteomic Analysis.....	79
2.13. Liquid Chromatography-Mass Spectrometry (LC-MS) of Phospholipids.....	83
2.14. Transcriptomics and Bioinformatics Analysis .....	84
3. Results .....	84
3.1. Characterization of Clone 92 EVs in the Absence of Lentiviral Particles .....	84
3.2 Characterization of Clone 92 EVs during Lentiviral Particles Production .....	95
4. Discussion.....	101
Supplementary materials.....	110
Author Contributions .....	110
Funding.....	111
Acknowledgements.....	111
Conflicts of Interest .....	111

References.....	112
Preface to Chapter 3.....	124
Chapter 3.....	125
Abstract.....	126
Keywords .....	126
1. Introduction .....	127
2. Materials and methods .....	129
2.1. Cell culture of HEK293SF cells in suspension.....	129
2.2. Production of conditioned medium containing EV .....	130
2.3. Fractionation of EV and LV/EV samples using iodixanol gradient .....	130
2.4. Quantification of functional viral titer by gene transfer assay (GTA) .....	131
2.5. Quantification of total particles by droplet digital polymerase chain reaction (ddPCR) .....	132
2.6. Quantification of particles by flow virometry.....	132
2.7. Titration of p24 viral capsid protein by ELISA.....	133
3. Results .....	134
3.1. Iodixanol gradient making .....	134
3.2. Quantitative characterization of EV to LV spectrum of populations.....	135
4. Discussion.....	140

---

Author Contributions .....	145
Conflict of Interest .....	145
Funding / Acknowledgements .....	145
References.....	145
General Discussion .....	151
Final Conclusion & Summary .....	157
Literature .....	158

## Abstract

Lentiviral vectors (LV), derived from the human immunodeficiency virus (HIV), are a powerful tool in the field of gene therapy. These vectors have been used to introduce therapeutic genes into the cells of patients for treating genetic diseases or cancer, traditionally by ex vivo modifications but now also aiming at direct in vivo applications. As LV are used in human health applications, a thorough knowledge of the final product is paramount. Challenges around the industrialization of LV production processes are numerous and the main platform for achieving large scale manufacturing often revolves around the use of the human embryonic kidney 293 cells platform.

In the past decades, extracellular vesicles (EV) have also received increased attention. They are nanosized particles known to be naturally secreted by any type of cells, including mammalian cells used in viral vector manufacturing processes such as HEK293. EV are significantly involved in cell communication and cell trafficking, transporting heterogenous lipid, protein, and nucleic acid cargos from donor to recipient cells. They are promisingly studied in the field of biomarkers but also as therapeutic delivering tools.

LV and EV are generated within the cells and their paths cross in many ways, starting from their similar biogenesis to their common biophysical properties. As such, this thesis aims at contributing to both fields, starting in the first chapter with highlighting the likely presence of EV in LV preparations and reviewing the inability of most bioprocessing units to separate one from another.

Using a lentiviral producer HEK293 derived cell line and a multi-omics approach, the second chapter dives into the characterization of EVs without induction of LV production,

thus establishing a host-EV profile. The study went further by characterizing the resulting mixed population of EV and LV after induction of LV production.

Subsequently, as suggested in the first chapter, EV and LV most likely existing in the form of a spectrum population rather than separate entities, in the last chapter, the product resulting from LV production was fractionated for further analyses using orthogonal methods, revealing not only the challenge faced when quantifying nanosized particles without true distinctive features but also heterogenous populations of EV and LV.

In conclusion, this work presents advancements in the characterization of LV preparations intended for human use with the focus on co-purified EV.

## Résumé

Les vecteurs lentiviraux (VL), dérivés du virus de l'immunodéficience humaine (VIH), sont un outil puissant dans le domaine des thérapies géniques et cellulaires. Ces vecteurs sont utilisés afin d'introduire des gènes thérapeutiques dans des cellules de patients pour le traitement de maladies génétiques ou cancers, traditionnellement par des modifications *ex vivo*, mais également de nos jours avec des visées d'application directe *in vivo*. Les VL étant utilisés à des fins d'applications en santé humaine, une connaissance approfondie du produit final est primordiale. Les défis autour de l'industrialisation des procédés de production de VL sont nombreux et la fabrication à grande échelle repose souvent sur l'utilisation de la plateforme des cellules rénales embryonniques humaines (HEK293).

Au cours des dernières décennies, les vésicules extracellulaires (VE) ont également reçu une attention accrue. Il s'agit de nanoparticules sécrétées de manière naturelle par n'importe quel type de cellules, incluant les cellules de mammifères utilisées dans les procédés de fabrication de vecteurs viraux telles que les HEK293. Les VE sont significativement impliqués dans la communication et le trafic intra-cellulaires, en transportant des cargaisons hétérogènes de lipides, protéines et acides nucléiques d'une cellule donneuse vers une cellule réceptrice. Les recherches autour des VE sont prometteuses non seulement en tant que biomarqueurs mais également en tant qu'outils thérapeutiques.

Les VL et les VE sont issues des mêmes cellules et leurs chemins vont se croiser de multiples façons, à commencer par leur biogénèse très similaire, jusqu'à leurs propriétés biophysiques très semblables. Cette thèse a donc pour but de contribuer aux deux

domaines, en commençant par mettre en lumière dans le premier chapitre la présence probable de VE dans les préparations de VL, en examinant l'inaptitude de la majorité des systèmes de bioprocédés à les séparer les uns des autres.

En utilisant une lignée cellulaire productrice de VL dérivée des HEK293 ainsi qu'une approche multi-omiques, le deuxième chapitre introduit dans un premier temps la caractérisation des VE sans induction de production de VL, permettant d'établir un profil de VE de cellules hôtes. L'étude va plus loin par la suite dans la caractérisation de la population mixte de VE et VL résultant de l'induction de la production de VL.

Consécutivement, tel que suggéré dans le premier chapitre, les VE et VL existant le plus probablement sous forme d'une distribution de populations plus ou moins continue, plutôt que sous forme d'entités séparées, dans le chapitre final, le produit résultant de la production de VL a été fractionné pour des analyses approfondies utilisant des méthodes orthogonales, dévoilant non seulement la difficulté à quantifier des nanoparticules sans réel signe distinctif, mais également les populations hétérogènes de VE et VL.

En conclusion, ce travail présente des progrès dans la caractérisation des préparations lentivirales à usage humain en mettant un accent sur la présence de VE co-purifiés dans ces préparations.

## Acknowledgements

I never thought this day would come. I know that at the time I am writing these lines, I am only submitting the thesis to my wonderful supervisor Dr. Amine Kamen, but it does feel like the most important milestone to complete this long PhD journey.

I would like to express my most sincere gratitude to my supervisor and mentor Prof. Amine Kamen. You gave me this incredible opportunity despite my unusual situation, saying that if the motivation was there, there was no reason for me not to succeed. And thanks to you, the motivation, despite some ups and downs, remained throughout the course of this adventure. You are the main reason why I didn't give up, and believe it, I came very close to from time to time. Thank you for not giving up on me, for your patience, for not showing me your worries even when I caused you some! I feel very lucky to have evolved under your supervision.

Further on, I would like to thank Prof. Christopher Moraes and Prof. Georgios Mitsis for their guidance and advice as part of my PhD thesis advisory committee. I truly appreciated the feedback you gave me.

I would like to thank all my labmates of the Kamen lab over the years for contributing a way or another to the completion of my work. I would like to thank Dr. Alina Venereo Sanchez in particular, who introduced me in the first place to Amine, you were right, it worked out eventually, and you showed me the way with your own PhD defense as I was just starting my own project. Good luck with your entrepreneurship adventure! Special thanks also to Dr. Jean-François Gélinas for his endless support especially during the publication process of my first article, not only as a co-author, but also as a mentor and

relatable pair. Thank you to the “historical” team, that I am proud to call Dr. Pranav Joshi, Dr. Sascha Kiesslich, and soon to be Dr. David Sharon. You all paved the way, and I am proud to walk in your steps. Thank you for the great memories at Thomson House and more. Thank you to my lab soul sister, Michelle Tran, who I am sure will become Dr. Michelle Tran shortly. Thank you for always being there for me, for sharing the same doubts but never giving up either. You are dear to me forever. Thank you to Angélique and Pablo, the last members I had the chance to meet. Your fresh motivation and hard work were inspiring. Part of the Kamen lab at the start, I would like to thank Xavier Elisseeff for helping with my labwork. It was a pleasure working together.

I am also grateful to all the people at the McGill and UQAM facilities, special thanks to Denis Flipo and Hélène Pagé-Veillette for their help with flow cytometry. Furthermore, I would like to thank all faculty, staff and students from the Department of Bioengineering and the Department of Biomedical Engineering, especially Xavier Elisseeff again, as lab manager this time, and Pina Sorrini, thank you for always rescuing me. I am truly grateful for the financial support provided by the Natural Sciences and Engineering Research Council of Canada (NSERC) and the McGill Faculty of Engineering in forms of scholarships.

Last, but definitely not least, I want to express my gratitude and love to my family and friends for supporting me all those years. Thank you to my amazing husband, Vincent, without whom I could not have made it. Your continuous support despite my stressed mood was essential. Thank you to my wonderful children, Jade, Héloïse, Inès and Lucas, who asked me once “what are doctors who do not treat people for?”. I hope I will have the answer some day, but I certainly hope that you will be proud of me anyway. MERCI !

## **Contribution to Original Knowledge**

The research work presented in this thesis expands the challenges faced with the presence of extracellular vesicles when dealing with enveloped virus production for therapeutic applications, especially lentiviral vectors used in cell and gene therapy.

The study in chapter 1 reviews current downstream technologies used in the manufacturing process of viral vaccines and viral vectors using enveloped viruses, as well as the analytical tools used to characterize the product. The review describes which properties of the virus the purification techniques are based on, how effective the processes are at removing EVs and the applicability of analytical methods to distinguish EVs. The review's aim is to highlight the fact that methods currently employed in large-scale production do not have sufficient capability at discriminating coproduced extracellular vesicles from the enveloped virus of interest. The need to better characterize copurified EVs in enveloped virus products is critically underlined and the major challenges faced in the field of viral vectors and viral vaccines with the knowledge of EVs characteristics and likely presence in the final product are introduced, especially in lentiviral vector production intended for gene therapy.

The study in chapter 2 starts with the characterization of EVs without induction of LV production. Various analytical methods were used including omics to get a baseline profile of EVs produced in the HEK293SF-LVP-CMVGFPq-92 cell line. Subsequently, the chapter also digs into characterizing the resulting mixed population of EVs and LVs upon induction of lentiviral vector production.

The study in chapter 3 is the continuation of chapter 2 as it aims at assessing sub-populations of EVs and LVs upon induction of lentiviral vector production. After fractionation, orthogonal analytical methods were used to quantify the different entities, based on distinct features such as the presence of viral genome or GFP in the particles. The study also highlights the difficulty to provide absolute quantification of the species.

## Contribution of Authors

The present thesis consists of three manuscripts - two published (Chapter 1 and 2) and one to be submitted (Chapter 3). I am the first author of all three manuscripts. The contributions of all authors to each manuscript are listed below.

**Chapter 1:**            **Critical Assessment of Purification and Analytical Technologies for Enveloped Viral Vector and Vaccine Processing and Their Current Limitations in Resolving Co-Expressed Extracellular Vesicles**

Published in        *Vaccines* 2021, 9(8)

Authors:            **Aline Do Minh**, Amine A. Kamen

Contributions:    Conceptualization, **A.D.M.** and A.A.K.; Formal analysis, **A.D.M.**; Investigation, **A.D.M.**; Writing—original draft preparation, **A.D.M.**; Writing—review and editing, A.A.K.; Funding acquisition, **A.D.M.** and A.A.K.; and Supervision, A.A.K.

**Chapter 2:**            **Characterization of Extracellular Vesicles Secreted in Lentiviral Producing HEK293SF Cell Cultures**

Published in        *Viruses* 2021, 13(5)

Authors:            **Aline Do Minh**, Alexandra T. Star, Jacek Stupak, Kelly M. Fulton, Arsalan S. Haqqani, Jean-François Gélinas, Jianjun Li, Susan M. Twine and Amine A. Kamen

Contributions: Conceptualization, **A.D.M.** and A.A.K.; Methodology, **A.D.M.**, A.T.S., J.S., K.M.F., S.M.T. and A.A.K.; Investigation, **A.D.M.**, A.T.S. and J.S.; Data Curation, A.S.H., Writing—Original Draft, **A.D.M.** and A.T.S.; Writing—Review and Editing, J.-F.G., K.M.F., J.L., S.M.T. and A.A.K.; Funding Acquisition, **A.D.M.**, S.M.T. and A.A.K.; Resources, S.M.T., J.L. and A.A.K.; and Supervision A.A.K.

**Chapter 3: From extracellular vesicles to lentiviral vectors: characterization of a spectrum of populations in a stable HEK293 producer cell line**

To be submitted to: *TBD*

Authors: **Aline Do Minh**, Xavier Elisseeff, Amine A. Kamen

Contributions: Conceptualization, **A.D.M.** and A.A.K.; Methodology, **A.D.M.** and A.A.K.; Investigation, **A.D.M.**, X.E., Writing – Original Draft, **A.D.M.**; Writing – Review & Editing, A.A.K.; Funding Acquisition, **A.D.M.** and A.A.K.; Resources, A.K.; and Supervision, A.A.K.

## List of Figures

<b>Figure 1:</b> Expected EV, LV and intermediate entities during production of lentiviral vector .....	28
<b>Figure 2:</b> General sequence of viral vector and viral vaccine production bioprocesses. ....	31
<b>Figure 3:</b> Analysis of Clone 92 supernatant by flow virometry: Quantification of GFP+ events and CTV+/FM4+ events over cell culture days as measured on the BD Fortessa flow cytometer.....	86
<b>Figure 4:</b> Preliminary characterization of C92EVSEC .....	88
<b>Figure 5:</b> Proteomic analysis of C92EVSEC.....	91
<b>Figure 6:</b> Phospholipids identified in C92EVSEC.....	92
<b>Figure 7:</b> Gene ontology (GO) enrichment analysis in <sup>C92</sup> EV <sub>SEC</sub> , top 25 ontology terms...	94
<b>Figure 8:</b> Top 10 miRNA found in <sup>C92</sup> EV <sub>SEC</sub> . .....	95
<b>Figure 9:</b> Comparison between Clone 92 supernatants with no induction and 3 days post-induction (3 dpi) by flow virometry: Quantification of flow virometry subpopulations of large particles and total GFP+ particles in each studied condition .....	96
<b>Figure 10:</b> Comparison between <sup>C92</sup> EV <sub>UC</sub> and <sup>C92</sup> EV/LV <sub>UC</sub> .....	97
<b>Figure 11:</b> Area-proportional Venn diagram for the total number of identified proteins in <sup>C92</sup> EV <sub>UC</sub> and <sup>C92</sup> EV/LV <sub>UC</sub> within the combined Vesiclepedia and ExoCarta database. ....	98
<b>Figure 12:</b> Phospholipids identified in Clone 92 EVs and LVs compared to Clone 92 parent cells .....	101
<b>Figure 13:</b> Density of iodixanol fractions after 250,000xg centrifugation .....	134
<b>Figure 14:</b> WPRE particles quantified by ddPCR in iodixanol fractions .....	135

<b>Figure 15:</b> Functional viral titer measured by GTA.....	137
<b>Figure 16:</b> Physical particle titer measured by p24 ELISA .....	138
<b>Figure 17:</b> Fluorescent particle titer measured by flow virometry .....	139

## List of Tables

<b>Table 1:</b> Examples of approved vaccines and gene therapy products using whole enveloped viruses .....	24
<b>Table 2:</b> Physical characteristics of extracellular vesicles and some enveloped viruses ....	29
<b>Table 3:</b> Analytical assays most commonly used in-process and with end product in enveloped viral vec-tor and vaccine manufacturing .....	43
<b>Table 4:</b> Nomenclature for EV and LV samples in Clone 92 cell line using different isolation methods in two conditions: without induction of LV production or after induction of LV production using cumate and doxycycline. ....	74
<b>Table 5:</b> In-process quantification of GFP+ particles by flow virometry and total protein by RC/DC during one repeat of Clone 92 EVs isolation process.....	87
<b>Table 6:</b> Nucleic acid quantification in $C^{92}EV_{SEC}$ .....	92
<b>Table 7:</b> Summary of protein classes identified in both $C^{92}EV_{UC}$ and $C^{92}EV/LV_{UC}$ , or only in either $C^{92}EV_{UC}$ or $C^{92}EV/LV_{UC}$ . ....	99
<b>Table 8:</b> Overview of EV/LV fractions landscape .....	140

## List of Acronyms

CAR-T	Chimeric Antigen Receptor T cell
DMEM	Dulbecco's Modified Eagle's Medium
ddPCR	droplet digital polymerase chain reaction
EV	Extracellular Vesicle
FBS	Fetal Bovine Serum
FDA	US Food and Drug Administration
GFP	green fluorescent protein
HEK	Human Embryonic Kidney cells
HIV	human immunodeficiency viruses
hpi	hours post-infection
LV	Lentiviral Vector
MISEV	Minimal information for studies of extracellular vesicles
PBS	phosphate-buffered saline buffer
SEC	size exclusion chromatography
UC	ultracentrifugation
VG	viral genome
VSV-g	vesicular stomatitis virus glycoprotein

## Introduction

Viral vectors and viral vaccines undeniably belong to the landscape of modern therapeutics. They can be produced by living organisms, from embryonated chicken eggs to adherent cell cultures or in suspension. In the past decade, gene and cell therapy became increasingly popular tools to treat diseases such as cardiovascular, genetic disorders, cancer, as well as a wide spectrum of orphan diseases (Naldini, 2015). Gene therapy consists of transferring genetic material (RNA or DNA) to a patient to correct a missing or malfunctioning gene to treat a disease. In cell therapy, on the other hand, live and intact cells are transferred to a patient to treat the disease. Gene and cell therapy are often used in combination, as it is the case in Chimeric Antigen Receptor T cell (CAR T) therapy, where the patient's own immune cells are modified to express a surface receptor to stimulate an immune response against cancer cells (Wang, Guo, & Han, 2017). Different viruses have been engineered to be used in gene therapy as gene delivery vectors. Adenovirus, adeno-associated virus (AAV) and lentiviral vectors (LV) have become dominant in the field (Sharon & Kamen, 2017).

LV have several advantages to offer over other viral vectors (Ansorge et al., 2009). Their ability to mediate long-term therapeutic transgene expression makes them ideal candidates for gene and cell therapy. However, challenges, such as achieving high yield and suitable purity for *in vivo* and *ex vivo* clinical use, need to be overcome for large scale production for broader applications than orphan diseases (Merten, Hebben, & Bovolenta, 2016). In this context, the discovery and recent interest in extracellular vesicles (EVs) raise an unprecedented concern as some EVs, such as exosomes and small shedding microvesicles,

not only share size distribution with lentiviral particles, but also biochemical and biophysical properties (Nolte-'t Hoen, Cremer, Gallo, & Margolis, 2016). This issue needs to be addressed since EVs are released concomitantly by the cells and, thus, will be found in the lentiviral preparation. As lentiviral-mediated gene therapies are intended for human use, they are strictly regulated by health authorities and any impurities in the viral preparation have to be characterized as per regulatory requirements (White, Whittaker, Gandara, & Stoll, 2017).

Human embryonic kidney (HEK293) cells are widely used to produce viral vaccines and viral vectors (Schweizer & Merten, 2010). Thus, they are selected as the cell culture platform for this project. Like most cells, HEK293 cells generate EVs, which are difficult to separate from LV produced at the same time.

## **Objectives**

The aim of this PhD research project is to qualitatively and quantitatively characterize the EV content of LV preparations, which in turn will help in assessing product safety and identity. The hypothesis is that gaining an understanding of the characteristics of EVs during LV production will provide an accurate product profile for lentiviral-mediated gene therapies and eventually help improve the LV purification process.

Aim 1: Characterize EVs during LV production from a proteomic, lipidomic and transcriptomic point of view.

Aim 2: Quantify the different entities from host EVs to infectious viral particles during LV production.

## Chapter 1

# Critical Assessment of Purification and Analytical Technologies for Enveloped Viral Vector and Vaccine Processing and Their Current Limitations in Resolving Co-Expressed Extracellular Vesicles

Authors: **Aline Do Minh**, Amine A. Kamen

Author affiliation : Department of Bioengineering, McGill University, 3480 University, Montréal, Québec H3A 0E9, Canada

Journal: Vaccines

Year: 2021

Volume: 9

DOI: <https://doi.org/10.3390/vaccines9080823>

Status: Published

Article history: Received 26 June 2021; Revised 19 July 2021; Accepted 20 July 2021; Published 26 July 2021

## **Abstract**

Viral vectors and viral vaccines are invaluable tools in prevention and treatment of diseases. Many infectious diseases are controlled using vaccines designed from subunits or whole viral structures, whereas other genetic diseases and cancers are being treated by viruses used as vehicles for delivering genetic material in gene therapy or as therapeutic agents in virotherapy protocols. Viral vectors and vaccines are produced in different platforms, from traditional embryonated chicken eggs to more advanced cell cultures. All these expression systems, like most cells and cellular tissues, are known to spontaneously release extracellular vesicles (EVs). EVs share similar sizes, biophysical characteristics and even biogenesis pathways with enveloped viruses, which are currently used as key ingredients in a number of viral vectors and licensed vaccine products. Herein, we review distinctive features and similarities between EVs and enveloped viruses as we revisit the downstream processing steps and analytical technologies currently implemented to produce and document viral vector and vaccine products. Within a context of well-established viral vector and vaccine safety profiles, this review provides insights on the likely presence of EVs in the final formulation of enveloped virus products and discusses the potential to further resolve and document these components.

## **Keywords**

extracellular vesicles; enveloped viruses; lentiviral vectors; viral vaccines; purification process; analytical technologies

## 1. Introduction

Viral vectors and viral vaccines have been part of the medical landscape for decades, as approved products or under evaluation in numerous clinical trials. About 14% of vaccines approved by the FDA involve enveloped viruses (FDA, 2021), while out of the 15 gene therapy products approved worldwide in 2019, six of them use enveloped viruses (F. Wang et al., 2019), and 39% of gene therapy clinical trials are using enveloped viruses (GTCT, 2021). Enveloped viruses are encased in a lipid bilayer which, in most cases, fuses with the target host cell membrane to infect cells. These enveloped viruses are produced in various systems, including traditional embryonated chicken eggs or more advanced cell culture technologies such as MRC-5 cells, Vero cells and HEK293-derived cell lines. Table 1 summarizes vaccines and gene therapy products using whole enveloped viruses. The manufacturing of viral vector and viral vaccine products has always been paved with challenges related to the downstream processing. Purification process unit operations usually start with harvest and clarification, followed by intermediate purification steps, before polishing and formulation steps (Moleirinho, Silva, Alves, Carrondo, & Peixoto, 2020). Although techniques have greatly improved over the years to generate purer high-quality products and reproducible processes while maintaining or decreasing the cost of goods, regulatory agencies are increasingly stringent regarding product identity and characterization of the end products and level of acceptable impurities as a way to ensure public safety and maintain public trust in this class of medicine.

**Table 1:** Examples of approved vaccines and gene therapy products using whole enveloped viruses. VSV: vesicular stomatitis virus, JEV: Japanese encephalitis virus, VZV: varicella-zoster virus, YFV: yellow fever virus, HSV-1: oncolytic herpes simplex virus-1.

	Virus	Trade Name	Manufacturer	Production System	Target Disease/Indication	Reference
Viral vaccine	VSV	ERVEBO	Merck Sharp & Dohme (MSD)	Vero cells	Ebola	(U.S. Food & Drug Administration, 2021b)
	Influenza virus	FluMist	Medimmune	Specific pathogen-free (SPF) eggs	Influenza	(U.S. Food & Drug Administration, 2021b)
	JEV	Ixiaro	Valneva Austria GmbH	Vero cells	Japanese encephalitis	(U.S. Food & Drug Administration, 2021b)
	Measles virus	M-M-R II ProQuad	MSD	Chick embryo cell culture	Measles	(U.S. Food & Drug Administration, 2021b)
	Mumps virus	M-M-R II ProQuad	MSD	Chick embryo cell culture	Mumps	(U.S. Food & Drug Administration, 2021b)
		M-M-R II	MSD			(Suni, Meurman, Hirvonen, & Vaheri, 1984; U.S. Food & Drug Administration, 2021b)
	Rubella virus	ProQuad		WI-38 human diploid lung fibroblasts MRC-5 cells	Rubella	(Suni, Meurman, Hirvonen, & Vaheri, 1984; U.S. Food & Drug Administration, 2021b)
		Rudivax	Sanofi Pasteur MSD			
	VZV	ProQuad ZOSTAVAX	MSD	MRC-5 cells	Varicella	(U.S. Food & Drug Administration, 2021b)

		VARIVAX		WI-38 human diploid lung fibroblasts		Administration, 2021b)
	Vaccinia virus	JYNNEOS	Bavarian Nordic A/S Emergent Product Development Gaithersburg, Inc.	Primary chicken embryo fibroblast cells	Smallpox	(U.S. Food & Drug Administration, 2021b)
		ACAM2000		Vero cells		(U.S. Food & Drug Administration, 2021b)
	YFV	YF-Vax	Sanofi Pasteur, Inc	Avian leukosis virus-free chicken embryos	Yellow fever	(U.S. Food & Drug Administration, 2021b)
Gene therapy		KYMRIAH	Novartis	HEK293-derived cells	Precursor B-cell lymphoblastic leukemia-lymphoma	Administration, 2021a)
	Lentivirus	Zynteglo	Bluebird bio	HEK293-derived cells	Beta-thalassemia	(European Medicines Agency, 2021c)
		Strimvelis		HEK293-derived cells	Severe combined immunodeficiency	(European Medicines Agency, 2021a)
	Retrovirus	Zalmoxis		HEK293-derived cells	Adjunctive treatment in haploidentical HSC transplantation	(European Medicines Agency, 2021b)
		YESCARTA		HEK293-derived cells	Lymphoma	(U.S. Food & Drug Administration, 2021a)
	HSV-1	IMLYGIC		HEK293-derived cells	Melanoma	(U.S. Food & Drug Administration, 2021a)

Different biological systems are used to produce enveloped viruses. All of them, as with most cells and cellular tissues, secrete naturally extracellular vesicles (EVs). The interest

towards those vesicles has recently increased as they may be used as therapeutic tools or biomarkers (Raposo & Stoorvogel, 2013). They are cell membrane-derived blebs that transport lipids, proteins and nucleic acids including DNA, mRNA, micro RNAs (miRNAs) and non-coding RNAs (ncRNAs). Their subpopulations are highly heterogenic in size and composition. EVs are extensively studied for their role in cell-to-cell communication and their ability to deliver their cargos from donor to recipient cells (Raposo & Stahl, 2019). Exosomes and microvesicles are the most commonly cited EV subtypes (Phillips, Willms, & Hill, 2021). Minimal information for studies of extracellular vesicles 2018 (MISEV 2018) (They et al., 2018) recommends classifying EVs by their physical characteristics (size or density), small EVs referring to particles smaller than 200 nm and medium/large EVs being larger than 200 nm. Other characteristics such as their bio-chemical composition or their subcellular origin have also been considered. The EV cargo composition depends on many factors, including the cell line from which they derive. However, the mechanism behind cargo sorting is still under careful investigation. Their budding pathways have also been analyzed. As EV subtypes do not have the same in-tracellular origin, their generation and release are not ruled by the same processes, even though they may share some mechanisms. Multivesicular bodies are formed from the fusion of endosomes, which derive from the invagination of the cell membrane, with molecular cargos sorted in the endoplasmic reticulum and processed in the Golgi complex. The lysosomal pathway leads to the degradation of the multivesicular bodies' content upon fusion with lysosomes. In the secretory pathway, the content of the multivesicular bodies is released into the extracellular environment in the form of exosomes upon maturation and fusion to the plasma

membrane. The key component for the exosome biogenesis within the endosomes is the endosomal sorting complex required for transport (ESCRT) (Andreu & Yanez-Mo, 2014). The ESCRT molecular machinery includes four multi-protein complexes (ESCRT-0, -I, -II, -III) and associated accessory proteins Alix and VPS4.

The existence of an ESCRT-independent mechanism was also unraveled, potentially involving other partners such as heat shock proteins, cholesterol, tetraspanins, phosphatidic acids and ceramides (Kowal, Tkach, & Théry, 2014). The reason why some multivesicular bodies undergo the secretory pathway or the degradation pathway remains to be understood. The mechanism underlying the generation of microvesicles is also not well understood. It was demonstrated that ESCRT-I component Tsg101 was involved in protein sorting into microvesicles (Nabhan, Hu, Oh, Cohen, & Lu, 2012), confirming that mechanistic elements may be shared in exosome and microvesicle biogenesis.

Viruses, as per their nature, take over many functions of the cells they are infecting. Viral nucleic acids and viral proteins of many enveloped viruses have been incorporated into host EVs. For instance, HIV Nef protein can be incorporated into EVs (McNamara et al., 2018), while HIV trans-activating response (TAR) element RNA was also detected in EVs (Sampey et al., 2016). It has been hypothesized that viruses hijack the host pathways for vesicle trafficking (Gould, Booth, & Hildreth, 2003), and one cannot deny the similarities between the biogenesis of viruses and EVs due to the implication of common proteins such as the ESCRT machinery once again, SNARE, SNAP and the cargos resemblance (Nolte-Hoen, Cremer, Gallo, & Margolis, 2016).

When it comes to viruses mixed with coproduced EVs, the distinction becomes even more challenging as EVs exist in a wide spectrum of populations, which is further broadened by virus production. EVs produced by cells that are also producing viruses likely contain viral proteins and parts of viral genetic material. Thus, it is reasonable to expect that, in the context of enveloped virus production, diverse vesicles are released. On one extreme, there are EVs that are entirely made of host cell components, while on the other extreme, there are infectious viruses. Ranging between these two entities, there are many intermediate structures, such as non-infectious particles that could be considered as incomplete viral particles or as EVs that have incorporated fragments of the viral genome and viral (glyco)proteins (Figure 1).

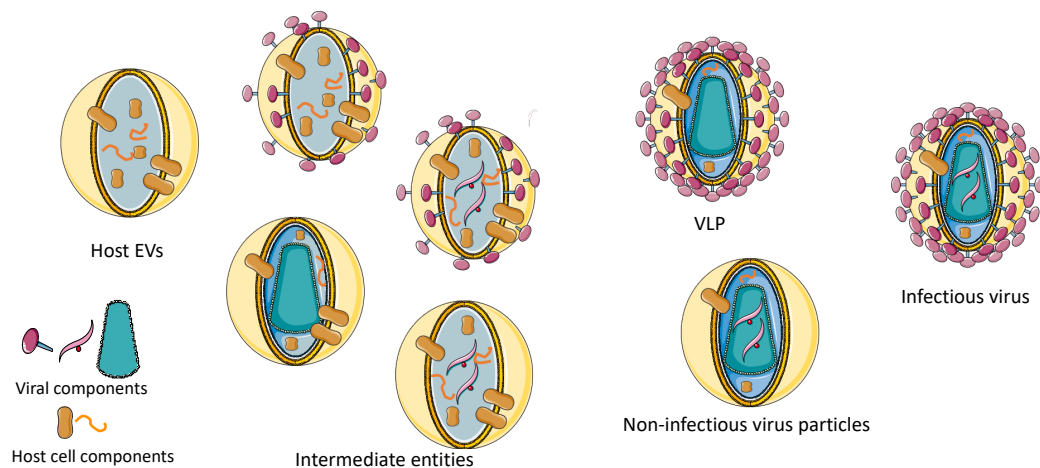


**Figure 1:** Expected EV, LV and intermediate entities during production of lentiviral vector (Figure created using Servier Medical Art by Servier). Viral components (left to right): envelope protein, viral genome, viral capsid.

Few studies have been designed to compare viruses to coproduced EVs in cell culture produced systems using omics approaches (Do Minh et al., 2021; Sviben et al., 2018). Sviben et al. compare mumps and measles produced in Vero cells to the coproduced EVs, while

Do Minh et al. compare lentiviral vectors to coproduced EVs in a HEK293-derived cell line. Do Minh et al. indeed identified subpopulations such as host EVs with or without the “viral genome”, non-functional LVs despite carrying the viral genome and fully functional LV particles. Other conclusions from both studies unsurprisingly reveal that EVs and the studied viruses share many features, including protein cargos, rendering specific markers difficult to establish. More studies on retroviruses (Segura et al., 2008) also associated CD63 with highly purified retroviral vectors, while the tetraspanin is often used as an exosome marker (Batrakova & Kim, 2015). Some studies claimed the separation of HIV from coproduced EVs (Cantin, Diou, Belanger, Tremblay, & Gilbert, 2008; DeMarino et al., 2019; Konadu et al., 2016) using density gradients. Besides the similar density of HIV-1 and small EVs questioning the reliability of the method, the separation process used is also far from being ideal for large scale manufacturing. Table 2 describes the size range of EVs and how they compare to other particles such as viruses.

**Table 2:** Physical characteristics of extracellular vesicles and some enveloped viruses. VSV: vesicular stomatitis virus, HSV-1: oncolytic herpes simplex virus-1.

	<b>Particle</b>	<b>Size range</b>	<b>Density</b>
<b>EVs</b>	Exosome	30–150 nm	1.13–1.21 g.ml <sup>-1</sup>
	Microvesicle	100–1000 nm	1.03–1.08 g.ml <sup>-1</sup>
	Apoptotic body	50–5000 nm	1.16–1.28 g.ml <sup>-1</sup>
<b>Enveloped viruses</b>	VSV	70–170 nm	1.19–1.20 g.ml <sup>-1</sup>
	Influenza A virus	80–120 nm	1.2 g.ml <sup>-1</sup>
	Lentivirus	80–100 nm	1.16–1.18 g.ml <sup>-1</sup>
	γ-retrovirus	80–120 nm	1.15–1.17 g.ml <sup>-1</sup>
	HSV-1	155–240 nm	1.27 g.ml <sup>-1</sup>

Similar downstream process unit operations are used in both fields. The isolation of enveloped viruses and EVs was for instance traditionally achieved using ultracentrifugation. More advanced techniques including chromatography and filtration are being increasingly developed. However, it is likely that the presence of EVs is largely unassessed and undocumented so far in the manufacturing of enveloped viruses, since the composition of EVs greatly resembles that of the targeted viral product.

In this review, we go through distinctive features and similarities between EVs and enveloped viruses as we describe the downstream processes and analytical methods currently used in the production of viral vectors and vaccines. Large scale technologies used in the field of viral vectors and vaccines for the purification of enveloped viruses are the main focus of this review. To assess the process reproducibility and robustness, analytical tools used for characterizing the critical quality attributes of the final viral products are also reviewed.

## **2. Viral Purification Processes**

No unique stream exists in the downstream processing of viral vectors and vaccines. Indeed, not only does each virus have its own properties and behavior, but the treatment that viruses can undergo also depends on the nature of the final product: Should the virus be inactivated or live-attenuated retaining infectivity properties, does the particle structure have to be maintained for immunogenicity, or should the virus, that might be defective, retain the properties to effectively transduce cells and express the targeted transgene, as is the case for viral vectors used in gene therapy or vaccination? Traditional techniques for

purifying EVs and viruses involved ultracentrifugation and filtration and are still being used extensively. However, more advanced chromatographic steps and scalable technologies are being implemented. Common steps and process unit operations are presented in a generic sequence summarizing the purification strategy (Figure 2). In the case of enveloped viruses, lysis of the cells is not required as the viruses bud out of the cell membranes. Therefore, the first clarification step aims at removing cells and cell debris. Centrifugation and filtration are the most commonly used techniques at this stage. In general, one or multiple purification steps follow in order to concentrate the virus and remove host cell proteins (HCPs) and host cell DNA. They might include tangential flow filtration and chromatographic unit operations. Buffer-exchange steps and nuclease treatment steps are often required at different downstream process stages. Below, we describe the general sequences of enveloped virus purification streams using (ultra-) centrifugation and various filtration and chromatography techniques.

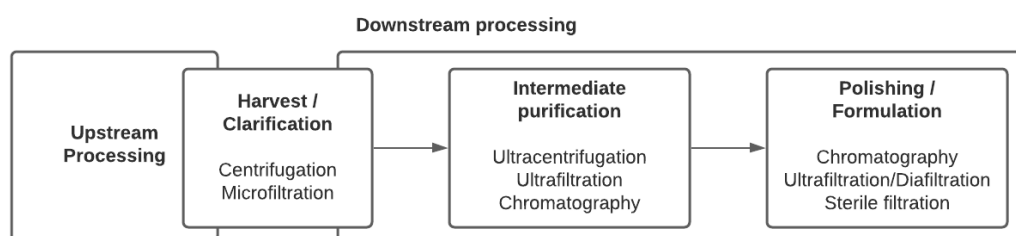


**Figure 2:** General sequence of viral vector and viral vaccine production bioprocesses.

### 2.1. Harvest and Clarification

In both cell culture or egg production systems, the transition step between upstream and downstream processing is known as the harvest. As stated, in the case of enveloped viruses or EVs, since particles directly bud out of the cells, there is no need to use de-

tergents to lyse the cells. Therefore, downstream processing starts directly with removing cells and large debris. It is often completed in two steps, combining centrifugation and filtration.

### **2.1.1. Centrifugation**

Centrifugation is a common way to remove cells and large cellular debris by pelleting them. It is still used broadly despite the high cost and difficulty to scale up as it offers good recovery (Besnard et al., 2016). Based on their lower density, viruses and EVs are therefore both recovered in the supernatant during this step.

### **2.1.2. Microfiltration**

Microfiltration is referred to using filters with membrane cut-offs usually between 0.1 and 10  $\mu\text{m}$ . Different filtration techniques are used with such filters, the main ones being normal-flow filtration (NFF) and tangential flow filtration (TFF). TFF, according to its name, differs from NFF in the flow directionality. Both have been extensively and very efficiently used in the separation and purification of biotherapeutics.

Different types of filters can be used in NFF: dead-end filters and depth filters. Dead-end filters have defined pore sizes, and excluded particles are retained only at the surface, whereas depth filters are made of porous material, which can retain particles of different sizes across the membrane's thickness (Schmidt, Wieschalka, & Wagner, 2017), rendering membrane fouling less problematic. Depth filters can also be positively charged to effectively capture host cell DNA and HCPs. Both types of filters have the advantage of being easy to scale up and cost-effectiveness. A scalable process using a dual 0.45–0.2  $\mu\text{m}$

filter has been proposed to clarify retroviral vectors produced in HEK293-derived cells (Segura, Kamen, Trudel, & Garnier, 2005). NFF has also been used effectively for decades in the clarification process of influenza virus produced in em-bryonated chicken eggs (Goyal, Hanssen, & Gerba, 1980).

In TFF, biological fluids recirculate in parallel to the membrane surface, preventing cake formation. Particles smaller than the pore size flow through the membrane in the permeate, while larger particles are retained by the membrane and are recovered in the retentate. TFF is also a highly scalable method and has been successfully implemented in the manufacturing process of smallpox and monkeypox vaccine JYNNEOS (U.S. Food & Drug Administration, 2019).

Given that these filters separate particles mainly based on their size and given the overlapping size range of viruses and EVs, both types of particles remain in the filtrate or permeate during this step.

## **2.2. Concentration and Intermediate Purification**

### ***2.2.1. Traditional Ultracentrifugation***

Traditional techniques for virus separations were based on their physical characteristics such as their size and density. Ultracentrifugation is a well-established technique that has been used for decades to pellet low-density particles. It can be used in one step, stepwise (differential (ultra-) centrifugation), with continuous density gradients or discontinuous density gradients called cushions with media such as cesium chloride, iodixanol or sucrose.

In the field of gene therapy, lentiviral vectors have been concentrated and partially purified using ultracentrifugation (Moreira et al., 2021). Iodixanol gradients (Kishishita, Takeda, Anuegoonpipat, & Anantapreecha, 2013) or sucrose cushions (Olgun, Tasyurek, Sanlioglu, & Sanlioglu, 2019) have been used for purifying lentivirus preparations. Ultracentrifugation steps using sucrose gradients have also been used to purify retrovirus (Rodrigues, Carrondo, Alves, & Cruz, 2007).

In the field of vaccines, ultracentrifugation and zonal-rate separation on sucrose cushions has been used widely for the purification of influenza virus. The FluMist vaccine, for example, employs ultracentrifugation in the production process. Japanese Encephalitis virus for the preparation of Ixiaro vaccine is purified using sucrose density gradients (U.S. Food & Drug Administration, 2018).

In the field of EVs, differential ultracentrifugation was for a while the gold standard to isolate EVs (They, Amigorena, Raposo, & Clayton, 2006), with sequential steps of increased centrifugal force. It is no longer the method of choice, however, as it is cumbersome, induces higher variability than other techniques and has been shown to damage and aggregate EVs (Mol, Goumans, Doevendans, Sluijter, & Vader, 2017). Ultracentrifugation with sucrose or iodixanol gradients is another popular approach to isolating EVs (Van Deun et al., 2014).

Ultracentrifugation using continuous density gradients is limited by the volume that can be processed (usually less than 50 mL); it is therefore mostly used for pre-clinical material or small-scale research samples. Continuous-flow centrifugation overcomes this volume limitation and is still being used at a large scale in vaccine manufacturing, es-

pecially in the case of influenza vaccine and Japanese encephalitis vaccine. However, it does not translate well for lentiviral vectors, which are subject to a loss of infectivity by ultracentrifugation with or without sucrose gradients (Perry & Rayat, 2021). Continuous-flow centrifugation equipment is also high-maintenance, costly and voluminous. Moreover, due to the overlapping density of EVs and viruses (Table 2), effective separation cannot be achieved. Ultracentrifugation is therefore not a suitable method to separate enveloped viruses from EVs, and viral manufacturing processes that rely on ultracentrifugation in downstream processing should expect retention of EVs in the bulk product if an additional step segregating the two entities is not considered.

### ***2.2.2. Ultrafiltration Tangential Flow Filtration***

Ultrafiltration (UF) is another membrane separation technique with tighter pore sizes than in microfiltration, usually ranging from 1 to 100 nm. It is most commonly used in TFF mode to concentrate the products of interest, and combined with diafiltration (DF), it allows buffer exchange. This well-controlled and scalable technology induces very low shear stress, which makes it very popular in various biomanufacturing processes. UF/DF is widely used in the field of influenza virus production (Wolff & Reichl, 2008) using different membrane molecular weight cut-offs (MWCO), from 100 to 750 kDa. UF/DF is also a method of choice in the purification of retroviral and lentiviral vectors using 100 to 300 kDa membranes (Geraerts, Michiels, Baekelandt, Debyser, & Gijssbers, 2005; Rodrigues, Carvalho, et al., 2007). UF/DF has also been employed in the field of EVs, especially for its scalability advantage (Do Minh et al., 2021; Lobb et al., 2015).

In UF/DF TFF, most viruses and EVs are larger than the molecular weight cut-off of the membrane. As they have very similar size ranges, as in any filtration technique, they are both recovered in the same phase, here in the retentate, while smaller particles pass through the permeate. Therefore, TFF cannot be used for separating EVs from enveloped viruses.

### ***2.2.3. Chromatography***

Chromatography is a commonly used process unit in the downstream processing of viral vectors and viral vaccines. Its role is to capture the particle of interest (bind-elute mode) or impurities (flow-through mode). If the virus is bound to the chromatographic material, it is then eluted, allowing its purification and concentration. Separation by chromatography is based on the physicochemical interactions of the particles of interest with the solid phase in opposition to the contaminants or impurities.

Different supports exist for the solid phase, also called stationary phase.

The most traditional one is resin-based chromatography, using packed-bed columns of microbeads with specific chemical properties. Packed-bed chromatography is, however, mainly used in small molecule purification such as antibodies, as the larger size of viruses affects their diffusion into the pores of the adsorbent resin thus reducing the dynamic binding capacity.

Alternative chromatographic supports are convective media such as membrane adsorbers and monoliths through which processing time, capacity and recovery are improved for viral processes rendering them more cost effective. Membrane adsorbers are a combination of liquid chromatography and membrane filtration (Orr, Zhong, Moo-

Young, & Chou, 2013). They offer reduced diffusion times compared to packed-bed chromatography, with high flow rate operation capabilities and low pressure drops. The low dead volume of the system also yields reduced buffer consumption. Although re-usability is always an option, another advantage of membrane adsorbers resides in their suggested single-use format, removing the need for lengthy validated clean-in-place and regeneration procedures and eliminating the risk of cross-contamination. Membrane adsorbers have been successfully used for scalable processes of lentiviral and retroviral vectors with high titers (Zimmermann et al., 2011).

The disposability advantage also goes for monoliths. Monoliths, also known as convective interaction media (CIM) are made of porous materials organized in a single block with highly cross-linked macropores with a diameter range of 10 to 4000 nm (Lynch, Ren, Beckner, He, & Liu, 2019). Similar to membrane chromatography, mass transport is essentially convective, allowing high flow rates and low pressure drops. Most chromatographic monoliths are made of polymethacrylate material and are operated at a large scale with radial flow devices. Monoliths have shown great performance in the purification of influenza virus and lentiviral vectors as compared to other chromatographic means (Kramberger, Urbas, & Štrancar, 2015). Rubella virus is another example of an enveloped viral vaccine and has been efficiently concentrated and purified using a monolith with almost 100% recovery and maintained infectivity (Forcic et al., 2011).

Chromatographic materials can also be characterized by surface chemistry. Ion-exchange, hydrophobic interaction, affinity, size-exclusion and mixed-mode are the main types.

Ion-exchange chromatography (IEX) is the most commonly used technique and is based on difference in charge between the viral envelope and the stationary phase. It is mostly operated in bind-elute mode. IEX usually offers high resolution especially when using elution gradients to fractionate closely related biomolecules. Depending on the particle of interest's net charge, either anion or cation exchange is employed. Most viruses are negatively charged at physiological pH due to their isoelectric point (pI) being below 7.4. Interestingly, egg-derived influenza virus has been purified by both anion-exchange (AIEX) and cation-exchange (CIEX) chromatography, although AIEX was more favorable (Wolff & Reichl, 2008). Lentiviral vectors, as well as retroviral vectors have been purified at a large scale using AEX, yielding 22% to over 60% of recovery of infectious particles (Moreira et al., 2021; Rodrigues, Carvalho, et al., 2007).

The use of hydrophobic interaction chromatography (HIC) is scarcer. It is mainly known for the purification of vaccinia virus (Hansen, Rene Faber, Udo Reichl, Michael Wolff, & Gram, 2011). The reason behind the low popularity of the method is due to the high salt concentration used for desorption, which can be detrimental to the virus integrity and functionality, especially in the case of viral vectors used in gene therapy.

Affinity chromatography (AC) separation is based on specific interactions between the particles of interest and the stationary phase and is used in bind-elute mode. It has attracted interest in recent years. The advantage of AC is the high specificity of the interaction, yielding highly pure product in one step. Mechanisms of affinity include specific antigen-antibody interactions, which, when employed for the purification of measles virus (Njayou & Quash, 1991), outperformed ultracentrifugation. Mumps virus purification using

AC with a monolithic column coupled with polyclonal antibodies is another example (Brgles, Sviben, Forčić, & Halassy, 2016). Lectin affinity chromatography uses lectin ligands binding to specific carbohydrates via carbohydrate recognition domains. It was used in the purification of influenza A virus (Opitz, Salaklang, Büttner, Reichl, & Wolff, 2007) and in the purification of HSV-1 (Olofsson, Jeansson, & Lycke, 1981). Immobilized metal affinity chromatography (IMAC) is based on metal ion affinity such as zinc, cobalt, nickel or a combination of copper, cobalt and nickel and is used for the purification of influenza virus (Opitz, Hohlweg, Reichl, & Wolff, 2009), HSV-1 (Jiang et al., 2004), retroviral vectors (Ye, Jin, Atai, Schultz, & Ibeh, 2004) and lentiviral vectors (Cheeks et al., 2009), respectively. An additional example of AC mechanism is based on heparin affinity and has been very popular for the purification of many enveloped vi-ruses, including HSV-1, vaccinia Ankara virus and retroviral and lentiviral vectors (Zhao et al., 2019). Despite the great performance of AC, it is not often implemented at a large scale due to the high cost of ligand design and immobilization.

Mixed-mode chromatography (MMC) is based on the combination of various multimodal binding mechanisms, such as ligands combining ionic interaction, hydrophobic interaction and hydrogen bonding. Hydroxyapatite, a complex crystalline compound, which resin binds at the same time as negatively charged phosphate groups and positively charged functional groups, is a good example of MMC. It has shown recovery of up to 46% in the purification of retroviral vectors (Kuiper, Sanches, Walford, & Slater, 2002).

In the field of EVs, the use of AIEEX has also been reported to efficiently isolate EVs from HEK293T cell cultures (Heath et al., 2018). No studies attempting to separate viruses from

coproduced EVs have been reported thus far. Despite the sizeable challenge, as charges between intermediate entities can exhibit slight differences, the possibility thus remains that this technique could separate EVs from viruses, as a recent study in another context showed the feasibility of separating full and empty adeno-associated virus (AAV) capsids (Joshi, Bernier, Moço, et al., 2021).

When approaching AC techniques in the field of EVs, immunoaffinity appears appealing and has been widely employed in the isolation of EVs from cell culture or body fluids (Liangsupree, Multia, & Riekkola, 2021). Tetraspanin proteins found at the surface of EVs are often reported as target molecules. However, specificity has not been demonstrated for efficient separation of EVs from viruses. Indeed, tetraspanins were also associated with viruses, such as CD63 with retroviral vectors and CD81 with lentiviral vectors (Do Minh et al., 2021; Segura et al., 2008). Distinctive markers have yet to be accurately identified, and they may differ depending on the expression system and the produced enveloped virus. As documented in previous studies, EVs coproduced with enveloped viruses carry similar membrane proteins, and more extensive studies would be needed to identify and validate any specific markers that would enable separation of these two entities.

### **2.3. Polishing**

Polishing is one of the last steps in bioprocessing, allowing the removal of remaining impurities, and can be completed after the final formulation of the product. This step is critical as it should ensure the purity, quality and potency of the final product according to stringent regulatory requirements.

Size exclusion chromatography (SEC) is the most commonly used chromatographic technique, based on the molecular size difference between the particle of interest and the impurities. SEC is used for example in the late-stage purification of lentiviral vectors (Boudeffa et al., 2019). Although still broadly used, SEC induces dilution of the final product and has usually low capacity.

Another MMC example used for polishing is the combination of size exclusion and binding properties of the Capto™ Core 700 and 400 resins. These are used in flow-through mode as the particles of interest are recovered in the flow-through, while impurities bind to the high-capacity column. It was originally designed for the removal of ovalbumin in the purification of influenza virus produced in eggs (Blom et al., 2014) but has since been applied to other viruses such as lentiviral vectors (Boudeffa et al., 2019).

Polishing can also be achieved by UF/DF, which is covered in Section 2.2.2.

SEC and more recently Capto™ Core have been successfully implemented in the isolation processes of EVs (Corso et al., 2017; Liangsupree et al., 2021; Lobb et al., 2015).

Both are well-controlled technologies and scalable; however, since their separation principle is based on size, they cannot efficiently separate EVs from viruses due to their size similarities.

### **3. Analytical Tools in Virus Production**

Process analysis technology deployment is critical for effective bioprocess development. Importantly, the final product destined for vaccine and gene therapy applications needs to be adequately characterized to ensure that it meets the claimed identity, purity,

safety, quantity and potency. Analytical tools should have the ability to characterize the final product but also to monitor the performance of the bioprocess, showing it is robust and well-controlled. The need for advanced analytical technologies has been emphasized in recent years as the critical quality attributes of biologics have been refined. Measurements made throughout the process have to be reliable, accurate and reproducible. A good overview of assays used in virus-based therapeutics has been recently published (Moleirinho et al., 2020) (Table 3). Identity of viruses can be determined by sequencing the genome DNA, identifying the viral proteins by Western blot or mass spectrometry, or confirming the isoelectric point if known. Purity assessment is usually related to impurity quantification, such as HCPs or HC-DNA, the quantities of which are strictly regulated in viral vaccines. Safety of the final product measures the level of microbial contaminants using bioburden and sterility tests, endotoxins and mycoplasma. Quantity is an attribute that is especially monitored throughout the process in intermediate products as well as in the end product, allowing the evaluation of the efficiency of each process unit. Total viral particles and vector genome particles are measured, as well as infectious particles in the case of viruses that need to retain infectivity, whereas transduction efficiency and expression of transgene are measured with defective viral particles. More generally, functional activity determining potency of the product can be assessed with cell-based or in vivo assays. In the following section, the most relevant analytical techniques used in the field of viral vectors and viral vaccine manufacturing are summarized. Some of these techniques can be applied to EV characterization, and their potential to segregate between EVs and viral entities is discussed.

**Table 3:** Analytical assays most commonly used in-process and with end product in enveloped viral vector and vaccine manufacturing (adapted from Moleirinho et al. (Moleirinho et al., 2020)).

Critical Quality Attribute	Assay (Parameter)
Identity	PCR-based assay (genomic DNA)
	Western blot (viral protein)
	Sequencing (genomic DNA)
	Mass spectrometry (viral protein)
	Isoelectric focusing (isoelectric point)
Purity	Electron microscopy (viral structure)
	ELISA (residual HCPs)
	Mass spectrometry (residual HCPs)
	PCR-based assay (residual HC-DNA)
Safety	Bioburden (microbial contaminants)
	Sterility test (microbial contaminants)
	Endotoxin assay (endotoxin)
	Mycoplasma testing (mycoplasma)
Quantity	PCR-based assay (vector genome particles)
	Plaque assay (infectious particles)
	TCID <sub>50</sub> (infectious particles)
	ELISA (total vector particles)
	NTA (total vector particles)
	TRPS (total vector particles)
	FFF-MALS (total vector particles)
	Flow virometry (total vector particles)
Potency	Cell-based assay (functional activity)
	In vivo assay (functional activity)

### 3.1. Identity and Purity

Sodium dodecyl sulfate polyacrylamide gel electrophoresis (SDS-PAGE) is a well-established technique to determine purity of a bioproduct, using different staining strategies to reveal proteins present in the viral preparation. It can be combined with

Western blotting to identify specific viral proteins. MS also allows the identification of viral proteins and residual HCPs. ELISA tests are available for both HCP and specific viral antigen quantification.

Host cell components including HCPs can also be associated with enveloped viruses as shown by Segura et al. (Segura et al., 2008). Which HCPs are attributed to incorporation by the viruses or by the presence of EVs has yet to be resolved. Similarly, viral proteins could also modify host cell EVs. HCPs and viral protein-based assays can therefore be biased by the presence of EVs, viruses and intermediate entities.

Electron microscopy techniques are useful to visualize virus structural integrity. Full and empty particles can be distinguished by negative staining. Viruses with distinctive shapes can easily be distinguished from EVs. Recent approaches aimed at exploiting data from transmission electron microscopy (TEM) to achieve quantitative analysis (Kotrbová et al., 2019). The principles are based on shape, rendering the distinction between viruses and EVs difficult in the case of close shaped particles such as lentiviral and retroviral vectors. Moreover, the technique would need extensive optimization and standardization as it is subjective due to operator handling, reducing its reproducibility (Rikkert, Nieuwland, Terstappen, & Coumans, 2019).

### **3.2. Quantity and Potency**

Quantification of viral particles has always been a challenge. Orthogonal methods relying on different technologies and measuring different aspects of the virus complement each other to deliver more accurate measurements. Depending on the virus, different approaches are used.

Quantification of particles based on the presence of the viral genome can be achieved using polymerase chain reaction (PCR) methods, including real-time PCR (qPCR) and more recently droplet digital PCR (ddPCR), which eliminates the need for a standard curve. ddPCR has for instance been developed for the quantification of the influenza virus (Feng et al., 2017), lentiviral vectors (Y. Wang, Bergelson, & Feschenko, 2018) and VSV-based vaccine (Gélinas, Kiesslich, Gilbert, & Kamen, 2020). However, PCR techniques are based on specific primers, which have to be designed in such a way that they are specific to the measured particles. In Do Minh et al. (Do Minh et al., 2021), primers used in ddPCR targeted the woodchuck hepatitis virus post-transcriptional regulatory element (WPRE), which is commonly used in viral vector design to enhance transgene expression, the presence of WPRE thus indicating the presence of the viral genome. The cell line used in the study expressed the green fluorescence protein (GFP) transgene constitutively. In the absence of lentiviral vector production, ddPCR still yielded a titer when measuring isolated EVs, revealing that host EVs did incorporate sequences of the viral genome. The development of PCR-based methods needs therefore to be designed in such a way that viral specific elements are measured in order to distinguish coproduced EVs.

Physical quantification of viruses enables fast enumeration of total particles. Methods include nanoparticle tracking analysis (NTA), tunable resistive pulse sensing (TRPS) and multi-angle laser light scattering (MALLS) coupled with asymmetrical field flow fractionation (FFF-MALLS). NTA, based on the Brownian motion of particles in suspension, and TRPS, measuring transient change in electrical resistance as particles pass through the nanopore proportionally to their size (Yang & Yamamoto, 2016), can also estimate particle

size distribution. In FFF-MALLS, particles are eluted in order of size and simultaneously detected by light scattered from different angles. All techniques have been used in the field of viral vectors (Moreira et al., 2021), vaccines (Bousse et al., 2013) and EVs (van der Pol et al., 2010). Although their detection methods differ, they are all based on particle size, in their lower limit of detection range for NTA and TRPS, rendering the distinction between viruses and coproduced EVs not possible.

Chromatography-based techniques using high-performance liquid chromatography (HPLC) present several advantages in terms of speed, accuracy and reproducibility for measuring total particles (Kramberger et al., 2015). Different chemistries on different chromatographic supports can be used, such as AIEX and SEC on a favored monolith. Intact virus particles can be separated from other cellular impurities or incomplete virus particles. This approach creates a quick picture of a process step and an impurity profile of the intermediate product. One drawback of HPLC when intended for accurate virus quantification is that it requires highly pure and fully characterized virus material to develop the method and the reference material stock. HPLC has been developed for the quantification of the influenza virus (Lorbetskie et al., 2011), retroviral vectors (J. Transfiguracion, Coelho, & Kamen, 2004) and lentiviral vectors (Julia Transfiguracion et al., 2020). Although the last of these studies did acknowledge the presence of EVs in lentiviral preparations, and the method was optimized in order to minimize their effect on the quantification of lentiviral vectors, the actual proportion of EVs in the final product could not be estimated as the analysis of a sample with no virus fell below the linear range of the method. The use of HPLC to quantify EVs and viruses cannot be excluded, but

extensive optimization is expected, as shown in the field of AAV where full and empty capsid could be identified by AIEX-HPLC (Joshi, Bernier, Chahal, & Kamen, 2021).

New technologies are being developed, including the ViroCyt virus counter. The proprietary technology uses a double fluorescence staining strategy: staining viral genomes (and nucleic acids in general) and viral capsids proteins, thereby allowing specific detection of the particles. Its performance showed a good correlation compared to other quantification methods in the quantification of filovirus (Rossi et al., 2015) and vaccinia virus (Americo, Earl, & Moss, 2017). The equipment design is based on flow cytometry principles, and the staining strategy can be applied to more generic flow virometry. Compared to flow cytometry, the term flow virometry refers to the nanoscale operation of the equipment (Lippe, 2018). In flow cytometry for cells, the threshold is normally set to light scatter, with the light scatter triggering the detection. However, in the case of 100 nm particles, forward-scattered light (FSC) would not differentiate these particles from noise. A difference can be seen with side-scattered light (SSC); however, in order to reduce noise, increasing the FSC threshold would lead to loss of the signal of the targeted particles. Using fluorescence-triggered detection overcomes that issue. Flow virometry has been used in the last decade to quantify different viruses such as HSV-1 (El Bilali, Duron, Gingras, & Lippé, 2017), vaccinia virus (Vera A. Tang et al., 2016) and retrovirus (V. A. Tang, Renner, Fritzsche, Burger, & Langlois, 2017). It is also a method of choice for the quantification of EVs (Nolan & Duggan, 2018). The staining strategies play a crucial role in flow virometry as they allow the detection and quantification of subpopulations. Although the use of dyes or

stains requires careful optimization, the technology could allow the distinction between EVs, viruses and intermediate populations to some extent.

Many other assays are used in the field of viral vaccines and viral vectors, including more virus specific assays such as the hemagglutination assay, single radial immunodiffusion (SRID) used in influenza vaccine production and cell-based assays used to determine infectivity or functionality of the virus, such as the tissue culture infective dose assay (TCID<sub>50</sub>) or the gene transfer assay (GTA). All these methods are of utmost importance in bioprocesses but are not discussed as they cannot contribute to estimating the proportion of copurified EVs in the final product.

#### **4. Conclusions**

The field of viral vectors and viral vaccines is expanding, motivating the development of advanced bioprocesses for their large-scale manufacturing. The translation to the clinic of these complex biomolecular structures for treatment and prevention of diseases is challenged by the new findings in the emerging field of EVs that share many features with enveloped viruses from their physical characteristics to their biogenesis.

Many process units used for the purification of viruses have been adapted to EV isolation and purification. This is an early indicator that both particles are likely to behave similarly in a cell culture environment, and therefore it is expected that EVs copurify in the case of enveloped virus production. This review sheds light on the current unlikelihood of EVs to be effectively separated from cell culture-produced enveloped viruses by current large-scale bioprocesses, according to their similar characteristics in terms of size, density,

charge and composition. The proportion of EVs in viral preparation also remains difficult to estimate as only a few methods show premises of capability to quantify both entities accurately using the same assay. The challenge is enhanced by the heterogeneous nature of both viral particles and EVs, which constitute more of a spectrum of populations rather than two distinct entities. Intermediate populations are therefore also more difficult to estimate, and their variations are manifold. The fact that EVs cannot be currently fully separated from viruses does not mean that they pose safety concerns as, on the contrary, they could serve as natural adjuvants in vaccine formulation. However, as per regulatory requirements, any component of the bulk medicinal product has to be carefully characterized, and EVs in enveloped virus preparations should not be an exception. Better analytical tools are therefore needed to gain expert knowledge on the actual proportion of EVs and intermediate entities in viral products.

## **Funding**

A.D.M. is funded by a Natural Sciences and Engineering Research Council of Canada (NSERC) doctoral scholarship. A.A.K. is a recipient of a Canada Research Chair (CRC/240394) of the government of Canada.

## **References**

Americo, J. L., Earl, P. L., & Moss, B. (2017). Droplet digital PCR for rapid enumeration of viral genomes and particles from cells and animals infected with orthopoxviruses. *Virology*, 511, 19-22. doi:10.1016/j.virol.2017.08.005

- Andreu, Z., & Yanez-Mo, M. (2014). Tetraspanins in extracellular vesicle formation and function. *Front Immunol*, 5, 442. doi:10.3389/fimmu.2014.00442
- Batrakova, E. V., & Kim, M. S. (2015). Using exosomes, naturally-equipped nanocarriers, for drug delivery. *J Control Release*, 219, 396-405. doi:10.1016/j.jconrel.2015.07.030
- Besnard, L., Fabre, V., Fettig, M., Gousseinov, E., Kawakami, Y., Laroudie, N., . . . Pattnaik, P. (2016). Clarification of vaccines: An overview of filter based technology trends and best practices. *Biotechnology Advances*, 34(1), 1-13. doi:10.1016/j.biotechadv.2015.11.005
- Blom, H., Åkerblom, A., Kon, T., Shaker, S., van der Pol, L., & Lundgren, M. (2014). Efficient chromatographic reduction of ovalbumin for egg-based influenza virus purification. *Vaccine*, 32(30), 3721-3724. doi:https://doi.org/10.1016/j.vaccine.2014.04.033
- Boudeffa, D., Bertin, B., Biek, A., Mormin, M., Leseigneur, F., Galy, A., & Merten, O. W. (2019). Toward a Scalable Purification Protocol of GaLV-TR-Pseudotyped Lentiviral Vectors. *Hum Gene Ther Methods*, 30(5), 153-171. doi:10.1089/hgtb.2019.076
- Bousse, T., Shore, D. A., Goldsmith, C. S., Hossain, M. J., Jang, Y., Davis, C. T., . . . Stevens, J. (2013). Quantitation of influenza virus using field flow fractionation and multi-angle light scattering for quantifying influenza A particles. *Journal of Virological Methods*, 193(2), 589-596. doi:10.1016/j.jviromet.2013.07.026
- Brgles, M., Sviben, D., Forčić, D., & Halassy, B. (2016). Nonspecific native elution of proteins and mumps virus in immunoaffinity chromatography. *Journal of Chromatography A*, 1447, 107-114. doi:https://doi.org/10.1016/j.chroma.2016.04.022

- Cantin, R., Diou, J., Belanger, D., Tremblay, A. M., & Gilbert, C. (2008). Discrimination between exosomes and HIV-1: Purification of both vesicles from cell-free supernatants. *Journal of Immunological Methods*, 338(1-2), 21-30. doi:10.1016/j.jim.2008.07.007
- Cheeks, M. C., Kamal, N., Sorrell, A., Darling, D., Farzaneh, F., & Slater, N. K. H. (2009). Immobilized metal affinity chromatography of histidine-tagged lentiviral vectors using monolithic adsorbents. *Journal of Chromatography A*, 1216(13), 2705-2711. doi:https://doi.org/10.1016/j.chroma.2008.08.029
- Corso, G., Mäger, I., Lee, Y., Görgens, A., Bultema, J., Giebel, B., . . . Andaloussi, S. E. (2017). Reproducible and scalable purification of extracellular vesicles using combined bind-elute and size exclusion chromatography. *Sci Rep*, 7(1), 11561. doi:10.1038/s41598-017-10646-x
- DeMarino, C., Barclay, R. A., Pleet, M. L., Pinto, D. O., Branscome, H., Paul, S., . . . Kashanchi, F. (2019). Purification of High Yield Extracellular Vesicle Preparations Away from Virus. *J Vis Exp*(151). doi:10.3791/59876
- Do Minh, A., Star, A. T., Stupak, J., Fulton, K. M., Haqqani, A. S., Gélinas, J.-F., . . . Kamen, A. A. (2021). Characterization of Extracellular Vesicles Secreted in Lentiviral Producing HEK293SF Cell Cultures. *Viruses*, 13(5), 797. Retrieved from <https://www.mdpi.com/1999-4915/13/5/797>
- El Bilali, N., Duron, J., Gingras, D., & Lippé, R. (2017). Quantitative Evaluation of Protein Heterogeneity within Herpes Simplex Virus 1 Particles. *Journal of Virology*, 91(10), e00320-00317. doi:10.1128/jvi.00320-17

European Medicines Agency. (2021a). Strimvelis. Retrieved from <https://www.ema.europa.eu/en/medicines/human/EPAR/strimvelis>

European Medicines Agency. (2021b). Zalmoxis. Retrieved from <https://www.ema.europa.eu/en/medicines/human/EPAR/zalmoxis>

European Medicines Agency. (2021c). Zynteglo. Retrieved from <https://www.ema.europa.eu/en/medicines/human/EPAR/zynteglo>

FDA. (2021). Vaccines Licensed for Use in the United States | FDA. Retrieved from <https://www.fda.gov/vaccines-blood-biologics/vaccines/vaccines-licensed-use-united-states>

Feng, Z., Zhao, X., Zou, X., Zhu, W., Chen, Y., Wang, D., & Shu, Y. (2017). Droplet Digital Polymerase Chain Reaction Method for Absolute Quantification of Influenza A Viruses. *Bing Du Xue Bao*, 33(1), 1-5.

Forcic, D., Brgles, M., Ivancic-Jelecki, J., Santak, M., Halassy, B., Barut, M., . . . Strancar, A. (2011). Concentration and purification of rubella virus using monolithic chromatographic support. *J Chromatogr B Analyt Technol Biomed Life Sci*, 879(13-14), 981-986. doi:10.1016/j.jchromb.2011.03.012

Gélinas, J. F., Kiesslich, S., Gilbert, R., & Kamen, A. A. (2020). Titration methods for rVSV-based vaccine manufacturing. *MethodsX*, 7, 100806. doi:10.1016/j.mex.2020.100806

Geraerts, M., Michiels, M., Baekelandt, V., Debyser, Z., & Gijssbers, R. (2005). Upscaling of lentiviral vector production by tangential flow filtration. *Journal of Gene Medicine*, 7(10), 1299-1310. doi:10.1002/jgm.778

- Gould, S. J., Booth, A. M., & Hildreth, J. E. (2003). The Trojan exosome hypothesis. *Proc Natl Acad Sci U S A*, 100(19), 10592-10597. doi:10.1073/pnas.1831413100
- Goyal, S. M., Hanssen, H., & Gerba, C. P. (1980). Simple method for the concentration of influenza virus from allantoic fluid on microporous filters. *Applied and Environmental Microbiology*, 39(3), 500. Retrieved from <http://aem.asm.org/content/39/3/500.abstract>
- GTCT. (2021). Gene Therapy Clinical Trials Worldwide. Retrieved from <http://www.abedia.com/wiley>
- Hansen, S. P., Rene Faber, Udo Reichl, Michael Wolff, & Gram, A. P. (2011). United States Patent No.
- Heath, N., Grant, L., De Oliveira, T. M., Rowlinson, R., Osteikoetxea, X., Dekker, N., & Overman, R. (2018). Rapid isolation and enrichment of extracellular vesicle preparations using anion exchange chromatography. *Scientific Reports*, 8(1), 5730. doi:10.1038/s41598-018-24163-y
- Jiang, C., Wechuck, J. B., Goins, W. F., Krisky, D. M., Wolfe, D., Ataii, M. M., & Glorioso, J. C. (2004). Immobilized Cobalt Affinity Chromatography Provides a Novel, Efficient Method for Herpes Simplex Virus Type 1 Gene Vector Purification. *Journal of Virology*, 78(17), 8994-9006. doi:10.1128/jvi.78.17.8994-9006.2004
- Joshi, P. R. H., Bernier, A., Chahal, P. S., & Kamen, A. (2021). Development and Validation of an Anion-Exchange High-Performance Liquid Chromatography Method for Analysis of Empty Capsids and Capsids Encapsidating Genetic Material in a Purified Preparation

of Recombinant Adeno-Associated Virus Serotype 5. *Hum Gene Ther.*  
doi:10.1089/hum.2020.317

Joshi, P. R. H., Bernier, A., Moço, P. D., Schrag, J., Chahal, P. S., & Kamen, A. (2021). Development of a scalable and robust AEX method for enriched rAAV preparations in genome-containing VCs of serotypes 5, 6, 8, and 9. *Mol Ther Methods Clin Dev*, 21, 341-356. doi:10.1016/j.omtm.2021.03.016

Kishishita, N., Takeda, N., Anuegoonpipat, A., & Anantapreecha, S. (2013). Development of a pseudotyped-lentiviral-vector-based neutralization assay for chikungunya virus infection. *Journal of Clinical Microbiology*, 51(5), 1389-1395. doi:10.1128/JCM.03109-12

Konadu, K. A., Huang, M. B., Roth, W., Armstrong, W., Powell, M., Villinger, F., & Bond, V. (2016). Isolation of Exosomes from the Plasma of HIV-1 Positive Individuals. *J Vis Exp*(107). doi:10.3791/53495

Kotrbová, A., Štěpka, K., Maška, M., Páleník, J. J., Ilkovic, L., Klemová, D., . . . Pospíchalová, V. (2019). TEM ExosomeAnalyzer: a computer-assisted software tool for quantitative evaluation of extracellular vesicles in transmission electron microscopy images. *J Extracell Vesicles*, 8(1), 1560808-1560808. doi:10.1080/20013078.2018.1560808

Kowal, J., Tkach, M., & Théry, C. (2014). Biogenesis and secretion of exosomes. *Current Opinion in Cell Biology*, 29, 116-125. doi:10.1016/j.ceb.2014.05.004

Kramberger, P., Urbas, L., & Štrancar, A. (2015). Downstream processing and chromatography based analytical methods for production of vaccines, gene therapy vectors, and bacteriophages. *Human Vaccines & Immunotherapeutics*, 11(4), 1010-1021. doi:10.1080/21645515.2015.1009817

- Kuiper, M., Sanches, R. M., Walford, J. A., & Slater, N. K. (2002). Purification of a functional gene therapy vector derived from Moloney murine leukaemia virus using membrane filtration and ceramic hydroxyapatite chromatography. *Biotechnology and Bioengineering*, 80(4), 445-453. doi:10.1002/bit.10388
- Liangsupree, T., Multia, E., & Riekkola, M.-L. (2021). Modern isolation and separation techniques for extracellular vesicles. *Journal of Chromatography A*, 1636, 461773. doi:https://doi.org/10.1016/j.chroma.2020.461773
- Lippe, R. (2018). Flow Virometry: a Powerful Tool To Functionally Characterize Viruses. *J Virol*, 92(3). doi:10.1128/jvi.01765-17
- Lobb, R. J., Becker, M., Wen Wen, S., Wong, C. S. F., Wiegmans, A. P., Leimgruber, A., & Möller, A. (2015). Optimized exosome isolation protocol for cell culture supernatant and human plasma. *J Extracell Vesicles*, 4(1), 27031. doi:10.3402/jev.v4.27031
- Lorbetskie, B., Wang, J., Gravel, C., Allen, C., Walsh, M., Rinfret, A., . . . Girard, M. (2011). Optimization and qualification of a quantitative reversed-phase HPLC method for hemagglutinin in influenza preparations and its comparative evaluation with biochemical assays. *Vaccine*, 29(18), 3377-3389. doi:10.1016/j.vaccine.2011.02.090
- Lynch, K. B., Ren, J., Beckner, M. A., He, C., & Liu, S. (2019). Monolith columns for liquid chromatographic separations of intact proteins: A review of recent advances and applications. *Analytica Chimica Acta*, 1046, 48-68. doi:https://doi.org/10.1016/j.aca.2018.09.021
- McNamara, R. P., Costantini, L. M., Myers, T. A., Schouest, B., Maness, N. J., Griffith, J. D., . . . Dittmer, D. P. (2018). Nef Secretion into Extracellular Vesicles or Exosomes Is

Conserved across Human and Simian Immunodeficiency Viruses. *mBio*, 9(1), e02344-02317. doi:10.1128/mBio.02344-17

Mol, E. A., Goumans, M.-J., Doevendans, P. A., Sluiter, J. P. G., & Vader, P. (2017). Higher functionality of extracellular vesicles isolated using size-exclusion chromatography compared to ultracentrifugation. *Nanomedicine: Nanotechnology, Biology and Medicine*, 13(6), 2061-2065. doi:https://doi.org/10.1016/j.nano.2017.03.011

Moleirinho, M. G., Silva, R. J. S., Alves, P. M., Carrondo, M. J. T., & Peixoto, C. (2020). Current challenges in biotherapeutic particles manufacturing. *Expert Opin Biol Ther*, 20(5), 451-465. doi:10.1080/14712598.2020.1693541

Moreira, A. S., Cavaco, D. G., Faria, T. Q., Alves, P. M., Carrondo, M. J. T., & Peixoto, C. (2021). Advances in Lentivirus Purification. *Biotechnol J*, 16(1), e2000019. doi:10.1002/biot.202000019

Nabhan, J. F., Hu, R., Oh, R. S., Cohen, S. N., & Lu, Q. (2012). Formation and release of arrestin domain-containing protein 1-mediated microvesicles (ARMMs) at plasma membrane by recruitment of TSG101 protein. *Proc Natl Acad Sci U S A*, 109(11), 4146-4151. doi:10.1073/pnas.1200448109

Njayou, M., & Quash, G. (1991). Purification of measles virus by affinity chromatography and by ultracentrifugation: a comparative study. *Journal of Virological Methods*, 32(1), 67-77. doi:https://doi.org/10.1016/0166-0934(91)90186-4

Nolan, J. P., & Duggan, E. (2018). Analysis of Individual Extracellular Vesicles by Flow Cytometry. In T. S. Hawley & R. G. Hawley (Eds.), *Flow Cytometry Protocols* (pp. 79-92). New York, NY: Springer New York.

- Nolte-'t Hoen, E., Cremer, T., Gallo, R. C., & Margolis, L. B. (2016). Extracellular vesicles and viruses: Are they close relatives? *Proc Natl Acad Sci U S A*, 113(33), 9155-9161. doi:10.1073/pnas.1605146113
- Olgun, H. B., Tasyurek, H. M., Sanlioglu, A. D., & Sanlioglu, S. (2019). High-Grade Purification of Third-Generation HIV-Based Lentiviral Vectors by Anion Exchange Chromatography for Experimental Gene and Stem Cell Therapy Applications. In K. Turksen (Ed.), *Skin Stem Cells: Methods and Protocols* (pp. 347-365). New York, NY: Springer New York.
- Olofsson, S., Jeansson, S., & Lycke, E. (1981). Unusual lectin-binding properties of a herpes simplex virus type 1-specific glycoprotein. *Journal of Virology*, 38(2), 564-570. Retrieved from <https://jvi.asm.org/content/jvi/38/2/564.full.pdf>
- Opitz, L., Hohlweg, J., Reichl, U., & Wolff, M. W. (2009). Purification of cell culture-derived influenza virus A/Puerto Rico/8/34 by membrane-based immobilized metal affinity chromatography. *Journal of Virological Methods*, 161(2), 312-316. doi:<https://doi.org/10.1016/j.jviromet.2009.06.025>
- Opitz, L., Salaklang, J., Büttner, H., Reichl, U., & Wolff, M. W. (2007). Lectin-affinity chromatography for downstream processing of MDCK cell culture derived human influenza A viruses. *Vaccine*, 25(5), 939-947. doi:<https://doi.org/10.1016/j.vaccine.2006.08.043>
- Orr, V., Zhong, L., Moo-Young, M., & Chou, C. P. (2013). Recent advances in bioprocessing application of membrane chromatography. *Biotechnology Advances*, 31(4), 450-465. doi:10.1016/j.biotechadv.2013.01.007

- Perry, C., & Rayat, A. (2021). Lentiviral Vector Bioprocessing. *Viruses*, 13(2). doi:10.3390/v13020268
- Phillips, W., Willms, E., & Hill, A. F. (2021). Understanding extracellular vesicle and nanoparticle heterogeneity: Novel methods and considerations. *Proteomics*, e200018. doi:10.1002/pmic.20200018
- Raposo, G., & Stahl, P. D. (2019). Extracellular vesicles: a new communication paradigm? *Nature Reviews Molecular Cell Biology*, 20(9), 509-510. doi:10.1038/s41580-019-0158-7
- Raposo, G., & Stoorvogel, W. (2013). Extracellular vesicles: Exosomes, microvesicles, and friends. *The Journal of Cell Biology*, 200(4), 373-383. doi:10.1083/jcb.201211138
- Rikkert, L. G., Nieuwland, R., Terstappen, L. W. M. M., & Coumans, F. A. W. (2019). Quality of extracellular vesicle images by transmission electron microscopy is operator and protocol dependent. *J Extracell Vesicles*, 8(1), 1555419. doi:10.1080/20013078.2018.1555419
- Rodrigues, T., Carrondo, M. J. T., Alves, P. M., & Cruz, P. E. (2007). Purification of retroviral vectors for clinical application: Biological implications and technological challenges. *Journal of Biotechnology*, 127(3), 520-541. doi:https://doi.org/10.1016/j.jbiotec.2006.07.028
- Rodrigues, T., Carvalho, A., Carmo, M., Carrondo, M. J. T., Alves, P. M., & Cruz, P. E. (2007). Scalable purification process for gene therapy retroviral vectors. *The Journal of Gene Medicine*, 9(4), 233-243. doi:https://doi.org/10.1002/jgm.1021
- Rossi, C. A., Kearney, B. J., Olschner, S. P., Williams, P. L., Robinson, C. G., Heinrich, M. L., . . . Schoepp, R. J. (2015). Evaluation of ViroCyt® Virus Counter for rapid filovirus quantitation. *Viruses*, 7(3), 857-872. doi:10.3390/v7030857

- Sampey, G. C., Saifuddin, M., Schwab, A., Barclay, R., Punya, S., Chung, M. C., . . . Kashanchi, F. (2016). Exosomes from HIV-1-infected Cells Stimulate Production of Pro-inflammatory Cytokines through Trans-activating Response (TAR) RNA. *Journal of Biological Chemistry*, 291(3), 1251-1266. doi:10.1074/jbc.M115.662171
- Schmidt, S. R., Wieschalka, S., & Wagner, R. (2017, 2017-01-20). Single-Use Depth Filters: Application in Clarifying Industrial Cell Cultures - BioProcess International. *BioProcess International*. Retrieved from <https://bioprocessintl.com/2017/single-use-depth-filters-application-clarifying-industrial-cell-cultures/>
- Segura, M. M., Garnier, A., Di Falco, M. R., Whissell, G., Meneses-Acosta, A., Arcand, N., & Kamen, A. (2008). Identification of host proteins associated with retroviral vector particles by proteomic analysis of highly purified vector preparations. *J Virol*, 82(3), 1107-1117. doi:10.1128/jvi.01909-07
- Segura, M. M., Kamen, A., Trudel, P., & Garnier, A. (2005). A novel purification strategy for retrovirus gene therapy vectors using heparin affinity chromatography. *Biotechnology and Bioengineering*, 90(4), 391-404. doi:10.1002/bit.20301
- Suni, J. I., Meurman, O., Hirvonen, P., & Vaheri, A. (1984). Vaccination with a live RA 27/3 strain rubella vaccine (Rudivax), a follow-up study. *Vaccine*, 2(4), 281-283. doi:10.1016/0264-410x(84)90045-8
- Sviben, D., Forcic, D., Halassy, B., Allmaier, G., Marchetti-Deschmann, M., & Brgles, M. (2018). Mass spectrometry-based investigation of measles and mumps virus proteome. *Virol J*, 15(1), 160. doi:10.1186/s12985-018-1073-9

- Tang, V. A., Renner, T. M., Fritzsche, A. K., Burger, D., & Langlois, M. A. (2017). Single-Particle Discrimination of Retroviruses from Extracellular Vesicles by Nanoscale Flow Cytometry. *Sci Rep*, 7(1), 17769. doi:10.1038/s41598-017-18227-8
- Tang, V. A., Renner, T. M., Varette, O., Le Boeuf, F., Wang, J., Diallo, J.-S., . . . Langlois, M.-A. (2016). Single-particle characterization of oncolytic vaccinia virus by flow virometry. *Vaccine*, 34(42), 5082-5089. doi:https://doi.org/10.1016/j.vaccine.2016.08.074
- Thery, C., Amigorena, S., Raposo, G., & Clayton, A. (2006). Isolation and characterization of exosomes from cell culture supernatants and biological fluids. *Curr Protoc Cell Biol*, Chapter 3, Unit 3.22. doi:10.1002/0471143030.cb0322s30
- Thery, C., Witwer, K. W., Aikawa, E., Alcaraz, M. J., Anderson, J. D., Andriantsitohaina, R., . . . Zuba-Surma, E. K. (2018). Minimal information for studies of extracellular vesicles 2018 (MISEV2018): a position statement of the International Society for Extracellular Vesicles and update of the MISEV2014 guidelines. *J Extracell Vesicles*, 7(1), 1535750. doi:10.1080/20013078.2018.1535750
- Transfiguracion, J., Coelho, H., & Kamen, A. (2004). High-performance liquid chromatographic total particles quantification of retroviral vectors pseudotyped with vesicular stomatitis virus-G glycoprotein. *J Chromatogr B Analyt Technol Biomed Life Sci*, 813(1-2), 167-173. doi:10.1016/j.jchromb.2004.09.034
- Transfiguracion, J., Tran, M. Y., Lanthier, S., Tremblay, S., Coulombe, N., Acchione, M., & Kamen, A. A. (2020). Rapid In-Process Monitoring of Lentiviral Vector Particles by High-Performance Liquid Chromatography. *Molecular Therapy - Methods & Clinical Development*, 18, 803-810. doi:10.1016/j.omtm.2020.08.005

U.S. Food & Drug Administration. (2018). Package Insert and Patient Information - IXIARO.

Retrieved from <https://www.fda.gov/media/75777/download>

U.S. Food & Drug Administration. (2019). Package Insert - JYNNEOS. Retrieved from

<https://www.fda.gov/media/131078/download>

U.S. Food & Drug Administration. (2021a). Approved Cellular and Gene Therapy Products

| FDA. Retrieved from <https://www.fda.gov/vaccines-blood-biologics/cellular-gene-therapy-products/approved-cellular-and-gene-therapy-products>

U.S. Food & Drug Administration. (2021b). Vaccines Licensed for Use in the United States

| FDA. Retrieved from <https://www.fda.gov/vaccines-blood-biologics/vaccines/vaccines-licensed-use-united-states>

van der Pol, E., Hoekstra, A. G., Sturk, A., Otto, C., van Leeuwen, T. G., & Nieuwland, R.

(2010). Optical and non-optical methods for detection and characterization of microparticles and exosomes. *J Thromb Haemost*, 8(12), 2596-2607. doi:10.1111/j.1538-7836.2010.04074.x

Van Deun, J., Mestdagh, P., Sormunen, R., Cocquyt, V., Vermaelen, K., Vandesompele, J., .

. . Hendrix, A. (2014). The impact of disparate isolation methods for extracellular vesicles on downstream RNA profiling. *J Extracell Vesicles*, 3, 10.3402/jev.v3i4.24858. doi:10.3402/jev.v3.24858

Wang, F., Qin, Z., Lu, H., He, S., Luo, J., Jin, C., & Song, X. (2019). Clinical translation of

gene medicine. *The Journal of Gene Medicine*, 21(7), e3108. doi:<https://doi.org/10.1002/jgm.3108>

- Wang, Y., Bergelson, S., & Feschenko, M. (2018). Determination of Lentiviral Infectious Titer by a Novel Droplet Digital PCR Method. *Hum Gene Ther Methods*, 29(2), 96-103. doi:10.1089/hgtb.2017.198
- Wolff, M. W., & Reichl, U. (2008). Downstream Processing: From Egg to Cell Culture-Derived Influenza Virus Particles. *Chem Eng Technol*, 31(6), 846-857. doi:10.1002/ceat.200800118
- Yang, L., & Yamamoto, T. (2016). Quantification of Virus Particles Using Nanopore-Based Resistive-Pulse Sensing Techniques. *Frontiers in Microbiology*, 7, 7. doi:10.3389/fmicb.2016.01500
- Ye, K., Jin, S., Atai, M. M., Schultz, J. S., & Ibeh, J. (2004). Tagging Retrovirus Vectors with a Metal Binding Peptide and One-Step Purification by Immobilized Metal Affinity Chromatography. *Journal of Virology*, 78(18), 9820-9827. doi:10.1128/jvi.78.18.9820-9827.2004
- Zhao, M., Vandersluis, M., Stout, J., Haupts, U., Sanders, M., & Jacquemart, R. (2019). Affinity chromatography for vaccines manufacturing: Finally ready for prime time? *Vaccine*, 37(36), 5491-5503. doi:https://doi.org/10.1016/j.vaccine.2018.02.090
- Zimmermann, K., Scheibe, O., Kocourek, A., Muelich, J., Jurkiewicz, E., & Pfeifer, A. (2011). Highly efficient concentration of lenti- and retroviral vector preparations by membrane adsorbers and ultrafiltration. *BMC Biotechnology*, 11(1), 55. doi:10.1186/1472-6750-11-55

## **Preface to Chapter 2**

The previous chapter reviewed current bioprocesses and analytical methods used to produce enveloped viral vectors and viral vaccines. As highlighted, there is a crucial need for developing new tools, if not with the attempt to separate extracellular vesicles from the produced virus of interest, at least to assess their attributes and quantitative contribution to the final product. The following work of this thesis will focus on the HEK293 cellular platform to produce lentiviral vectors intended for gene therapy.

The first step in order to further characterize extracellular vesicles in lentiviral preparation is to establish a baseline of EVs profile in the absence of LV in a lentiviral producer cell line. This is the scope of the next chapter, which starts with developing a scalable process for isolating EVs and using proteomic, lipidomic and transcriptomic tools for characterizing EVs. It then goes beyond with the characterization of the mixed population of LV and EV after induction of LV production.

## Chapter 2

# Characterization of Extracellular Vesicles Secreted in Lentiviral Producing HEK293SF Cell Cultures

Authors: Aline Do Minh <sup>1</sup>, Alexandra T. Star <sup>2</sup>, Jacek Stupak <sup>2</sup>, Kelly M. Fulton <sup>2</sup>,  
Arsalan S. Haqqani <sup>2</sup>, Jean-François Gélinas <sup>1,†</sup>, Jianjun Li <sup>2</sup>, Susan M.  
Twine <sup>2</sup> and Amine A. Kamen <sup>1,\*</sup>

Author affiliation : <sup>1</sup> Department of Bioengineering, McGill University, Montreal, QC,  
H3A 0E9, Canada; aline.dominh@mail.mcgill.ca (A.D.M.); jean-  
francois.gelinas.1@umontreal.ca (J.-F.G.)

<sup>2</sup> Human Health Therapeutics Research Centre, National Research  
Council Canada, Ottawa, ON, K1N 5A2, Canada; Alexandra.Star@nrc-  
cnrc.gc.ca (A.T.S.); Jacek.Stupak@nrc-cnrc.gc.ca (J.S.);  
Kelly.Fulton@nrc-cnrc.gc.ca (K.M.F.); Arsalan.Haqqani@nrc-  
cnrc.gc.ca (A.S.H.); Jianjun.Li@nrc-cnrc.gc.ca (J.L.);  
Susan.Twine@nrc-cnrc.gc.ca (S.M.T.)

\* Correspondance: amine.kamen@mcgill.ca

† Current address: Département de Médecine, Université de Montréal,  
Montreal, QC, H3T 1J4, Canada.

Journal: Viruses

Year: 2021

Volume: 13

DOI: <https://doi.org/10.3390/v13050797>

Status: Published

Article history: Received 28 March 2021; Revised 23 April 2021; Accepted 28 April 2021;  
Published 29 April 2021

## Abstract

Lentiviral vectors (LVs) are a powerful tool for gene and cell therapy and human embryonic kidney cells (HEK293) have been extensively used as a platform for production of these vectors. Like most cells and cellular tissues, HEK293 cells release extracellular vesicles (EVs). EVs released by cells share similar size, biophysical characteristics and even a biogenesis pathway with cell-produced enveloped viruses, making it a challenge to efficiently separate EVs from LVs. Thus, EVs co-purified with LVs during downstream processing, are considered “impurities” in the context of gene and cell therapy. A greater understanding of EVs co-purifying with LVs is needed to enable improved downstream processing. To that end, EVs from an inducible lentivirus producing cell line were studied under two conditions: non-induced and induced. EVs were identified in both conditions, with their presence confirmed by transmission electron microscopy and Western blot. EV cargos from each condition were then further characterized by a multi-omic approach. Nineteen proteins were identified by mass spectrometry as potential EV markers to differentiate EVs in LV preparations. Lipid composition of EV preparations before and after LV induction showed similar enrichment in phosphatidylserine. RNA cargos in EVs showed enrichment in transcripts involved in viral processes and binding functions. These findings provide insights on the product profile of lentiviral preparations and could support the development of improved separation strategies aimed at removing co-produced EVs.

## Keywords

extracellular vesicles; enveloped viruses; lentiviral vectors; exosome; proteomics; lipidomics; transcriptomics

### 1. Introduction

In the past decade, gene and cell therapies have become increasingly popular tools to treat diseases such as genetic disorders, cancer, cardiovascular disease, as well as a wide spectrum of orphan diseases (Naldini, 2015). Recently, the cell therapy field reported significant clinical achievements, including Chimeric Antigen Receptor T cell (CAR T) therapy, where the patient's own immune cells are modified to express a surface receptor to stimulate an immune response against cancer cells (Wang, Guo, & Han, 2017). While many viruses have been engineered to be used in gene and cell therapies as delivery vectors, adenovirus, adeno-associated virus (AAV) and lentiviral vectors (LV) have become dominant in the field (Sharon & Kamen, 2017).

LV have several advantages over other viral vectors (Ansorge et al., 2009). Their ability to mediate long-term therapeutic transgene expression (Escors & Breckpot, 2010) makes them the ideal candidate for cell therapy. However, challenges such as achieving sufficiently high yield and suitable purity for *in vivo* and *ex vivo* clinical applications need to be addressed. This is particularly crucial for large scale productions to meet the needs of large population treatments other than orphan diseases (Merten, Hebben, & Bovolenta, 2016). Achieving suitable purity of LVs is challenged by the presence of extracellular vesicles (EVs) such as exosomes and small shedding microvesicles, that co-purify with LVs, because

they not only share a similar size, but also many biochemical and biophysical properties (Nolte-'t Hoen, Cremer, Gallo, & Margolis, 2016).

EVs are cell membrane-derived vesicles that bleb from most cells and are found in most body fluids. The field of EVs has gained considerable attention in the past few years and their potential as drug delivery vehicles and biomarkers for diseases is actively investigated (Raposo & Stoorvogel, 2013). EVs are known to transport lipids, proteins and nucleic acids. The cargo composition of EVs depends on many features, such as cell type from which they are derived and the cell environment or medium for in vitro cultures. However, the mechanism behind cargo sorting is not well understood (Hessvik & Llorente, 2017).

Databases have been created to compile data pertaining to EV characterization, such as Vesiclepedia and ExoCarta (Kalra et al., 2012; Mathivanan & Simpson, 2009). Furthermore, guidelines standardizing the study of EVs, known as the Minimal Information for Studies of Extracellular Vesicles (MISEV 2018) have been established. Definitive markers, however, are currently not established. EVs often contain similar elements as the cell of origin but at different levels and can therefore only be described in terms of enrichment or depletion in relation to parental cells. Also, EV composition depends very much on the EV subtype. For instance, Endosomal Sorting Complex Required for Transport (ESCRT) machinery proteins (ALIX, TSG101, CD63, CD81 and CD9) are highly enriched in exosomes, while MMP2 and CK18 are mostly found in shedding microvesicles. EVs also have the ability to transport ribonucleic acid (RNA). Both coding and non-coding RNA were reported in next-generation sequencing studies, revealing the presence of miRNAs in EVs' cargo which are involved in transcription regulation, post-transcription regulation and sometimes viral

defence (Lasser et al., 2016). The lipid content of EVs is also important as EVs are enclosed within a single phospholipid bilayer with the lipid composition resembling that of the cell plasma membrane. In addition, exosomes are highly enriched in glycosphingolipids, sphingomyelin, cholesterol and phosphatidylserine. EV membranes also contain lipid-raft micro-domains, which are notably involved in virus morphogenesis and budding (Izquierdo-Useros, Puertas, Borràs, Blanco, & Martinez-Picado, 2011).

EVs and retroviruses share a biogenesis pathway using the ESCRT machinery, they incorporate similar host cell components as well as viral components (Cantin, Diou, Belanger, Tremblay, & Gilbert, 2008), and also share biophysical and biochemical properties, making their separation challenging. Typical purification methods, such as chromatography based on charge or size will be ineffective at discriminating EVs and LVs. This problem needs to be addressed since EVs are released concomitantly by the cells and, thus, will be found in lentiviral preparations. As lentiviral-mediated gene therapies are intended for human use, they are strictly regulated by health authorities and any impurities in the viral preparation have to be documented as per regulatory requirements (White, Whittaker, Gandara, & Stoll, 2017). Indeed, impurities such as host cell proteins and host cell DNA are only accepted at defined level. EVs, which contain both, would require extensive characterization in order to set appropriate product specifications.

Many studies have been conducted to characterize EVs isolated from different biological fluids, tissues and even cultured cells. However, only few studies focus on cell lines used to produce viruses for vaccination or gene and cell therapy (Lavado-García et al., 2020; Venereo-Sánchez et al., 2019). Moreover, these studies centered their attention on

virus-like-particles versus EVs, which influenced their choice of separation technique. Methods such as step ultracentrifugation (UC), sucrose cushion used by Venereo et al. (Venereo-Sánchez et al., 2019), or processes involving the qEV size exclusion chromatography (SEC) column with a sample loading volume of < 500 µL have very low throughputs due to the volume limitation of the techniques. Additionally, these methods are labour intensive, not controlled and, therefore, would induce high variability in the yield of isolated EVs. These processes are also not scalable to accommodate large volumes of samples when extensive analysis is required. Here, we want to emphasize the use of the human embryonic kidney (HEK293) cell line to produce viral vectors for gene and cell therapies (Schweizer & Merten, 2010). Like most cells, HEK293 cells continuously generate EVs, which will be difficult to separate from LV concomitantly produced in these cell cultures. Therefore, gaining an understanding of the characteristics of EVs generated during LV production will provide an accurate product profile for LV-mediated gene therapies, and eventually, insights to improving the LV purification process. LV production in HEK293 cells can be achieved by different methods (Do Minh, Tran, & Kamen, 2020): by transient transfection using 3 to 4 plasmids, using packaging cell lines where necessary genetic elements for the assembly and functioning of the vectors have been stably integrated, or using producer cell lines where the remaining transgene plasmid has been integrated.

In this study, we developed a scalable process to isolate EVs from cultures of an inducible HEK293 lentivirus (Clone 92) producing cell line. First, we evaluated EVs produced under no-inducing conditions to extensively characterize isolated EVs for

proteomic, lipidomic, and transcriptomic content. We then compared EVs from Clone 92 cells with and without LV induction. These data shed light on markers that may be exploited to improve separation approaches used during downstream processing and subsequently increase LV purity.

## **2. Materials and Methods**

### **2.1. Cell Culture of HEK293SF Cells in Suspension**

As a platform for lentiviral vector (LV) production, HEK293SF cell line (abbreviated hereafter as 293SF) and a stable producer cell line developed by the National Research Council Canada (NRC), HEK293SF-LVP-CMVGFPq-92 (abbreviated hereafter as Clone 92) were used in this study (Cote, Garnier, Massie, & Kamen, 1998; Manceur et al., 2017). Production of the LVR<sub>2</sub>-GFP (rHIV.VSV-g CMV GFP) vesicular stomatitis virus G (VSV-G)-pseudotyped lentiviral vector is induced in the Clone 92 cell line by the addition 1 µg/mL (w/v) doxycycline hyclate (Millipore Sigma, Etobicoke, Canada) (from a 1 mg/mL stock in nuclease-free water) and 10 µg/mL (w/v) 4-isopropylbenzoic acid (cumate) (Millipore Sigma) (from a 10 mg/mL stock in ethanol absolute) to produce a third-generation self-inactivating human immunodeficiency virus (SIN HIV)-based lentiviral vector which expresses the green fluorescence protein (GFP). 293SF and Clone 92 cells were cultured in shake flasks (from 20 to 300 mL working volumes) in HyCell TransFx-H medium (GE Healthcare, Chicago, Illinois) supplemented with 4-6 mM L Glutamine or GlutaMAX™ (Thermo Fisher Scientific, Waltham, Massachusetts) and 0.1% Kolliphor (Millipore Sigma) without serum or antibiotics, or in HEK GM medium (Xell AG, Bielefeld, Germany)

supplemented with 4-6 mM L Glutamine or GlutaMAX™ (Thermo Fisher Scientific). Cell growth was monitored by determining live cell density based on the principle of trypan blue dye exclusion on a Vi-Cell XR cell counter (Beckman Coulter, Brea, CA, United States of America (USA)). Cells were passaged twice a week by diluting to  $2.0 \times 10^5$  live cells per mL in fresh medium.

HEK293A cells (American Type Culture Collection, Manassas, VA, USA) were used for the gene transfer assay (GTA) (Graham, Smiley, Russell, & Nairn, 1977). They were maintained in a humidified incubator at 5% CO<sub>2</sub> and 37 °C in Dulbecco's Modified Eagle's Medium (DMEM) (Wisent, St-Bruno, Canada), supplemented with 2 mM L Glutamine and 5% Fetal Bovine Serum (FBS) (Corning Inc., Corning, New York, NY, USA) without antibiotics. Cells were passaged twice a week.

## **2.2. Production of Conditioned Medium Containing EVs**

293SF and Clone 92 (under non-induced conditions) cell lines were cultivated and the cell density was measured every day. When the cell density reached  $1 \times 10^6$  cells/mL, the cells were kept in culture for 2 additional days before harvest.

## **2.3. EV Isolation**

### **2.3.1. Ultrafiltration (UF) and Size Exclusion Chromatography (SEC)**

EVs in non-LV producing conditions from Clone 92 cell cultures were isolated using a combination of ultrafiltration followed by size exclusion chromatography as it was reported that this technique could yield more intact and pure particles (Lobb et al., 2015; Nordin et al., 2015). The cells were first removed by centrifugation. The cell pellet was kept at -20 °C

for further analysis and the supernatant was filtered through a 0.45  $\mu\text{m}$  vacuum polyvinylidene fluoride (PVDF) filter (VWR, Ville Mont-Royal, QC, Canada) to remove large particles. The filtrate was then subjected to ultrafiltration and diafiltration (DF) using a Vivaflow™ 50R membrane (Sartorius) with a 100 kDa MWCO pre-flushed with MilliQ water and phosphate-buffered saline (PBS) buffer (Wisent) containing 0.005% Kolliphor. The pressure and volume were monitored throughout the process. This membrane also allowed for large scale processing with volumes up to 1.5 L and reusability. The diafiltered concentrate was then loaded onto a HiScreen™ Cpto™ Core 700 SEC column (GE Healthcare) which resin exhibits both size exclusion and binding properties. The Cpto Core 700 column was operated in flowthrough mode on an ÄKTA avant (GE Healthcare), providing further control and allowing large volumes to be processed. The flowthrough was collected and stored at  $-80\text{ }^{\circ}\text{C}$  until further analysis. In some cases, the flowthrough was subjected to an additional concentration step using a MicroKros 10 kDa MWCO hollow fiber (Repligen, Rancho Dominguez, CA, USA) or an Amicon Ultra-4 centrifugal filter unit (Millipore Sigma).

### ***2.3.2. Ultracentrifugation***

The induction of Clone 92 cell cultures with cumate and doxycycline generates LV particles which are classified as biosafety level 2 (BSL2) material. As the isolation process described earlier was specifically designed for EVs, involving open handling and use of equipment not suitable for BSL 2 material, ultracentrifugation was used in order to compare EVs in non-LV producing conditions with EVs upon induction of LV production. The supernatant of Clone 92 cell culture, with and without induction, obtained after

centrifugation at  $1200\times g$  for 5 min, was filtered through a  $0.45\ \mu\text{m}$  filter and then subjected to a  $100,000\times g$  centrifugation for 70 min at  $4\ ^\circ\text{C}$ . The pellet was then washed with PBS and centrifuged again at  $100,000\times g$  for 70 min at  $4\ ^\circ\text{C}$ . The pellet was resuspended in 1 mL of PBS and stored at either  $2\text{--}8\ ^\circ\text{C}$  or  $-80\ ^\circ\text{C}$  until further analysis.

## 2.4. Nomenclature

Table 4 presents the nomenclature that will be used hereafter for the purpose of clarification. As the result of Clone 92 induction with cumate and doxycycline is a mixed population of EVs and LVs, the nomenclature was chosen to highlight that fact. When designating Clone 92 EVs in general without a specific isolation method, the abbreviation  $\text{C}^{92}\text{EVs}$  will be used.

**Table 4:** Nomenclature for EV and LV samples in Clone 92 cell line using different isolation methods in two conditions: without induction of LV production or after induction of LV production using cumate and doxycycline.

	No Induction	Induction
No isolation	$\text{C}^{92}\text{EV}_{\text{sup}}$	$\text{C}^{92}\text{EV/LV}_{\text{sup}}$
Isolation by UF/SEC	$\text{C}^{92}\text{EV}_{\text{SEC}}$	N/A <sup>1</sup>
Isolation by UC	$\text{C}^{92}\text{EV}_{\text{UC}}$	$\text{C}^{92}\text{EV/LV}_{\text{UC}}$

<sup>1</sup> N/A: not applicable.

## 2.5. Quantification of Functional Viral Titer by Gene Transfer Assay (GTA)

A flow cytometry-based GTA was used to determine functional viral titer (Manceur et al., 2017). Each well of a 24-well plate was seeded with  $1 \times 10^5$  cells of HEK293A. After leaving the cells adhere to the plate for 5 h, the medium was removed. EV and LV samples were serially diluted in DMEM (Wisent) supplemented with  $8\ \mu\text{g/mL}$  of polybrene (Millipore

Sigma) and incubated at 37 °C for 30 min. 200 µL of diluted sample were then added to the cells for transduction and the plates were incubated overnight at 37 °C before addition of 800 µL of fresh culture medium in each well the next day. Three days post-transduction (therefore, 48 h after medium addition), cells were harvested and run on the Accuri flow cytometer (Becton Dickinson, Franklin Lakes, NJ, USA) to quantify GFP expressing cells. Accepted values ranged between 2–20% fluorescent cells out of total cell count to avoid signal due to super infection.

## **2.6. Quantification of Total Particles by Digital Drop Polymerase Chain Reaction (ddPCR)**

RNA was first extracted from LV samples using the High Pure Viral Nucleic Acid Kit (Roche, Mannheim, Germany) according to the manufacturer's instructions. The extracted RNA was then reverse transcribed into complementary deoxyribonucleic acid (cDNA) using the iScript™ Select cDNA Synthesis Kit (Bio-Rad Laboratories, Hercules, CA, USA) according to the manufacturer's instructions and using gene-specific primers targeted towards the woodchuck hepatitis virus posttranscriptional regulatory element (WPRE) amplifying a 589-base pair fragment. Primer sequences were: forward primer (5'-GTCCTTTCCATGGCTGCTC-3'), reverse primer (5'-CCGAAGGGACGTAGCAGA-3') (Integrated DNA Technologies, Inc., Coralville, IA, USA). Serial dilutions of cDNA were prepared in nuclease-free water. ddPCR reactions were prepared with the QX200™ ddPCR™ EvaGreen Supermix (Bio-Rad) and the WPRE primer set. PCR mixtures (22 µL) were prepared for the QX200™ Droplet Generator (Bio-Rad), with final primer concentration of 0.8 µM. After droplet generation, the following PCR program was run: one cycle of 95 °C

for 10 min; 40 cycles of 95 °C for 30 sec and 60 °C for 30 sec; followed by a final extension at 72 °C for 10 min and a 4 °C hold. PCR results were analyzed with the Droplet reader and QuantaSoft (Bio-Rad).

## **2.7. Quantification of Total Particles by Flow Virometry**

A few studies used FM4-64FX and reported that the unbound fractions of the dye do not interfere with the flow cytometry measurements (Pospichalova et al., 2015; Tang, Renner, Fritzsche, Burger, & Langlois, 2017). Moreover, FM4-64FX was shown to efficiently label EVs as well as the retrovirus under study (Tang et al., 2017). Cell Trace Violet (CTV) is a similar dye to Carboxyfluoresceinsuccinimidyl ester (CFSE), which has been used in many flow cytometry studies on EVs (Morales-Kastresana et al., 2017; Pospichalova et al., 2015). CTV was reported as more efficient and it has a different fluorescence spectrum than GFP, which is helpful in avoiding crosstalk, since the samples bear GFP.

A double staining experiment was performed by labeling Clone 92 EV samples with a generic lipophilic dye, FM4-64FX (Thermo Fisher Scientific), and a protein-binding dye, Cell Trace Violet (CTV) (Thermo Fisher Scientific) according to the manufacturer's instructions. A three-laser BD LSRFortessa™ X-20 was used for acquisition and results were analyzed by FlowJo V10.2 (FlowJo LLC, Ashland, Oregon, USA). 405 nm filter with 450/50 fluorescent channel, and 488 nm filter with 530/30 and 780/60 fluorescent channels were used.

For small particle detection, a Cytoflex flow cytometer (Beckman Coulter, Indianapolis, IN, USA) with a photomultiplier tube (PMT) for forward scatter detection was used. Specifications for laser wavelengths and power were as follows: 488 nm–300 mW, 525/40

fluorescent channel. Acquisition was done with CytExpert (Beckman Coulter). Samples, unless otherwise indicated, were acquired at the lowest flow rate 10  $\mu\text{L}/\text{min}$ . The instrument cleaning procedure prior to acquisition was as follows: 20 min with Cleaning solution (Beckman Coulter) or 20 min with 0.1% bleach followed by 20 min with distilled water.

### **2.8. Imaging of EVs by Transmission Electron Microscopy (TEM)**

EV samples were prepared for negative staining TEM imaging according to Théry et al. (Théry, Amigorena, Raposo, & Clayton, 2006). Imaging was done on a CM 100 Transmission Electron Microscope (Philips, Eindhoven, The Netherlands) operating at 80 kV. Briefly, 10  $\mu\text{L}$  samples in 2% para-formaldehyde (PFA) were fixed on Formvar-carbon coated EM grids in 1% glutaraldehyde. Samples were then stained first in a solution of uranyl oxalate then embedded in a mixture of 4% uranyl acetate and 2% methyl cellulose for 10 min on ice. The stain was then removed by touching gently the edge of the grids on a filter paper. The grids were air dried prior to the TEM observation.

### **2.9. Immunoblot Analysis**

Proteins were resolved by sodium dodecyl sulfate-polyacrylamide gel electrophoresis (SDS-PAGE), transferred to nitrocellulose membranes, blocked with 5% non-fat powdered milk in PBS-tween (PBS-T). Membranes were then probed for Western blot (WB) using antibodies against EV-enriched proteins (anti-CD9 (rabbit), anti-CD81 (mouse) and anti-TSG101 (rabbit) (Abcam, Cambridge, United Kingdom)) and against non-EV enriched proteins (anti-Calnexin (rabbit) (Cell Signaling, Danvers, MA, USA)).

### **2.10. Protein and Nucleic Acid Quantification**

Protein concentration was determined using the RC/DC™ Protein Assay (Bio-Rad, Hercules, CA, USA) according to the manufacturer's instructions.

For DNA quantification, the nucleic acids of EVs were extracted using the High Pure Viral Nucleic Acid Kit (Roche, Mannheim, Germany). Then, the DNA content was quantified with the Quant-iT™ PicoGreen™ dsDNA Assay Kit (Thermo Fisher Scientific) following the manufacturer's instructions.

RNA extraction using the High Pure Nucleic Acid kit has been done previously (Venereo-Sánchez et al., 2019). This technique was however deemed not suitable for that purpose since poly(A) is used in this kit in a non-negligible concentration to precipitate the RNA. This would compromise RNA quantification since the Ribogreen kit used for total RNA quantification has a high affinity for poly(A) fractions. RNA was extracted using the Exosomal RNA Isolation Kit (Norgen, Thorold, ON, Canada). The extracted RNA was quantified with the Quant-iT™ RiboGreen™ RNA Assay Kit (Thermo Fisher Scientific) or the Qubit™ RNA assay (ThermoFisher).

### **2.11. EV Identification**

Protein markers from the Minimal Information for Studies of Extracellular Vesicles 2018 (MISEV 2018) guidelines were used to confirm enrichment of EVs from their parent cells (They et al., 2018). For general EV characterization, MISEV 2018 recommends showing three positive protein markers of EVs to demonstrate EV enrichment with ideally one trans-membrane/lipid bound protein and one cytosolic protein. In addition to demonstrating

protein enrichment, MISEV 2018 also recommends the depletion of cellular proteins using at least one negative protein marker for EVs.

## **2.12. Proteomic Analysis**

### **2.12.1. Filter-Aided Sample Preparation (FASP)**

All analyses were done on three biological replicates. The samples were thawed on ice, and then boiled to ensure deactivation of the virus. Samples were subsequently aliquoted for separate proteomic and phospholipid analyses. The samples used in proteomics studies were treated with 4× lysis buffer containing 14% SDS, 400 mM Tris-HCl (pH 8.5), 400 mM dithiothreitol (DTT), and Protease Inhibitor Cocktail (Millipore Sigma). The samples were then diluted with water to reduce the lysis buffer concentration to 1X, sonicated on ice with Sonic Dismembrator (Fisher Scientific, Ottawa, ON, Canada) and subsequently boiled at 95 °C for 10 min. The samples were alkylated with 20 mM iodoacetamide and then digested using a modified filter-aided sample preparation (FASP) method (Wisniewski, Zougman, Nagaraj, & Mann, 2009). Briefly, the samples were first buffer exchanged with 8 M urea using a 10 kDa MWCO filter in order to remove all detergent and alkylating reagents. A buffer exchange into 50 mM ammonium bicarbonate was then performed four times. Protein concentrations were determined by the Bradford protein assay (Bio-Rad), according to the manufacturer's instructions. The protein suspensions were then digested with 1 µg sequencing grade modified trypsin (Promega, Madison, WI, USA) at 37 °C overnight. The resulting peptides were collected by centrifugation and acidified with formic acid (final concentration of 0.25%). The EV samples were subsequently dried down in a speed vacuum centrifuge and resuspended in 25 µL of 0.1% formic acid. Cell

preparations and cell supernatants were diluted with 0.1% formic acid to yield a concentration of 0.02 µg/µL in 100 µL.

### ***2.12.2. Liquid Chromatography-Tandem Mass Spectrometry (LC MS/MS) Analysis***

The acidified peptides were separated by reversed-phase liquid chromatography (RPLC) using a nanoAcquity ultra-high-performance liquid chromatography (nUPLC) (Waters, Milford, MA, USA) coupled to LTQ-Orbitrap-XL ETD mass spectrometer (Thermo Fisher Scientific) with a nano-electrospray ionization (ESI) interface operated in positive ion mode. The analysis involved injection and loading of approximately 10 µL of the peptide sample onto an inline Pepmap100 300 µm × 5 mm C8 Acclaim 5 µm 100 Å precolumn (Thermo Fisher Scientific), and Nano-Acquity Symmetry C18, 5 µm, 180 µm × 2 cm Trap (Waters) followed by separation using a 100 µm I.D. × 10 cm 1.7 µm BEH130C18 nanoLC column (Waters). The mobile phase consisted of 0.1% (v/v) formic acid in HPLC grade water as solvent A and 0.1% (v/v) formic acid in acetonitrile as solvent B. The peptides were separated using a gradient ramping from 0.2% to 40% solvent B over 45 min, 40% to 95% solvent B over 4 min, and then re-equilibrating from 95% to 0.2% solvent B over 11 min at a flow rate of 500 nL/min. A 30-min clean-up gradient was run between samples to minimize carryover. Data was acquired on ions with mass/charge (m/z) ratio between 400 and 2000 Da in profile mode at a resolution of 60,000 in the Orbitrap followed by data-dependent analysis (DDA) MS/MS scans of the top three ions per scan using collision-induced dissociation (CID) for fragmentation and detection in the ion trap with the following settings: isolation width of 3.0, normalized collision energy of 35.0, activation Q of 0.250, and activation time of 30.000 ms.

### 2.12.3. Mascot Database Search

The raw files generated by MS analysis were converted to mascot generic files (mgf) and mzXML files using ProteoWizard (Chambers et al., 2012) (version 3.0.18250, ProteoWizard Software Foundation, Palo Alto, CA, USA). Files were submitted to Mascot search engine (Perkins, Pappin, Creasy, & Cottrell, 1999) (version 2.6.2, Matrix Science, London, United Kingdom) to search against protein sequence databases consisting of target and decoy sequences. The target sequences included the human Uniprot database (The UniProt Consortium, 2018) (release 2019) combined with HIV genome translated genome sequence and GFP sequences. The decoy database was constructed with reverse sequences from the target database. Searches were restricted to trypsin cleavage with one missed cleavage accepted. The peptide tolerance was set to  $\pm 5$  ppm with a fragment mass tolerance of  $\pm 0.8$  Da. Carbamidomethylation on cysteine residues was set as a fixed modification while oxidation of methionine residues was set as a variable modification. False discovery rate (FDR) in Mascot searching was calculated as follows:

$$FDR = \frac{N_{decoy}}{N_{target}}, \quad (1)$$

where  $N_{decoy}$  is the number of decoy hits identified and  $N_{target}$  is the number of target hits identified. To maximize the number of true positive peptides and minimize false positives, an FDR of <1% was selected, which corresponded to an average Mascot ion scores  $\geq 40$ .

#### 2.12.4. Proteomics Data Processing

Proteomics data analysis involved measurement and assignment of MS intensity signal to each identified protein and was performed using MatchRX software (MatchRX, Royal Oak, MI, USA) as described previously (Haqqani, Kelly, & Stanimirovic, 2008). Briefly, peak intensities of all the ions in each MS run were extracted from the mzXML files and assigned to Mascot-identified proteins using the MatchRX software using their m/z, retention times and neighbouring peak coordinates. Each MS intensity was adjusted using total median normalization as described previously (Haqqani et al., 2008). For each sample, total MS intensity signal was also calculated by summing intensities of all the MS intensity signals in the run and was used to estimate fraction of MS intensity (FMSI) of each protein as follows:

$$FMSI \text{ of a protein} = \frac{\text{sum of all intensities specific to the protein in the sample}}{\text{sum of all intensities in the sample}} \quad (2)$$

FMSI were used to examine the enrichment or depletion of each protein in EV fractions compared to Clone 92 cells or supernatants. Proteins showing more than two natural log difference (approximately 7-fold) were considered either enriched or depleted. Since FMSI values were calculated using MS intensities, they may not correspond to true protein abundance and hence were not used to compare levels amongst proteins.

The top 50 EV proteins were selected based on the following criteria for high confidence protein identification:

1. The protein's Mascot score had to be  $\geq 40$  (<1% FDR) with  $\geq 2$  peptides and an FMSI fold change  $\geq 7$  compared to cells and supernatant.

2. Keratins were not included in the top 50 list as their presence can be the result of sample processing.

3. The FMSI value in SEC isolated EVs had to be >0.

Venn diagrams were generated using the BioVenn website (Hulsen, de Vlieg, & Alkema, 2008). The common proteins identified in both the ExoCarta (Keerthikumar et al., 2016) and Vesiclepedia (Pathan et al., 2018) databases were used for comparison.

### **2.13. Liquid Chromatography-Mass Spectrometry (LC-MS) of Phospholipids**

LC-MS was carried out using a Synapt G2-Si mass spectrometer (Waters) coupled to a Dionex3000 HPLC (Thermo Fisher Scientific) using a Waters ESI source. Separations were performed on a 50 × 1 mm internal diameter 3.5 μm Zorbax XDB-C8 column (Agilent, Santa Clara, CA, USA), Solvent A was 5:1:4 IPA:MeOH:H<sub>2</sub>O (0.2% Formic Acid/0.028 NH<sub>4</sub>OH); while solvent B was IPA (0.2% Formic Acid/0.028 NH<sub>4</sub>OH). The following gradient program was used: 0% solvent B over 3 min, 0–95% solvent B over 12 min, 95% solvent B over 5 min, and re-equilibration at 0% solvent B for 10 min. Phospholipids were analyzed in negative-ion mode. A rolling collision energy between 45 and 160 eV was used for automated DDA MS/MS. Data interpretation was done manually using LIPID MAPS® Online Tools (Sud, Fahy, & Subramaniam, 2012). Data was normalized by first applying correction factors based on ionization efficiencies and response factors for each type of phospholipid, then percent compositions for each fraction were calculated.

### **2.14. Transcriptomics and Bioinformatics Analysis**

The quality of the RNA was assessed with the Qubit RNA assay. The sequencing library was prepared using the SMARTer smRNA-Seq kit for Illumina (Takara Bio USA, Mountain View, CA, USA), following the manufacturer's instructions, for miRNA samples, and the SMART-Seq v4 Ultra Low Input RNA kit (Takara Bio USA) for mRNA samples. The quality of the libraries was assessed using Qubit DNA assay (Thermo Fisher Scientific), Bioanalyzer 2100 (Agilent), and qPCR. Sequencing was performed on the NextSeq 500 system (Illumina, San Diego, CA, USA), using a 1x75bp SE sequencing strategy.

The gene expression levels in each mRNA sample were evaluated by aligning reads to the human GRCh38 reference genome and following published methods.(Pertea, Kim, Pertea, Leek, & Salzberg, 2016) The gene expression level was normalized by the number of fragments per kilobase per million mapped reads (FPKM). Enrichment analyses were performed using the GO Enrichment Analysis tool and Metascape Express Analysis (Ashburner et al., 2000; "The Gene Ontology Resource: 20 years and still GOing strong," 2019; H. Mi, Muruganujan, Ebert, Huang, & Thomas, 2019; Y. Zhou et al., 2019). Protein hits were classified by protein class using the Protein Analysis Through Evolutionary Relationships (PANTHER) tool (Huaiyu Mi et al., 2020).

## **3. Results**

### **3.1. Characterization of Clone 92 EVs in the Absence of Lentiviral Particles**

Although efforts have been dedicated to segregate EVs from retrovirus particles (Cantin et al., 2008; Konadu et al., 2016), it is currently not possible to fully separate EVs from LVs.

This is even more difficult on large scale processes. It is therefore important to understand the composition of basal EVs, meaning under non-inducing conditions, as they will constitute a subpopulation that will be found in LV preparation. Thus, the first part of the study focuses on the characterization of EVs generated by Clone 92 in the absence of lentiviral particles. As described in the materials and methods section, Clone 92 cells are cultured in suspension and serum-free medium, to avoid contamination by EVs associated with serum supplementation (They et al., 2006). It is also important to note that the viability of the cell cultures was maintained and monitored above 95% at all times to avoid the presence of apoptotic bodies.

### ***3.1.1. Quantification of EVs Using GFP Signal by Flow Virometry***

Clone 92 cells express GFP constitutively, allowing the detection of particles released by the cells as Clone 92 EVs will emit a fluorescence signal. The flow virometry quantification method was first validated using a double-labeling strategy. Samples of a non-induced Clone 92 culture supernatant referred to as  $^{C92}EV_{sup}$  were taken on day 0, 2, 3, 4 and 7 and labeled with FM4-64FX and CTV. Samples were then analyzed by flow cytometry without purification. Results are presented in Figure 3.

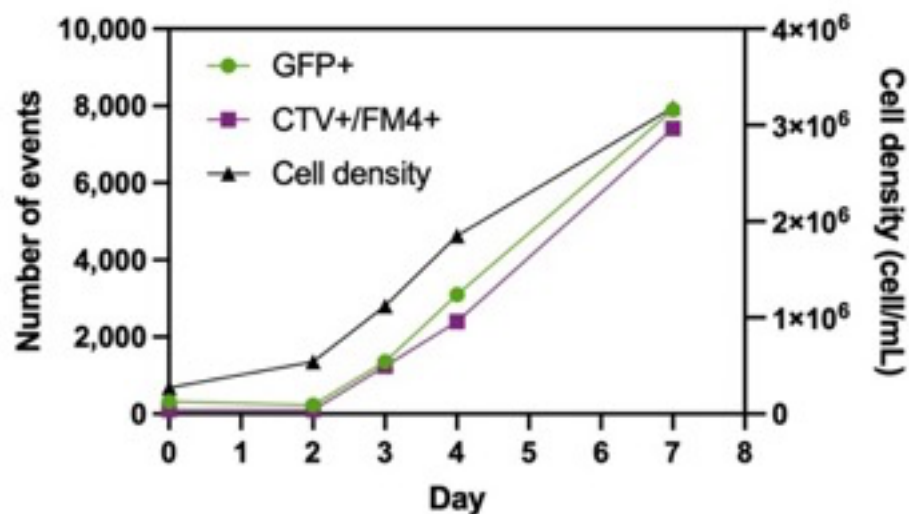


**Figure 3:** Analysis of Clone 92 supernatant by flow virometry: Quantification of GFP+ events and CTV+/FM4+ events over cell culture days as measured on the BD Fortessa flow cytometer.

Gating is shown in supplementary Figure S1. In Figure S1a, the gate represents GFP positive events. In Figure S1b, gating was done such as FM4-64FX positive and CTV positive events are found in quadrant Q2. In Figure S1a,b, HyCell medium serves as a negative control and shows no GFP+ signal nor FM4-64FX+/CTV+ signal before and after staining. The analysis was done on the samples mentioned above and the GFP+ events, CTV+/FM4-64FX+ events and the cell density were plotted over time on Figure 1. Figure 1 shows that GFP positive events correlated to FM4-64FX / CTV double positive events and are increasing as the cell density increases over time. Thus, this preliminary experiment showed the feasibility of detecting <sup>C92</sup>EVs using GFP fluorescence signal to enumerate the number of total particles. Subsequent flow virometry measurements were then done using only GFP signal.

Flow virometry was then used in order to estimate the number of particles bearing GFP, since GFP, which is constitutively expressed in that cell line, is being randomly

incorporated into  $^{C92}$ EVs. The gating used is presented in supplementary Figure S2, PBS being used as a negative control. Samples were diluted with PBS to keep a low abort rate (ideally below 2%) and the concentrations were corrected for the dilution.

### 3.1.2. Development of a Scalable EV Isolation Process Using Size Exclusion Chromatography (SEC)

For consistency and reproducibility, it was desirable that all analyses be performed on a single batch, thus requiring a large volume with high yield of isolated EVs to proceed with extensive characterization.

The isolation process involving UF/DF and SEC described in the materials and methods section, with or without the final concentration step, yielded EVs with an adequate volume and concentration according to the protein content and was considered as an appropriate process to produce EVs for further characterization.

This isolation process was performed 3 times and yielded 3 batches of  $^{C92}$ EV<sub>SEC</sub>.

Table 5 presents the mass balance of one repeat of the EV isolation process for Clone 92 culture showing recoveries at different steps in the process. Quantification was done by flow virometry in order to estimate the amount of in-process and  $^{C92}$ EV<sub>SEC</sub>.

**Table 5:** In-process quantification of GFP+ particles by flow virometry and total protein by RC/DC during one repeat of Clone 92 EVs isolation process.

In-Process Sample	Volume (mL)	GFP+ Particles (Part/mL)	GFP+ Particles Step Recovery (%)	Total Protein (µg/mL)
Supernatant	1478	$1.37 \times 10^9$	N/A <sup>1</sup>	85
Supernatant after 0.45 µm filtration	1473	$7.73 \times 10^8$	56	73
UF/DF <sup>2</sup> product	115	$4.01 \times 10^9$	68	181

UF/DF <sup>2</sup> product after 0.45 µm filtration	108	$2.90 \times 10^9$	84	188
UF/DF <sup>2</sup> permeate	1759	$2.81 \times 10^8$	-	32
SEC <sup>3</sup> EV peak	101	$3.15 \times 10^9$	102	75
SEC <sup>3</sup> post-EV peak	8	$2.99 \times 10^8$	103	44
Final concentrated EVs	10	$2.38 \times 10^{10}$	74	795

<sup>1</sup> N/A: not applicable, <sup>2</sup> UF/DF: ultrafiltration/diafiltration, <sup>3</sup> SEC: size exclusion chromatography.

Total protein quantification by RC/DC showed a reduction of 63% in the C<sub>92</sub>EV<sub>SEC</sub> peak as compared to the starting material. Gene transfer assay (GTA) was performed on undiluted C<sub>92</sub>EV<sub>SEC</sub> samples and did not show any functional titer confirming the absence of lentiviral activity.

### 3.1.3. Preliminary Characterization Confirms EV Identity

C<sub>92</sub>EV<sub>SEC</sub> were imaged by transmission electron microscopy (TEM). In Figure 4a, EVs are visible as cup-shaped indicated by white arrows. Their sizes range from about 50 to 100 nm.

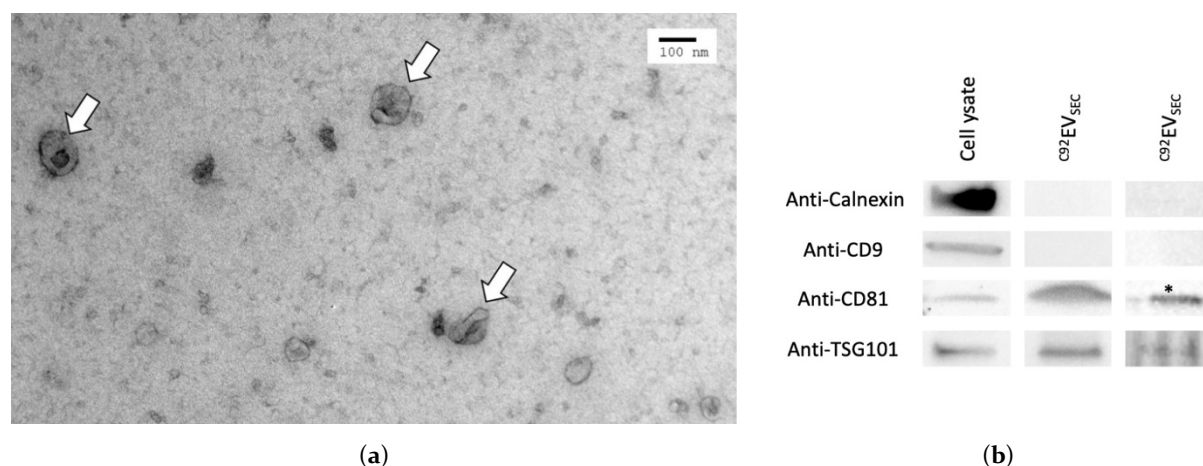


**Figure 4:** Preliminary characterization of C<sub>92</sub>EV<sub>SEC</sub>. (a) Electron microscopy images of C<sub>92</sub>EV<sub>SEC</sub>. Scale 100. nm. (b) Enriched proteins in C<sub>92</sub>EV<sub>SEC</sub> identified by Western Blot. \* Sample was concentrated before loading on the gel.

CD81, TSG101 and CD9 are markers expected to be present or enriched in EVs. By WB analysis, CD81 was detected in cell lysate and  $^{C92}EV_{SEC}$  samples, with an expected enrichment in  $^{C92}EV_{SEC}$  samples (Figure 2b). TSG101 was also present in cell lysate and  $^{C92}EV_{SEC}$ . The WB did not show CD9 in  $^{C92}EV_{SEC}$  samples, as the concentration of this common marker in the samples was either too low for detection or  $^{C92}EV_{SEC}$  might not be enriched in CD9. Calnexin is a protein embedded in the endoplasmic reticulum membrane and serves here as a negative marker to assess EVs purity. It was only found in cell lysate samples and not in  $^{C92}EV_{SEC}$  as expected.

### **3.1.4. Proteomic Cargo of $^{C92}EV_{SEC}$**

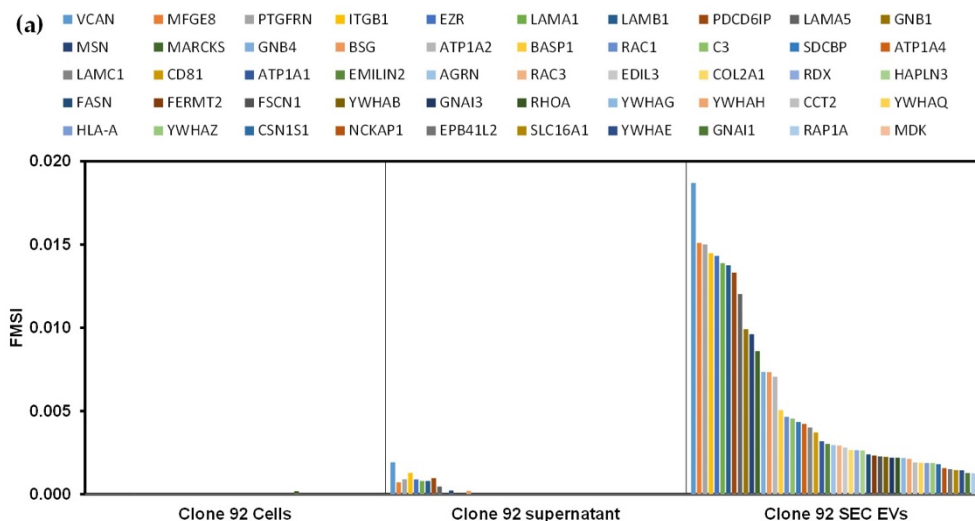
Mass spectrometry (MS) was used to estimate enrichment of extracellular vesicles (EVs) by looking at the FMSI contributed by each protein to the total MS intensity in each sample. The positive identification of transmembrane proteins cluster of differentiation 81 (CD81), basigin (BSG), and the cytosolic protein, programmed cell death 6 interacting protein (PDCD6IP), confirmed the enrichment of EVs in  $^{C92}EV_{SEC}$ . The FMSI of both CD81 and BSG was found to be enriched in  $^{C92}EV_{SEC}$  when compared to the Clone 92 cells, as well as the conditioned media prior to EV isolation called “supernatant” (Supplementary Figure S3). Additionally, protein PDCD6IP had a higher FMSI in the  $^{C92}EV_{SEC}$  than in the parental cells and associated supernatants (Supplementary Figure S3) suggesting enrichment in EV fractions. Endoplasmic reticulum chaperones (HSP90B1) and other heat shock proteins are good candidates as negative protein markers as they are found in the endoplasmic reticulum or mitochondria of cells and are not associated with the plasma membrane or endosomes. In this set of data, several heat shock proteins including HSP90B1, HSPD1, HSPA9, HSPE1 were depleted in

$C^{92}EV_{SEC}$  compared to the parental cells (Supplementary Figure S3). Taken together, these data indicate that the samples have been enriched for EVs.

MS was also used to detect the presence of GFP in the samples and confirm its presence in the  $C^{92}EV_{SEC}$ . GFP was detected in Clone 92 cells,  $C^{92}EV_{sup}$ , and  $C^{92}EV_{SEC}$  and not from the 293SF original cell line, as expected (Supplementary Figure S4). No HIV proteins were identified in any of the samples.

The FMSI of all identified proteins in  $C^{92}EV_{SEC}$  was plotted to identify enrichment in the EV samples compared to the parental cells. Out of the 204 proteins identified, 179 showed enrichment in EVs based on their FMSI, with the top 50 of enriched proteins in  $C^{92}EV_{SEC}$  shown in Figure 5a based on their FMSI.

The total number of identified proteins in  $C^{92}EV_{SEC}$  and the top 50 enriched proteins were compared to the combined Vesiclepedia database (Pathan et al., 2018) and ExoCarta database (Keerthikumar et al., 2016) in Figure 5b.



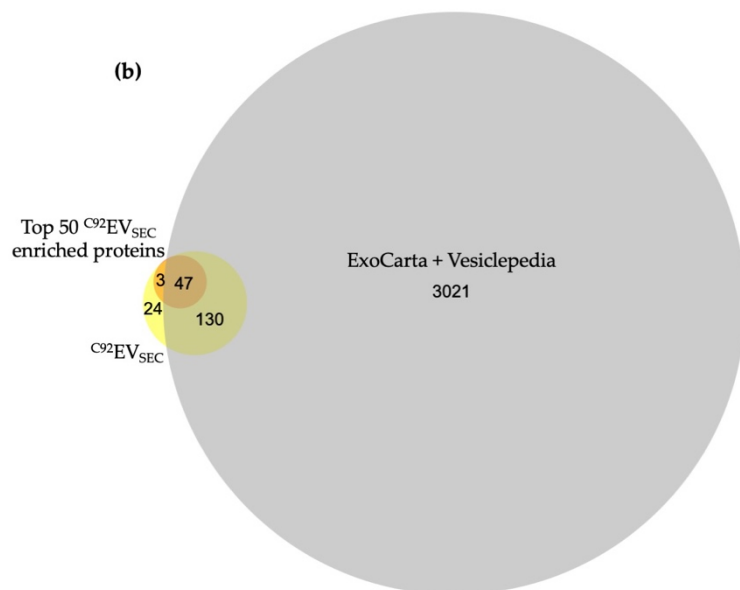


**Figure 5:** Proteomic analysis of  $C^{92}EV_{SEC}$ . (a) Top 50 enriched proteins identified in  $C^{92}EV_{SEC}$  based on the criteria described in Materials and Methods. (b) Area-proportional Venn diagram for the total number of identified proteins in  $C^{92}EV_{SEC}$  and the top 50 enriched proteins in  $C^{92}EV_{SEC}$  within the combined Vesiclepedia and ExoCarta database.

Among the total identified proteins in  $C^{92}EV_{SEC}$ , 27 were not found in the combined database, and 3 of these were in the top 50 enriched proteins in  $C^{92}EV_{SEC}$ : EMILIN2, MDK and ATP1A4. These proteins might be additional potential markers for  $C^{92}EVs$ .

### 3.1.5. Lipidomic Composition of $C^{92}EV_{SEC}$

EVs are formed by a lipid bilayer membrane. Given the size of EVs, lipids are a significant component of EVs and may play important biological roles. The field is still young; however, any data on lipids structuring EVs may give critical information related to their biogenesis.

The phospholipid species were quantified by liquid chromatography-mass spectrometry (LC-MS) in three samples of  $C^{92}EV_{SEC}$  (Figure 6). LIPID MAPS consortium guidelines were followed for lipid nomenclature and the annotation of lipid species was as

follows: lipid class followed by total number of carbons and degree unsaturation of respective acyl chains (e.g., PS 34:1) (Fahy et al., 2009).

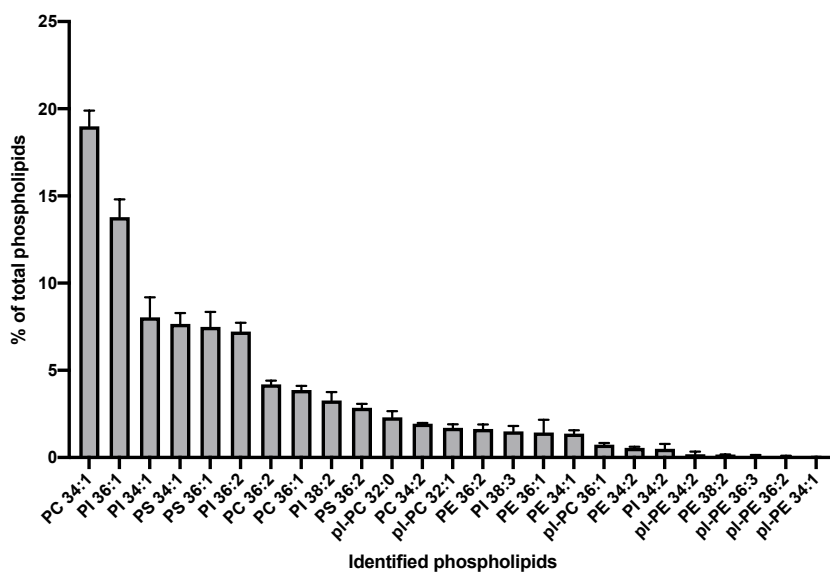


**Figure 6:** Phospholipids identified in C<sub>92</sub>EV<sub>SEC</sub>. PC: phosphatidylcholine, PI: phosphatidylinositol, PS: phosphatidylserine, pl-PC: plasmalogen-phosphatidylcholine, PE: phosphatidylethanolamine, pl-PE: plasmalogen-phosphatidylethanolamine. Error bars indicate standard error of the mean (SEM).

The most abundant phospholipids identified in C<sub>92</sub>EV<sub>SEC</sub> were phosphatidylcholine (PC) 34:1 and phosphatidylinositol (PI) 36:1. Hexose-ceramide (sphingolipids (SL)) were also abundantly detected at levels comparable to plasmalogen (PL), however they could not be quantified reliably.

### 3.1.6. Nucleic Acid Content and Gene Ontology

Picogreen (DNA) and Qubit (RNA) extracted from C<sub>92</sub>EV<sub>SEC</sub> were performed on two different batches of C<sub>92</sub>EV<sub>SEC</sub> in duplicate (Table 6).

**Table 6:** Nucleic acid quantification in C<sub>92</sub>EV<sub>SEC</sub>.

	C <sub>92</sub> EV <sub>SEC</sub> <sup>1</sup>
dsDNA (µg/mL)	0.4 ± 0.1
Total RNA (µg/mL)	9.7 ± 1.7

<sup>1</sup> Mean ± SD.

The 3000 most expressed genes present in replicate samples of  $C^{92}EV_{SEC}$  and ranked by FPKM were analyzed for enrichment. The GO enrichment analysis tool and Metascape were both used to provide a broader search in available databases. The top 25 ontology terms are shown on Figure 7.

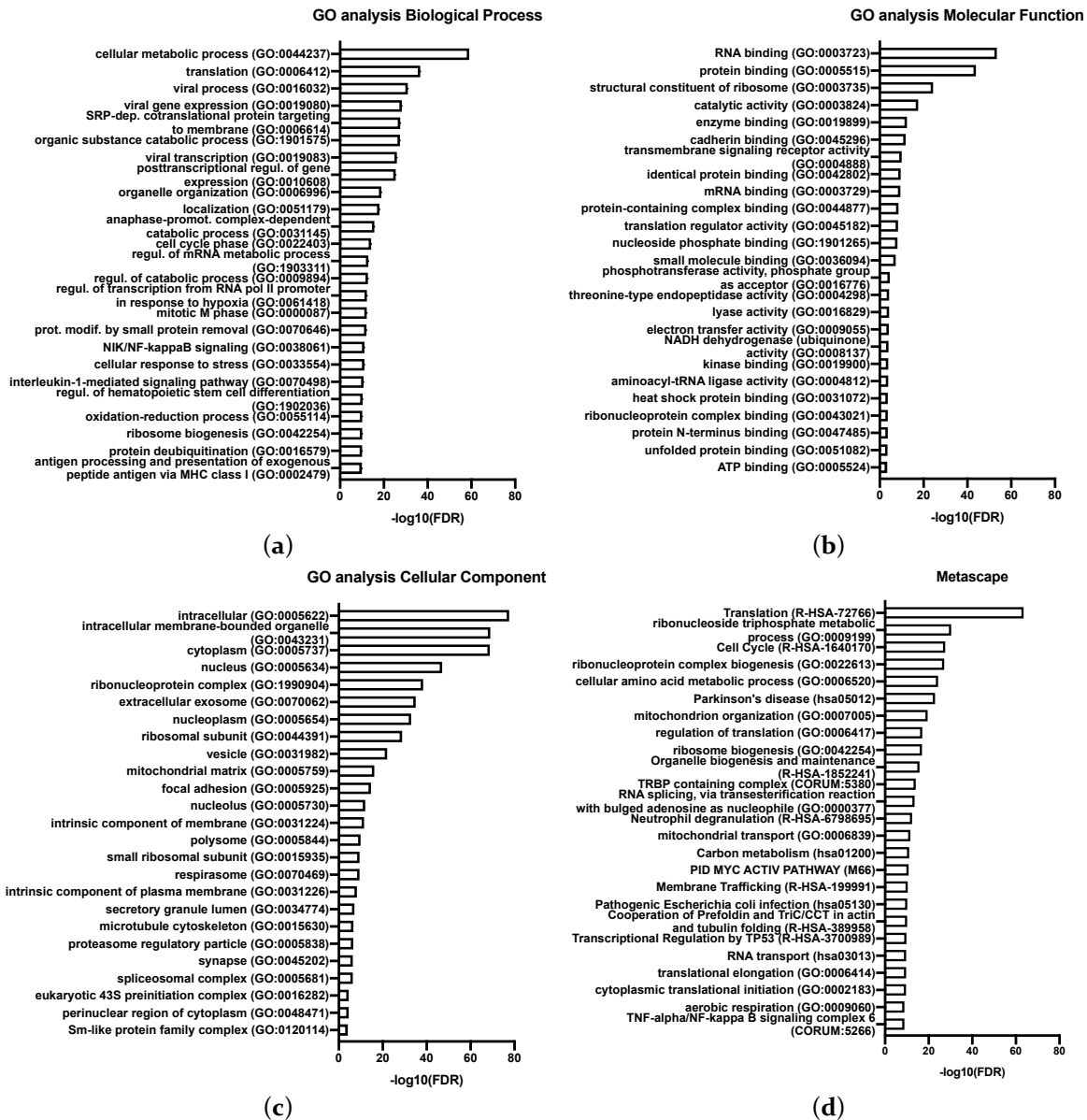


**Figure 7:** Gene ontology (GO) enrichment analysis in  $^{C92}EV_{SEC}$ , top 25 ontology terms. (a) GO, biological process, (b) GO, molecular function, (c) GO, cellular component, (d) Metascape. Only terms with an FDR < 0.01 were selected.

$^{C92}EV_{SEC}$  are enriched in genes involved in viral process, viral gene expression and viral transcription as seen in Figure 7a. The GO enrichment analysis for molecular function in Figure 7b reveals that many genes represented in EVs have a binding function such as RNA binding, protein binding and enzyme binding. Many intracellular components are abundantly found in  $^{C92}EV_{SEC}$  including intracellular membrane-bounded organelle and cytoplasm components, as well as genes associated with extracellular exosome (Figure 7c). Genes involved in DNA- and RNA-related functions are highly represented: RNA transport, viral transcription, regulation of mRNA metabolic process, transcription regulation activity, regulation of translation, etc. Other enriched genes are involved in immune system process and cellular response such as NIK/NF-kappaB signaling, anaphase-promoting complex-dependent catabolic process.

miRNAs are highly conserved, non-coding, small single-stranded RNA molecules and have the ability to regulate gene expression. They were also characterized in  $^{C92}EV_{SEC}$ . The 10 most abundant miRNAs found in  $^{C92}EV_{SEC}$  are shown in Figure 8.

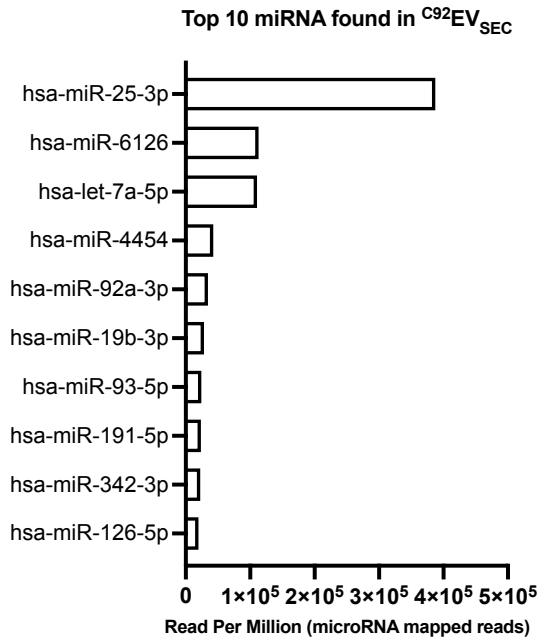


**Figure 8:** Top 10 miRNA found in  $C^{92}EV_{SEC}$ .

The most abundant miRNA found in  $C^{92}EV_{SEC}$  was hsa-miR-25-3p, with over 3 times more read per million than the next most abundant miRNA species hsa-miR-6126 and hsa-let-7a-5p.

### 3.2 Characterization of Clone 92 EVs during Lentiviral Particles Production

As previously indicated, it is not yet feasible to effectively separate EVs from LVs in a production process. In the second part of this study, we compared EVs from Clone 92 in absence of LV induction ( $C^{92}EV_{UC}$ ), and Clone 92 co-produced EVs following induction of LV production ( $C^{92}EV/LV_{UC}$ ). For consistency in the sample preparations, ultracentrifugation was used as described in Section 2.3.2.

### 3.2.1. Heterogeneity of EV and LV Populations

As flow virometry is based on GFP+ events, analysis can be performed directly on supernatant material.  $C^{92}EV_{sup}$  were therefore compared to  $C^{92}EV/LV_{sup}$  3 days post-induction (3 dpi). Results are shown in Figure 9.

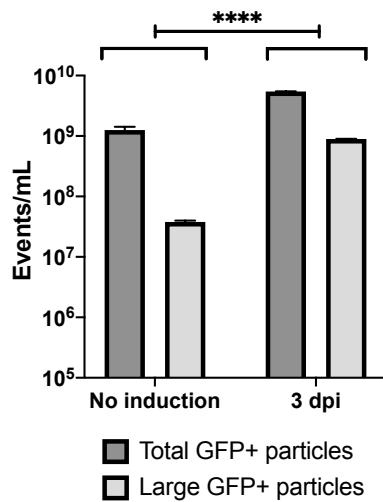


**Figure 9:** Comparison between Clone 92 supernatants with no induction and 3 days post-induction (3 dpi) by flow virometry: Quantification of flow virometry subpopulations of large particles and total GFP+ particles in each studied condition. Error bars indicate SEM. Significance is indicated by \*\*\*\* and is calculated via two-way ANOVA.

Using the same gating as in the first part of the study, total GFP+ events were higher in  $C^{92}EV/LV_{UC}$  3 dpi. Another population was additionally observed after induction (supplementary Figure S5, still fluorescent but larger in size. A third population which was not gated in Figure S5 would include non-fluorescent even larger particles. This population was also observed in some in-process samples without induction from Table 5, suggesting large particles with no GFP but their proportion could not be estimated due to their overlap with the noise.

$C^{92}EV_{UC}$  and  $C^{92}EV/LV_{UC}$  samples were analyzed by digital drop polymerase chain reaction (ddPCR) and gene transfer assay (GTA). Results are shown in Figure 10.

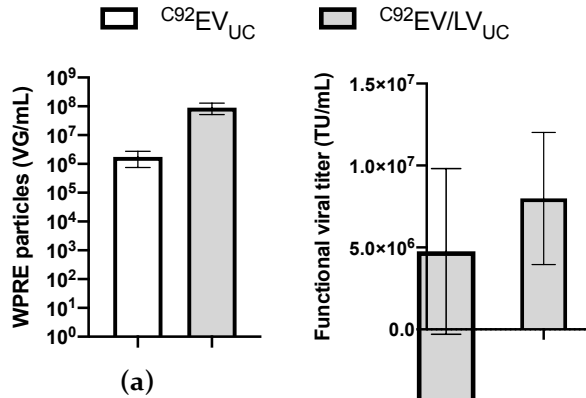


**Figure 10:** Comparison between  $C92EV_{UC}$  and  $C92EV/LV_{UC}$ . (a) Quantification of WPRE particles by ddPCR. (b) Quantification of functional viral titer by gene transfer assay (GTA). Error bars indicate SEM.

ddPCR allowed the quantification of particles containing the woodchuck hepatitis virus posttranscriptional regulatory element (WPRE). As seen on Figure 10a, both  $C92EV_{UC}$  and  $C92EV/LV_{UC}$  show a titer by ddPCR.  $C92EV/LV_{UC}$ 's titer is greater than  $C92EV_{UC}$ 's titer by two orders of magnitude.

GTA measures transgene expression (here GFP by flow cytometry) in transduced target cells to report functional viral vector particles. As in the first part of the study,  $C92EV_{UC}$  samples did not show any functional titer, confirming the absence of functional LVs particles when there is no induction.  $C92EV/LV_{UC}$  on the other hand confirmed the functionality of the produced LVs particles.

### 3.2.2. Protein Cargos of EVs and LVs have Common Features

$C92EV_{UC}$  and  $C92EV/LV_{UC}$  were also compared using MS. The samples contained protein markers from the MISEV 2018 guidelines: CD81 and PDCD61P were found to be present in  $C92EV_{UC}$  and  $C92EV/LV_{UC}$ . Additionally, prostaglandin F<sub>2</sub> receptor inhibitor (PTGFRN), a protein from the ExoCarta database was also found in both. CD9 was not identified in the samples, consistent with  $C92EV_{SEC}$  results. In addition, Calnexin and HSP90B1, common EVs

“negative markers”, were not identified in any of the samples, whether under inducing or non-inducing conditions. This suggests that either EVs are indeed recovered in  $C^{92}EV/LV_{UC}$  samples or that LVs package the same proteins as EVs. A total of 822 proteins were identified in  $C^{92}EV_{UC}$  and 1203 proteins were identified in  $C^{92}EV/LV_{UC}$ , with an overlap of about 48% as shown on Figure 11.

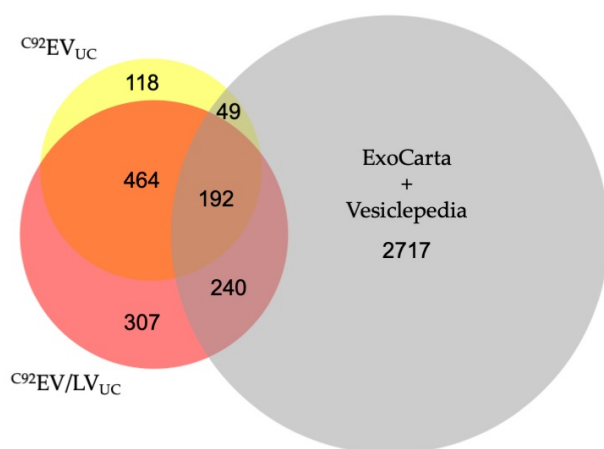


**Figure 11:** Area-proportional Venn diagram for the total number of identified proteins in  $C^{92}EV_{UC}$  and  $C^{92}EV/LV_{UC}$  within the combined Vesiclepedia and ExoCarta database.

Among all the identified proteins in  $C^{92}EV_{UC}$  and  $C^{92}EV/LV_{UC}$ , 167 were uniquely identified in  $C^{92}EV_{UC}$  and 548 were uniquely identified in  $C^{92}EV/LV_{UC}$  (Supplementary Table S1).

All identified proteins in  $C^{92}EV_{UC}$  and  $C^{92}EV/LV_{UC}$  were classified into 23 PANTHER protein classes (Table 7).

**Table 7:** Summary of protein classes identified in both  $^{C92}EV_{UC}$  and  $^{C92}EV/LV_{UC}$ , or only in either  $^{C92}EV_{UC}$  or  $^{C92}EV/LV_{UC}$ .

Category Name (Accession)	Protein Hits		
	Only in $^{C92}EV_{UC}$	Only in $^{C92}EV/LV_{UC}$	In both $^{C92}EV_{UC}$ and $^{C92}EV/LV_{UC}$
extracellular matrix protein (PC00102)	5	3	4
cytoskeletal protein (PC00085)	12	41	23
transporter (PC00227)	10	31	18
scaffold/adaptor protein (PC00226)	10	21	14
cell adhesion molecule (PC00069)	2	4	6
nucleic acid metabolism protein (PC00171)	10	57	31
intercellular signal molecule (PC00207)	1	6	3
protein-binding activity modulator (PC00095)	6	26	16
viral or transposable element protein (PC00237)	1	1	0
calcium-binding protein (PC00060)	1	5	5
gene-specific transcriptional regulator (PC00264)	11	24	14
defense/immunity protein (PC00090)	0	4	3
translational protein (PC00263)	4	55	20
metabolite interconversion enzyme (PC00262)	8	56	54
protein modifying enzyme (PC00260)	21	38	35
chromatin/chromatin-binding, or -regulatory protein (PC00077)	3	8	7
transfer/carrier protein (PC00219)	1	3	4
membrane traffic protein (PC00150)	1	13	13
chaperone (PC00072)	3	13	8
cell junction protein (PC00070)	0	2	0
structural protein (PC00211)	0	0	3
storage protein (PC00210)	0	0	1
transmembrane signal receptor (PC00197)	7	16	7

Metabolite interconversion enzymes and protein modifying enzymes were highly represented in all three categories (Table 7). Although also abundant in only  $^{C92}EV_{UC}$  and in both  $^{C92}EV_{UC}$  and  $^{C92}EV/LV_{UC}$ , nucleic acid metabolism proteins were even more

enriched in  $^{C92}EV/LV_{UC}$ . Translational proteins were abundantly found in  $^{C92}EV/LV_{UC}$  only and cytoskeletal proteins were dominant in the overlap population.

Additionally, GAG-POL and VSV-G was used to identify enrichment for LV particles. Both GAG-POL and VSV-G proteins were found to be significantly more enriched in samples after LV induction in  $^{C92}EV/LV_{UC}$  and below limits of detection/identification in  $^{C92}EV_{UC}$ .

GFP was identified in both  $^{C92}EV_{UC}$  and  $^{C92}EV/LV_{UC}$ . Lower level of GFP was seen in samples before induction.

### ***3.2.3. Phospholipid Content in EVs and LVs***

The phospholipid species were quantified by liquid chromatography-mass spectrometry (LC-MS) and compared between Clone 92 cells (cell pellet),  $^{C92}EV_{UC}$  and  $^{C92}EV/LV_{UC}$ . The identified phospholipids in  $^{C92}EV_{UC}$  and  $^{C92}EV/LV_{UC}$  were ranked by highest positive fold change to most negative fold change compared to the parent cells (Figure 12).

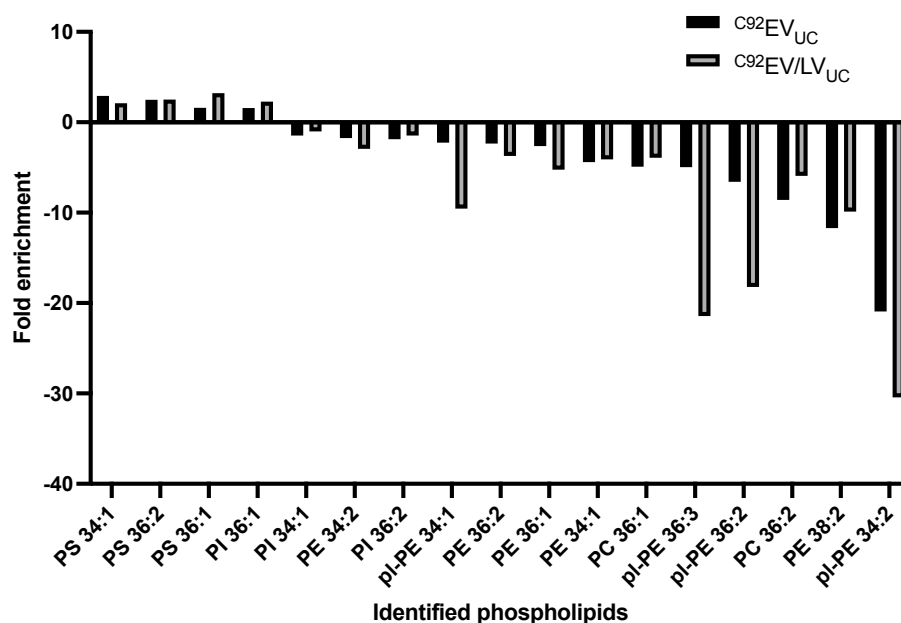


**Figure 12:** Phospholipids identified in Clone 92 EVs and LVs compared to Clone 92 parent cells. PS: phosphatidylserine, PI: phosphatidylinositol, PE: phosphatidylethanolamine, pl-PE: plasmalogen-phosphatidylethanolamine PC: phosphatidylcholine. Error bars indicate SEM.

Differences were not statistically significant, but some semi-quantitative observations are noted and could have biological implications.  $C^{92}EV_{UC}$  membranes and  $C^{92}EV/LV_{UC}$  membranes are enriched in the same PL compared to the cell membrane: phosphatidylserine (PS) 34:1, PS 36:2, PS 36:1 and phosphatidylinositol (PI) PI 36:1. Interestingly,  $C^{92}EV_{UC}$  and  $C^{92}EV/LV_{UC}$  are enriched and depleted in the same PL compared to their parent cell. Plasmalogen-PE (pl-PE) are 1.5 to almost 5 times more depleted in  $C^{92}EV/LV_{UC}$  than in  $C^{92}EV_{UC}$ .

#### 4. Discussion

EVs have gained a lot of attention in the past few years, as potential biomarkers and as drug delivery vehicles. Many studies have been carried out on EVs isolated from biofluids or even cultured cells. Yet, investigations do not report on EVs as secondary products in

viral vaccines or viral vectors productions. Most cell lines, especially mammalian cell lines, are known to release EVs and cell lines used as platform for biological products are no exception. The experiments completed in this study provide a comprehensive characterization of EVs produced in HEK293SF cell lines that are widely used in viral vectors and viral vaccines production. Enveloped viruses-based products including LVs are especially targeted here for their biophysical similarities to EVs as the preparations most certainly contain both EVs and viruses. To this end a large set of experiments has been done to characterize EVs associated with an inducible HEK293SF lentivirus producing cell line (Clone 92) cultured under non-induced conditions.

The characterization of EVs is greatly impacted by the isolation method (Van Deun et al., 2014). Herein a process was developed that would allow all selected analyses to be performed on one single batch of EVs for results consistency. The isolation method combining SEC and UF was selected for its scalability. Moreover, an additional advantage of developing a scalable process applicable to isolation of EVs associated with HEK293SF human cell line is the generalization of this process to multiple therapeutic products derived from the HEK293SF manufacturing platform. Indeed, EVs produced in HEK293SF cell cultures might be loaded with therapeutic cargos and used as drug delivery vehicles (Luan et al., 2017). EVs associated with the two cell lines HEK293SF and HEK293-derived lentivirus producing cell, Clone 92 cultures were investigated. Since no significant differences were found between EVs isolated from the two cell lines and because of the intrinsic GFP labeling property of Clone 92 allowing for flow virometry measurements, these studies focused on Clone 92.

EVs reported in the literature have different cellular origins and therefore no definite markers of populations have been identified. Enriched proteins are, however, observed. In this study, although we did not discriminate between exosomes and microvesicles, only enriched proteins associated with exosomes were considered for identification. Additionally, the study focused on EVs co-produced with enveloped virus products, more specifically lentiviral vectors, consequently the size of the particles observed ranged from 80 to 100 nm, which mainly corresponds to the size of exosomes and only small microvesicles.

Other orthogonal methods are available for EV and LV quantification. However, significant discrepancies in absolute values with other techniques should be expected. For example, nanoparticle tracking analysis (NTA) is based on the Brownian motion of particles in suspension and is used to determine the size distribution of purified EVs (Soo et al., 2012) and for quantification (van der Pol et al., 2010). This method lacks specificity and often leads to overestimation of the total particles measured. A method for in-process LV quantification was recently published (Transfiguracion et al., 2020) involving High-Performance Liquid Chromatography (HPLC). Although the authors optimized the method for minimizing the impact of EVs, they did acknowledge the presence of EVs in the quantification of LV particles and their proportion could not be estimated since the measure of a sample with no LV particles falls outside of the claimed linear range of the method.

The different methods used in this study highlight different features of EVs. Flow virometry results reflect the presence of GFP in <sup>C92</sup>EVs. As reported, the GFP+ analysis

would be a better estimate of the total particles. However, it is likely that intermediate populations that do not carry GFP or have slightly different size or granularity are excluded. Moreover, this quantification method is applicable to  $^{C92}$ EVs because of the fluorescence detection and is not applicable to EVs that do not carry GFP due to the challenges associated with signal detection which does not allow differentiating EVs from the signal background in the flow cytometer analyses. ddPCR analysis targeted WPRE as a probe. Indeed, as mentioned before, the GFP transgene and therefore the WPRE element which ensures high level transgene expression, are expressed constitutively. The quantification of WPRE therefore indicates the presence of the transgene, usually referred as “viral genome” when dealing with LVs particles. ddPCR results revealed that the “viral genome” is being incorporated in a fraction of EVs, although no viral protein or viral activity is present in EVs based on the proteomic and GTA analysis. This observation might be of interest for the design and development of therapeutic EVs for delivery of specific nucleic acid cargos. The results by flow virometry differ from the ddPCR data by at least 3 orders of magnitude in  $^{C92}EV_{SEC}$  suggesting that all EVs do not incorporate the “viral genome” sequences. The GTA and ddPCR data in LVs also reveals a difference. Indeed, the functional viral titer is lower than the VG titer as previously documented in Transfiguracion et al. (Transfiguracion et al., 2020). This underlines the difficulty in assessing absolute quantification of EVs and LVs, but it also underlines the heterogeneous nature of EVs and LVs. In that respect, EVs and LVs are not unique populations but rather a broad distribution of populations that incorporate different cellular components. Here, the results suggest that Clone 92 LV preparations are at least composed of EVs which have incorporated the “viral genome”, EVs

which do not have the “viral genome”, LVs with the viral genome but are not functional, and fully functional LV particles.

Proteomic results of  $^{C92}EV_{SEC}$  showed that GFP was indeed detected in these EVs; however, no HIV proteins were found. Although Gag-Pol is under a constitutive promoter, Rev, which is tightly regulated by the cumate switch in the design of Clone 92 (Broussau et al., 2008; Manceur et al., 2017), induction is required for Gag efficient expression. Thus, HIV proteins are not expected to be found in Clone 92 EVs when there is no induction by cumate and doxycycline. Results confirm here the tight regulation from the switches. Proteomic analyses of Clone 92 EVs not only confirmed EVs identity, thus validating the isolation process, but they also revealed the presence of proteins commonly found in EV databases. In fact, 47 of the top 50 proteins (Figure 5a) are known markers of EVs. These markers were also used to confirm the isolation of EVs in  $^{C92}EV_{UC}$  and  $^{C92}EV/LV_{UC}$ . The absence of cellular markers CANX, HSP90B1 and HSPA5 in the two EV populations has also demonstrated EV enrichment. Nineteen proteins of interest have been identified that are common between the  $^{C92}EV_{SEC}$ ,  $^{C92}EV_{UC}$  and  $^{C92}EV/LV_{UC}$ : FASN (fatty acid synthase), MFGE8 (lactadherin), PDCD6IP (programmed cell death 6-interacting protein), CD81 (CD81 antigen), PTGFRN (prostaglandin F<sub>2</sub> receptor negative regulator), EZR (ezrin), ATP1A1 (sodium/potassium-transporting ATPase subunit alpha-1), YWHAQ (14-3-3 protein theta), GNB1 (guanine nucleotide binding protein G(I)/G(S)/G(T) subunit beta-1), RHOA (transforming protein RhoA), ITGB1 (integrin beta-1), MSN (moesin), YWHAG (14-3-3 protein gamma), YWHAE (14-3-3 protein epsilon), BSG (basigin), CCT2 (T-complex protein 1 subunit beta), SLC16A1 (monocarboxylate transporter 1), YWHAZ (14-3-3 protein zeta/delta), and RAC1 (ras-related

C3 botulinum toxin substrate 1). These proteins have been previously identified as exosome markers in ExoCarta, which further supports their use as indicators of the presence of EVs. All nineteen of these proteins are enriched in  $^{C92}EV_{SEC}$  when compared to the Clone 92 cells and supernatant (Figure 5a). The five proteins FASN, MFGE8, PDCD6IP, CD81 and PTGFRN are found to be about equally enriched in both  $^{C92}EV_{UC}$  and  $^{C92}EV/LV_{UC}$  samples. The remaining fourteen proteins are found to be significantly enriched in the  $^{C92}EV/LV_{UC}$  when compared to  $^{C92}EV_{UC}$ . This could indicate that these proteins are also present in LV particles, or there are more EVs containing these proteins being produced during LV induction as well. Future work in separating EV and LV populations will help to confirm these markers. More proteins enriched in EVs compared to the conditioned medium and parental cells were also identified (Figure 5) and could be additional potential new markers for  $^{C92}EVs$ , such as Midkine (MDK in Figure 5a), a secreted protein that regulates multiple biological processes including cell proliferation, cell adhesion, cell growth, cell survival, and cell migration (Sakaguchi et al., 2003).

Discrepancies between proteins identified in  $^{C92}EV_{SEC}$  and  $^{C92}EV_{UC}$  were observed. Only 108 proteins (~11%) overlapped between  $^{C92}EV_{SEC}$  and  $^{C92}EV_{UC}$ . The lack of overlap is likely due to the difference in the EV isolation methods underlining again the importance of this step. The high percentage of protein overlap (~48%) in  $^{C92}EV_{UC}$  and  $^{C92}EV/LV_{UC}$  reinforces the observation that EVs and LVs have a lot of common features.

Interestingly, a number of proteins identified in  $^{C92}EV/LV_{UC}$  were previously reported to be associated with HIV-1 virus, including EEF1A1, a translational protein (Zhao, Azam, & Thorpe, 2005), NONO, a nucleic acid metabolism protein (Zolotukhin et al., 2003),

GAPDH, a metabolite interconversion enzyme (Saphire, Gally, & Bark, 2006), PPIA, a protein involved in host-virus interaction (Thali et al., 1994). NONO, GAPDH and PPIA were also found in  $^{C92}EV_{UC}$  thus indicating once again the similarities between EVs and LVs. The large number of cytoskeletal proteins in both  $^{C92}EV_{UC}$  and  $^{C92}EV/LV_{UC}$  was expected as cytoskeletal proteins have been implicated in virus transport and release (Sasaki et al., 1995), indicating that the budding mechanism of both LV and EV rely on cytoskeletal proteins for the translocation process.

Lipid composition of EVs has mainly been described in biological fluids but not in EVs associated with HEK292SF cell cultures (Skotland, Sandvig, & Llorente, 2017)..  $^{C92}EV_{UC}$  and  $^{C92}EV/LV_{UC}$  share a similar lipid composition, with an enrichment in phosphatidylserine as compared to the parental cells, consistent with the findings of other studies (Kreimer et al., 2015).  $^{C92}EV_{UC}$  and  $^{C92}EV/LV_{UC}$  also contained less phosphatidylcholine and phosphatidylethanolamine than their parental cells. It has been reported that the change in distribution of these lipids was involved in the budding of microvesicles (Hugel, Martínez, Kunzelmann, & Freyssinet, 2005). Sphingolipid and cholesterol analysis in LVs/EVs samples would be a good addition to this lipidomic characterization to confirm enrichment in ceramide and cholesterol in EVs and LVs as reported in these studies on lipids involved in the budding process (Bianco et al., 2009; Kreimer et al., 2015). The higher depletion of plasmalogen-PE in  $^{C92}EV/LV_{UC}$  compared to  $^{C92}EV_{UC}$  might be interesting to further study as pl-PE could play an important role in membrane dynamics and intracellular signaling (Nagan & Zoeller, 2001). Discrepancies in the lipidomic profiles observed between  $^{C92}EV_{SEC}$  and  $^{C92}EV_{UC}$  is again likely due to the difference in the EV

isolation methods. Techniques for studying lipids should also be further improved to quantify more accurately lipid species, which could conduct to identifying lipid markers for Clone 92 EVs or LVs.

DNA quantification is of importance especially when it comes to biologics and viral vectors and vaccines particularly because of the stringent regulation. In the field of EVs, DNA identification is often investigated with the perspective of using them as biomarkers. Additional DNA sequencing can be expected in the future.  $^{C92}$ EV cargoes also revealed different types of RNA, including miRNA. The gene ontology analyses of  $^{C92}$ EV<sub>SEC</sub> confirmed the main components and functions attributed to EVs. For instance, the abundance of genes with binding functions can explain a mechanism of cargo sorting by which RNAs will interact with specific proteins to be packaged into EVs for cell-to-cell transport. The enrichment in genes involved in viral process, viral gene expression and viral transcription can be linked to the fact that EVs and some viruses including retroviruses share the same biogenesis pathways, including the ESCRT-dependant pathway. miRNAs are highly conserved, non-coding, small single-stranded RNA molecules and have the ability to regulate gene expression. They are also involved in diseases mechanisms and have been previously identified in EVs (Valadi et al., 2007). It was therefore critical to characterize them in  $^{C92}$ EV<sub>SEC</sub>. Most miRNA found in  $^{C92}$ EV<sub>SEC</sub> were also found in biofluids (Momen-Heravi, Getting, & Moschos, 2018). The most abundant miRNAs identified in  $^{C92}$ EV<sub>SEC</sub> (Figure 8) play a role in all sort of diseases: miR-25-3p and miR-93-5p in gastric cancer (Li et al., 2018; Ning et al., 2020), miR-19b-3p and let-7a-5p in colon cancer (Ghanbari et al., 2016; Jiang et al., 2017). Multiple cancers showed abnormal expression of miR-92a-3p

while ovarian cancer cells are suggested to release exosomes containing miR-6126 abundantly (Cun & Yang, 2018; Kanlikilicer et al., 2016). Some miRNAs found in  $C^{92}EV_{SEC}$  may have a positive regulating role, such as miR-93-5p in glioma or myocardial damage (J. Liu et al., 2018; Wu, Liu, & Zhu, 2019), miR-191-5p in lung cancer (L. Y. Zhou, Zhang, Tong, & Liu, 2020), or miR-342-3p in liver cancer (W. Liu et al., 2018). Although it has been suggested that miRNAs are packaged into EVs as a way to dispose of excessive miRNAs, the TRBP containing complex, a member of the RNA-induced silencing complex (RISC) involved in RNA silencing (Haase et al., 2005) is also enriched in  $C^{92}EV_{SEC}$ . So not only do  $C^{92}EVs$  contain miRNA but they could also provide recipient cells with the miRNA processing machinery which is needed to process those miRNAs (Chendrimada et al., 2005). More studies on miRNA uptake from EVs should be conducted. Until then, the effect of miRNA on recipient cells cannot be excluded given the role of miRNAs in a number of diseases.

The fact that EVs share biogenesis pathways and biophysical properties with viral products produced in cell culture platforms such as lentiviral vectors produced in HEK293SF cells and derived cell lines, supports the need to characterize host cell EVs. As discussed above, the production of viral products will induce changes to EVs. In the context of cell and gene therapy, for future in vivo gene delivery of LVs, it will be critical to further investigate EV changes and the subsequent intermediate populations upon virus production to determine accurately the product profile and specifications. The effect of co-purified EVs in LV preparations on recipient cells also needs to be evaluated. Indeed, if EVs

are proven to be safe, as an associated component to enveloped viral vectors and viral vaccines, they might also have a possible adjuvanting role in the vaccine formulation.

## Supplementary materials

The following are available online at <https://www.mdpi.com/article/10.3390/v13050797/s1>, Figure S1: Analysis of Clone 92 supernatant by flow virometry, Figure S2: Flow virometry density plots showing size (violet side scatter) and green fluorescence (GFP) in the negative control PBS and an in-process Clone 92 sample (here supernatant at a dilution factor of 100), Figure S3: Enrichment of EVs shown by the increase in signal for CD81, BSG, and PDCD6IP and the depletion of cellular protein in EVs shown by a decrease in signal for HSPA5 and HSP90B1 compared to parent cells, Figure S4: Presence of GFP in cells, supernatant and EVs from Clone 92, Figure S5: Flow virometry density plots showing size (violet side scatter) and green fluorescence (GFP) in the negative control PBS and in Clone 92 supernatants, Table S1: List of all proteins identified in <sup>C92</sup>EV<sub>UC</sub> and <sup>C92</sup>EV/LV<sub>UC</sub> with a Mascot score >30 and more than 1 peptide.

## Author Contributions

Conceptualization, A.D.M. and A.A.K.; Methodology, A.D.M., A.T.S., J.S., K.M.F., S.M.T. and A.A.K.; Investigation, A.D.M., A.T.S. and J.S., Data Curation, A.S.H., Writing—Original Draft, A.D.M. and A.T.S.; Writing—Review and Editing, J.-F.G., K.M.F., J.L., S.M.T. and A.A.K.; Funding Acquisition, A.D.M., S.M.T. and A.A.K.; Resources, S.M.T., J.L. and A.A.K.;

and Supervision A.A.K. All authors have read and agreed to the published version of the manuscript.

## **Funding**

A.D.M. is funded by a Natural Sciences and Engineering Research Council of Canada (NSERC) doctoral scholarship. A.A.K. is a recipient of a Canada Research Chair (CRC/240394) of government of Canada.

## **Acknowledgements**

We would like to thank Xavier Elisseeff and Alice Bernier for their help with some EV isolations. We also thank Marie-Angélique Sené and David Sharon for their input in processing transcriptomics data. We would like to acknowledge Sam Williamson, and Luc Tessier for their help with mass spectrometry set-up at NRC, and Simon Foote for the data-file conversion pipeline for submission to Mascot.

## **Conflicts of Interest**

The authors declare no conflict of interest. The funders had no role in the design of the study; in the collection, analyses, or interpretation of data; in the writing of the manuscript, or in the decision to publish the results.

## References

- Ansorge, S., Lanthier, S., Transfiguracion, J., Durocher, Y., Henry, O., & Kamen, A. (2009). Development of a scalable process for high-yield lentiviral vector production by transient transfection of HEK293 suspension cultures. *Journal of Gene Medicine*, 11(10), 868-876. doi:10.1002/jgm.1370
- Ashburner, M., Ball, C. A., Blake, J. A., Botstein, D., Butler, H., Cherry, J. M., . . . Sherlock, G. (2000). Gene ontology: tool for the unification of biology. The Gene Ontology Consortium. *Nat Genet*, 25(1), 25-29. doi:10.1038/75556
- Bianco, F., Perrotta, C., Novellino, L., Francolini, M., Riganti, L., Menna, E., . . . Verderio, C. (2009). Acid sphingomyelinase activity triggers microparticle release from glial cells. *EMBO Journal*, 28(8), 1043-1054. doi:10.1038/emboj.2009.45
- Broussau, S., Jabbour, N., Lachapelle, G., Durocher, Y., Tom, R., Transfiguracion, J., . . . Massie, B. (2008). Inducible packaging cells for large-scale production of lentiviral vectors in serum-free suspension culture. *Mol Ther*, 16(3), 500-507. doi:10.1038/sj.mt.6300383
- Cantin, R., Diou, J., Belanger, D., Tremblay, A. M., & Gilbert, C. (2008). Discrimination between exosomes and HIV-1: Purification of both vesicles from cell-free supernatants. *Journal of Immunological Methods*, 338(1-2), 21-30. doi:10.1016/j.jim.2008.07.007
- Chambers, M. C., Maclean, B., Burke, R., Amodei, D., Ruderman, D. L., Neumann, S., . . . Mallick, P. (2012). A cross-platform toolkit for mass spectrometry and proteomics. *Nature Biotechnology*, 30(10), 918-920. doi:10.1038/nbt.2377

- Chendrimada, T. P., Gregory, R. I., Kumaraswamy, E., Norman, J., Cooch, N., Nishikura, K., & Shiekhattar, R. (2005). TRBP recruits the Dicer complex to Ago2 for microRNA processing and gene silencing. *Nature*, 436(7051), 740-744. doi:10.1038/nature03868
- Cote, J., Garnier, A., Massie, B., & Kamen, A. (1998). Serum-free production of recombinant proteins and adenoviral vectors by 293SF-3F6 cells. *Biotechnology and Bioengineering*, 59(5), 567-575.
- Cun, J., & Yang, Q. (2018). Bioinformatics-based interaction analysis of miR-92a-3p and key genes in tamoxifen-resistant breast cancer cells. *Biomed Pharmacother*, 107, 117-128. doi:10.1016/j.biopha.2018.07.158
- Do Minh, A., Tran, M. Y., & Kamen, A. A. (2020). Lentiviral Vector Production in Suspension Culture Using Serum-Free Medium for the Transduction of CAR-T Cells. *Methods Mol Biol*, 2086, 77-83. doi:10.1007/978-1-0716-0146-4\_6
- Escors, D., & Breckpot, K. (2010). Lentiviral vectors in gene therapy: their current status and future potential. *Arch Immunol Ther Exp (Warsz)*, 58(2), 107-119. doi:10.1007/s00005-010-0063-4
- Fahy, E., Subramaniam, S., Murphy, R. C., Nishijima, M., Raetz, C. R. H., Shimizu, T., . . . Dennis, E. A. (2009). Update of the LIPID MAPS comprehensive classification system for lipids. *Journal of Lipid Research*, 50 Suppl(Suppl), S9-S14. doi:10.1194/jlr.R800095-JLR200
- The Gene Ontology Resource: 20 years and still GOing strong. (2019). *Nucleic Acids Res*, 47(D1), D330-d338. doi:10.1093/nar/gky1055

- Ghanbari, R., Mosakhani, N., Sarhadi, V. K., Armengol, G., Nouraei, N., Mohammadkhani, A., . . . Knuutila, S. (2016). Simultaneous Underexpression of let-7a-5p and let-7f-5p microRNAs in Plasma and Stool Samples from Early Stage Colorectal Carcinoma. *Biomarkers in cancer*, 7(Suppl 1), 39-48. doi:10.4137/BIC.S25252
- Graham, F. L., Smiley, J., Russell, W. C., & Nairn, R. (1977). Characteristics of a human cell line transformed by DNA from human adenovirus type 5. *J Gen Virol*, 36(1), 59-74. doi:10.1099/0022-1317-36-1-59
- Haase, A. D., Jaskiewicz, L., Zhang, H., Laine, S., Sack, R., Gatignol, A., & Filipowicz, W. (2005). TRBP, a regulator of cellular PKR and HIV-1 virus expression, interacts with Dicer and functions in RNA silencing. *EMBO Rep*, 6(10), 961-967. doi:10.1038/sj.embor.7400509
- Haqqani, A. S., Kelly, J. F., & Stanimirovic, D. B. (2008). Quantitative protein profiling by mass spectrometry using label-free proteomics. *Methods Mol Biol*, 439, 241-256. doi:10.1007/978-1-59745-188-8\_17
- Hessvik, N. P., & Llorente, A. (2017). Current knowledge on exosome biogenesis and release. *Cell Mol Life Sci*. doi:10.1007/s00018-017-2595-9
- Hugel, B., Martínez, M. C., Kunzelmann, C., & Freyssinet, J. M. (2005). Membrane microparticles: two sides of the coin. *Physiology (Bethesda)*, 20, 22-27. doi:10.1152/physiol.00029.2004
- Hulsen, T., de Vlieg, J., & Alkema, W. (2008). BioVenn – a web application for the comparison and visualization of biological lists using area-proportional Venn diagrams. *BMC Genomics*, 9(1), 488. doi:10.1186/1471-2164-9-488

- Izquierdo-Useros, N., Puertas, M. C., Borràs, F. E., Blanco, J., & Martinez-Picado, J. (2011). Exosomes and retroviruses: The chicken or the egg? *Cellular Microbiology*, 13(1), 10-17. doi:10.1111/j.1462-5822.2010.01542.x
- Jiang, T., Ye, L., Han, Z., Liu, Y., Yang, Y., Peng, Z., & Fan, J. (2017). miR-19b-3p promotes colon cancer proliferation and oxaliplatin-based chemoresistance by targeting SMAD4: validation by bioinformatics and experimental analyses. *J Exp Clin Cancer Res*, 36(1), 131. doi:10.1186/s13046-017-0602-5
- Kalra, H., Simpson, R. J., Ji, H., Aikawa, E., Altevogt, P., Askenase, P., . . . Mathivanan, S. (2012). Vesiclepedia: A Compendium for Extracellular Vesicles with Continuous Community Annotation. *PLoS Biology*, 10(12), e1001450. doi:10.1371/journal.pbio.1001450
- Kanlikilicer, P., Rashed, M. H., Bayraktar, R., Mitra, R., Ivan, C., Aslan, B., . . . Lopez-Berestein, G. (2016). Ubiquitous Release of Exosomal Tumor Suppressor miR-6126 from Ovarian Cancer Cells. *Cancer Res*, 76(24), 7194-7207. doi:10.1158/0008-5472.Can-16-0714
- Keerthikumar, S., Chisanga, D., Ariyaratne, D., Al Saffar, H., Anand, S., Zhao, K., . . . Mathivanan, S. (2016). ExoCarta: A Web-Based Compendium of Exosomal Cargo. *Journal of Molecular Biology*, 428(4), 688-692. doi:https://doi.org/10.1016/j.jmb.2015.09.019
- Konadu, K. A., Huang, M. B., Roth, W., Armstrong, W., Powell, M., Villinger, F., & Bond, V. (2016). Isolation of Exosomes from the Plasma of HIV-1 Positive Individuals. *J Vis Exp*(107). doi:10.3791/53495

- Kreimer, S., Belov, A. M., Ghiran, I., Murthy, S. K., Frank, D. A., & Ivanov, A. R. (2015). Mass-spectrometry-based molecular characterization of extracellular vesicles: lipidomics and proteomics. *J Proteome Res*, 14(6), 2367-2384. doi:10.1021/pr501279t
- Lasser, C., They, C., Buzas, E. I., Mathivanan, S., Zhao, W., Gho, Y. S., & Lotvall, J. (2016). The International Society for Extracellular Vesicles launches the first massive open online course on extracellular vesicles. *J Extracell Vesicles*, 5, 34299. doi:10.3402/jev.v5.34299
- Lavado-García, J., González-Domínguez, I., Cervera, L., Jorge, I., Vázquez, J., & Gòdia, F. (2020). Molecular Characterization of the Coproduced Extracellular Vesicles in HEK293 during Virus-Like Particle Production. *J Proteome Res*. doi:10.1021/acs.jproteome.0c00581
- Li, L., Zhao, J., Huang, S., Wang, Y., Zhu, L., Cao, Y., . . . Deng, J. (2018). MiR-93-5p promotes gastric cancer-cell progression via inactivation of the Hippo signaling pathway. *Gene*, 641, 240-247. doi:10.1016/j.gene.2017.09.071
- Liu, J., Jiang, M., Deng, S., Lu, J., Huang, H., Zhang, Y., . . . Wang, H. (2018). miR-93-5p-Containing Exosomes Treatment Attenuates Acute Myocardial Infarction-Induced Myocardial Damage. *Mol Ther Nucleic Acids*, 11, 103-115. doi:10.1016/j.omtn.2018.01.010
- Liu, W., Kang, L., Han, J., Wang, Y., Shen, C., Yan, Z., . . . Zhao, C. (2018). miR-342-3p suppresses hepatocellular carcinoma proliferation through inhibition of IGF-1R-mediated Warburg effect. *Onco Targets Ther*, 11, 1643-1653. doi:10.2147/ott.S161586

- Lobb, R. J., Becker, M., Wen Wen, S., Wong, C. S. F., Wiegmans, A. P., Leimgruber, A., & Möller, A. (2015). Optimized exosome isolation protocol for cell culture supernatant and human plasma. *J Extracell Vesicles*, 4(1), 27031. doi:10.3402/jev.v4.27031
- Luan, X., Sansanaphongpricha, K., Myers, I., Chen, H., Yuan, H., & Sun, D. (2017). Engineering exosomes as refined biological nanoplatfroms for drug delivery. *Acta Pharmacologica Sinica*, 38(6), 754-763. doi:10.1038/aps.2017.12
- Manceur, A. P., Kim, H., Misic, V., Andreev, N., Dorion-Thibaudeau, J., Lanthier, S., . . . Ansoerge, S. (2017). Scalable lentiviral vector production using stable HEK293SF producer cell lines. *Hum Gene Ther Methods*. doi:10.1089/hgtb.2017.086
- Mathivanan, S., & Simpson, R. J. (2009). ExoCarta: A compendium of exosomal proteins and RNA. *Proteomics*, 9(21), 4997-5000. doi:10.1002/pmic.200900351
- Merten, O. W., Hebben, M., & Bovolenta, C. (2016). Production of lentiviral vectors. *Mol Ther Methods Clin Dev*, 3, 16017. doi:10.1038/mtm.2016.17
- Mi, H., Ebert, D., Muruganujan, A., Mills, C., Albou, L.-P., Mushayamaha, T., & Thomas, P. D. (2020). PANTHER version 16: a revised family classification, tree-based classification tool, enhancer regions and extensive API. *Nucleic Acids Research*, 49(D1), D394-D403. doi:10.1093/nar/gkaa1106
- Mi, H., Muruganujan, A., Ebert, D., Huang, X., & Thomas, P. D. (2019). PANTHER version 14: more genomes, a new PANTHER GO-slim and improvements in enrichment analysis tools. *Nucleic Acids Res*, 47(D1), D419-d426. doi:10.1093/nar/gky1038

- Momen-Heravi, F., Getting, S. J., & Moschos, S. A. (2018). Extracellular vesicles and their nucleic acids for biomarker discovery. *Pharmacology & Therapeutics*. doi:<https://doi.org/10.1016/j.pharmthera.2018.08.002>
- Morales-Kastresana, A., Telford, B., Musich, T. A., McKinnon, K., Clayborne, C., Braig, Z., . . . Jones, J. C. (2017). Labeling Extracellular Vesicles for Nanoscale Flow Cytometry. *Scientific Reports*, 7(1), 1878. doi:[10.1038/s41598-017-01731-2](https://doi.org/10.1038/s41598-017-01731-2)
- Nagan, N., & Zoeller, R. A. (2001). Plasmalogens: biosynthesis and functions. *Progress in Lipid Research*, 40(3), 199-229. doi:[https://doi.org/10.1016/S0163-7827\(01\)00003-0](https://doi.org/10.1016/S0163-7827(01)00003-0)
- Naldini, L. (2015). Gene therapy returns to centre stage. *Nature*, 526(7573), 351-360. doi:[10.1038/nature15818](https://doi.org/10.1038/nature15818)
- Ning, L., Zhang, M., Zhu, Q., Hao, F., Shen, W., & Chen, D. (2020). miR-25-3p inhibition impairs tumorigenesis and invasion in gastric cancer cells in vitro and in vivo. *Bioengineered*, 11(1), 81-90. doi:[10.1080/21655979.2019.1710924](https://doi.org/10.1080/21655979.2019.1710924)
- Nolte-'t Hoen, E., Cremer, T., Gallo, R. C., & Margolis, L. B. (2016). Extracellular vesicles and viruses: Are they close relatives? *Proc Natl Acad Sci U S A*, 113(33), 9155-9161. doi:[10.1073/pnas.1605146113](https://doi.org/10.1073/pnas.1605146113)
- Nordin, J. Z., Lee, Y., Vader, P., Mäger, I., Johansson, H. J., Heusermann, W., . . . Andaloussi, S. E. L. (2015). Ultrafiltration with size-exclusion liquid chromatography for high yield isolation of extracellular vesicles preserving intact biophysical and functional properties. *Nanomedicine: Nanotechnology, Biology and Medicine*, 11(4), 879-883. doi:<https://doi.org/10.1016/j.nano.2015.01.003>

- Pathan, M., Fonseka, P., Chitti, S. V., Kang, T., Sanwlani, R., Van Deun, J., . . . Mathivanan, S. (2018). Vesiclepedia 2019: a compendium of RNA, proteins, lipids and metabolites in extracellular vesicles. *Nucleic Acids Res.* doi:10.1093/nar/gky1029
- Perkins, D. N., Pappin, D. J. C., Creasy, D. M., & Cottrell, J. S. (1999). Probability-based protein identification by searching sequence databases using mass spectrometry data. *Electrophoresis*, 20(18), 3551-3567. doi:10.1002/(sici)1522-2683(19991201)20:18<3551::Aid-elps3551>3.0.Co;2-2
- Pertea, M., Kim, D., Pertea, G. M., Leek, J. T., & Salzberg, S. L. (2016). Transcript-level expression analysis of RNA-seq experiments with HISAT, StringTie and Ballgown. *Nat Protoc*, 11(9), 1650-1667. doi:10.1038/nprot.2016.095
- Pospichalova, V., Svoboda, J., Dave, Z., Kotrbova, A., Kaiser, K., Klemova, D., . . . Bryja, V. (2015). Simplified protocol for flow cytometry analysis of fluorescently labeled exosomes and microvesicles using dedicated flow cytometer. *J Extracell Vesicles*, 4, 25530. doi:10.3402/jev.v4.25530
- Raposo, G., & Stoorvogel, W. (2013). Extracellular vesicles: Exosomes, microvesicles, and friends. *The Journal of Cell Biology*, 200(4), 373-383. doi:10.1083/jcb.201211138
- Sakaguchi, N., Muramatsu, H., Ichihara-Tanaka, K., Maeda, N., Noda, M., Yamamoto, T., . . . Muramatsu, T. (2003). Receptor-type protein tyrosine phosphatase zeta as a component of the signaling receptor complex for midkine-dependent survival of embryonic neurons. *Neurosci Res*, 45(2), 219-224. doi:10.1016/s0168-0102(02)00226-2
- Saphire, A. C., Gallay, P. A., & Bark, S. J. (2006). Proteomic analysis of human immunodeficiency virus using liquid chromatography/tandem mass spectrometry

- effectively distinguishes specific incorporated host proteins. *J Proteome Res*, 5(3), 530-538. doi:10.1021/pro50276b
- Sasaki, H., Nakamura, M., Ohno, T., Matsuda, Y., Yuda, Y., & Nonomura, Y. (1995). Myosin-actin interaction plays an important role in human immunodeficiency virus type 1 release from host cells. *Proceedings of the National Academy of Sciences*, 92(6), 2026-2030. doi:10.1073/pnas.92.6.2026
- Schweizer, M., & Merten, O. W. (2010). Large-scale production means for the manufacturing of lentiviral vectors. *Current Gene Therapy*, 10(6), 474-486.
- Sharon, D., & Kamen, A. (2017). Advancements in the design and scalable production of viral gene transfer vectors. *Biotechnol Bioeng*. doi:10.1002/bit.26461
- Skotland, T., Sandvig, K., & Llorente, A. (2017). Lipids in exosomes: Current knowledge and the way forward. *Progress in Lipid Research*, 66, 30-41. doi:https://doi.org/10.1016/j.plipres.2017.03.001
- Soo, C. Y., Song, Y., Zheng, Y., Campbell, E. C., Riches, A. C., Gunn-Moore, F., & Powis, S. J. (2012). Nanoparticle tracking analysis monitors microvesicle and exosome secretion from immune cells. *Immunology*, 136(2), 192-197. doi:10.1111/j.1365-2567.2012.03569.x
- Sud, M., Fahy, E., & Subramaniam, S. (2012). Template-based combinatorial enumeration of virtual compound libraries for lipids. *Journal of Cheminformatics*, 4(1), 23. doi:10.1186/1758-2946-4-23
- Tang, V. A., Renner, T. M., Fritzsche, A. K., Burger, D., & Langlois, M. A. (2017). Single-Particle Discrimination of Retroviruses from Extracellular Vesicles by Nanoscale Flow Cytometry. *Sci Rep*, 7(1), 17769. doi:10.1038/s41598-017-18227-8

- Thali, M., Bukovsky, A., Kondo, E., Rosenwirth, B., Walsh, C. T., Sodroski, J., & Göttlinger, H. G. (1994). Functional association of cyclophilin A with HIV-1 virions. *Nature*, 372(6504), 363-365. doi:10.1038/372363a0
- The UniProt Consortium. (2018). UniProt: a worldwide hub of protein knowledge. *Nucleic Acids Research*, 47(D1), D506-D515. doi:10.1093/nar/gky1049
- Thery, C., Amigorena, S., Raposo, G., & Clayton, A. (2006). Isolation and characterization of exosomes from cell culture supernatants and biological fluids. *Curr Protoc Cell Biol*, Chapter 3, Unit 3.22. doi:10.1002/0471143030.cb0322s30
- Thery, C., Witwer, K. W., Aikawa, E., Alcaraz, M. J., Anderson, J. D., Andriantsitohaina, R., . . . Zuba-Surma, E. K. (2018). Minimal information for studies of extracellular vesicles 2018 (MISEV2018): a position statement of the International Society for Extracellular Vesicles and update of the MISEV2014 guidelines. *J Extracell Vesicles*, 7(1), 1535750. doi:10.1080/20013078.2018.1535750
- Transfiguracion, J., Tran, M. Y., Lanthier, S., Tremblay, S., Coulombe, N., Acchione, M., & Kamen, A. A. (2020). Rapid In-Process Monitoring of Lentiviral Vector Particles by High-Performance Liquid Chromatography. *Molecular Therapy - Methods & Clinical Development*, 18, 803-810. doi:10.1016/j.omtm.2020.08.005
- Valadi, H., Ekström, K., Bossios, A., Sjöstrand, M., Lee, J. J., & Lötvall, J. O. (2007). Exosome-mediated transfer of mRNAs and microRNAs is a novel mechanism of genetic exchange between cells. *Nature Cell Biology*, 9(6), 654-659. doi:10.1038/ncb1596
- van der Pol, E., Hoekstra, A. G., Sturk, A., Otto, C., van Leeuwen, T. G., & Nieuwland, R. (2010). Optical and non-optical methods for detection and characterization of

- microparticles and exosomes. *J Thromb Haemost*, 8(12), 2596-2607. doi:10.1111/j.1538-7836.2010.04074.x
- Van Deun, J., Mestdagh, P., Sormunen, R., Cocquyt, V., Vermaelen, K., Vandesompele, J., . . . Hendrix, A. (2014). The impact of disparate isolation methods for extracellular vesicles on downstream RNA profiling. *J Extracell Vesicles*, 3, 10.3402/jev.v3i4.24858. doi:10.3402/jev.v3.24858
- Venereo-Sánchez, A., Fulton, K., Koczka, K., Twine, S., Chahal, P., Ansorge, S., . . . Kamen, A. (2019). Characterization of influenza H1N1 Gag virus-like particles and extracellular vesicles co-produced in HEK-293SF. *Vaccine*. doi:https://doi.org/10.1016/j.vaccine.2019.07.057
- Wang, Z., Guo, Y., & Han, W. (2017). Current status and perspectives of chimeric antigen receptor modified T cells for cancer treatment. *Protein Cell*, 8(12), 896-925. doi:10.1007/s13238-017-0400-z
- White, M., Whittaker, R., Gandara, C., & Stoll, E. A. (2017). A Guide to Approaching Regulatory Considerations for Lentiviral-Mediated Gene Therapies. *Hum Gene Ther Methods*, 28(4), 163-176. doi:10.1089/hgtb.2017.096
- Wisniewski, J. R., Zougman, A., Nagaraj, N., & Mann, M. (2009). Universal sample preparation method for proteome analysis. *Nature Methods*, 6(5), 359-362. doi:10.1038/nmeth.1322
- Wu, H., Liu, L., & Zhu, J. M. (2019). MiR-93-5p inhibited proliferation and metastasis of glioma cells by targeting MMP2. *Eur Rev Med Pharmacol Sci*, 23(21), 9517-9524. doi:10.26355/eurrev\_201911\_19446

- Zhao, Y., Azam, S., & Thorpe, R. (2005). Comparative studies on cellular gene regulation by HIV-1 based vectors: implications for quality control of vector production. *Gene Therapy*, 12(4), 311-319. doi:10.1038/sj.gt.3302414
- Zhou, L. Y., Zhang, F. W., Tong, J., & Liu, F. (2020). MiR-191-5p inhibits lung adenocarcinoma by repressing SATB1 to inhibit Wnt pathway. *Mol Genet Genomic Med*, 8(1), e1043. doi:10.1002/mgg3.1043
- Zhou, Y., Zhou, B., Pache, L., Chang, M., Khodabakhshi, A. H., Tanaseichuk, O., . . . Chanda, S. K. (2019). Metascape provides a biologist-oriented resource for the analysis of systems-level datasets. *Nat Commun*, 10(1), 1523. doi:10.1038/s41467-019-09234-6
- Zolotukhin, A. S., Michalowski, D., Bear, J., Smulevitch, S. V., Traish, A. M., Peng, R., . . . Felber, B. K. (2003). PSF acts through the human immunodeficiency virus type 1 mRNA instability elements to regulate virus expression. *Molecular and Cellular Biology*, 23(18), 6618-6630. doi:10.1128/mcb.23.18.6618-6630.2003

## **Preface to Chapter 3**

Chapter 2 shed light on similarities between EVs and LVs, from their biogenesis to their cargo, as well as differences on a molecular level which could help better distinguishing them. However, distinction may be challenging to achieve, as highlighted in chapter 1, there seem to be a continuum of populations rather than actual distinct ones.

The scope of the third chapter of this thesis is to further study the spectrum populations of extracellular vesicles and viral particles generated when producing lentiviral vectors in a HEK293 producer cell line. Orthogonal methods based on particle features such as the presence of p24 viral capsid protein or the presence of viral genome are used to quantify the different entities.

## Chapter 3

### **From extracellular vesicles to lentiviral vectors: characterization of a spectrum of populations generated by a stable HEK293 producer cell line.**

Authors: **Aline Do Minh**, Xavier Elisseeff, Amine A. Kamen \*

Author affiliation : Department of Bioengineering, McGill University, Montréal, QC,  
Canada

Notes: \* Corresponding author.

Journal: Frontiers in Bioengineering and Biotechnology

Year: 2022

Status: To be submitted for publication

## **Abstract**

Lentiviral vectors (LV) constitute a major player in the field of cell and gene therapy. One of the challenges encountered when producing LV is the inevitable presence of extracellular vesicles (EV) naturally secreted by any type of cells and sharing many similarities with LV particles of interest, rendering their separation almost impossible. In that respect, characterizing LV, EV and intermediate derived entities during LV productions becomes highly relevant if not required to reach an adequate product knowledge and associated extended characterization to establish the critical quality attributes of the final product.

In this study, fractionation was used to characterize LV, EV and resulting intermediate species from an inducible LV producer cell line. Selected orthogonal methods including flow virometry and droplet digital PCR (ddPCR) were used to quantify particles with specific features. These results confirm once more the difficulty of an absolute quantification due to the diversity of LV/EV populations, and the opportunity to further enrich functional LV in the densest iodixanol fractions. They also bring to light new leads for better exploiting the potential of these analytical tools.

## **Keywords**

extracellular vesicles, lentiviral vectors, gene therapy, exosome, ddPCR, flow virometry

## 1. Introduction

Extracellular vesicles (EV) are nanosized particles naturally produced by any type of cells. They have been shown to be involved in a diversity of roles including cell to cell communication (They et al., 2018). They have been heavily studied over the past decades because of their potential as biomarkers or therapeutic delivery tools (Barile and Vassalli, 2017). They are however difficult to quantify on their own due to the resolution limit of most technologies. In the field of cell and gene therapy, lentiviral vectors (LV) are viral particles of the same size range as EV and are promisingly used for treating neurologic, genetic, or metabolic diseases (Escors and Breckpot, 2010). The production of LV is often carried out in mammalian cellular platforms such as human embryonic kidney 293 (HEK 293) derived cells (Ansorge et al., 2010). When EVs are co-produced with LV during LV production, the quantification becomes even more challenging. The challenge resides not only in the detection, but also in the fact that EVs exist in a wide spectrum of populations, and it is expected that this spectrum is further broadened by LV production (Do Minh and Kamen, 2021). EVs coproduced by virus producing cells will incorporate viral proteins and parts of viral genetic material. Thus, during LV production, diverse vesicles including incomplete viral particles, EVs with viral components, fully infectious viruses, and host cell EVs are likely to be released.

It is not possible to discriminate them based on their size or charge, and, to date, distinguishing markers are not absolute, in the sense that only enrichment can be claimed. However, few teams have reported successful isolation of EVs from viral particles from the plasma of HIV-1 positive individuals (Konadu et al., 2016) and from cell culture (Cantin et

al., 2008, Boker et al., 2017) using 6-18% iodixanol gradients. In this context, fractionation would be an appropriate method to study intermediate populations. However, strict separation does not appear realistic since those populations are most likely distributed in size as a continuum rather than separate entities.

The determination of virus production yield can be achieved by several means using different analytical methods to measure virus concentration. Indeed, different assays are at hand to quantify specific attributes of the virus. The number of infectious viral particles can be measured by plaque assays or gene transfer assays while polymerase chain reaction (PCR) techniques are used to measure the number of viral genomes (Wang et al., 2018). On the other hand, enzyme-linked immunosorbent assays can be used to count the number of viral antigens. Total viral particles quantification is also claimed by using transmission electron microscopy (Heider and Metzner, 2014) or high-performance liquid chromatography (Transfiguracion et al., 2020). However, when using each of these assays in the current routine testing of viral products, the presence of extracellular vesicles is likely to be omitted, most of the time leading to overestimation of the virus titer. The approach of using orthogonal methods is highly relevant though, as it can reveal different features of subpopulations of particles.

Flow virometry has been introduced in the past few years as a promising flow cytometry tool to be applied to nanosized particles (Lippe, 2018). Due to its multiplexing capability, flow virometry is a method of choice when there is a need for different markers to be observed simultaneously. In a previous study (Do Minh et al., 2021), flow virometry was successfully used to quantify EV and LV particles using their intrinsic GFP signal. That

study used a multi-omics approach to compare EV and LV produced in a HEK 293 derived cell line. Many similarities including lipid composition were uncovered, as well as distinctive features between both populations with protein cargo uniquely found in EV.

The aim of the current study is to use density gradient as a mean to further characterize subpopulations of host EV, infectious LV and the intermediate entities described above from cultures of an inducible HEK 293 lentivirus producing cell line. Orthogonal quantitative methods were selected to underline different characteristics of LV particles such as envelope or capsid marker. These data bring additional knowledge on the nature of particles produced during lentiviral vector production in the context of cell and gene therapy interventions.

## **2. Materials and methods**

### **2.1. Cell culture of HEK293SF cells in suspension**

As a platform for LV production, the stable 293SF producer cell line developed by the National Research Council Canada (NRC), HEK293SF-LVP-CMVGFPq-92 (abbreviated hereafter as Clone 92) (Manceur et al., 2017) was used in this study. As previously described, production of the LVR2-GFP (rHIV.VSV-g CMV GFP) lentiviral vector is induced in the Clone 92 cell line by the addition 1 µg/mL (w/v) doxycycline hyclate (Millipore Sigma, Etobicoke, ON, Canada) and 10 µg/mL (w/v) 4-isopropylbenzoic acid (cumate) (Millipore Sigma) to produce a third-generation SIN HIV-based lentiviral vector which expresses the green fluorescence protein (GFP). Clone 92 cells were cultured in shake flasks (from 20 to 300 mL working volumes) in HyCell TransFx-H medium (GE Healthcare, Chicago, IL,

United States) supplemented with 4-6 mM L Glutamine or GlutaMAX™ (ThermoFisher Scientific, Waltham, MA, USA) and 0.1% Kolliphor (Millipore Sigma) without serum or antibiotics. Cell growth was monitored by determining live cell density based on the principle of Trypan blue dye exclusion on a Vi-Cell XR cell counter (Beckman Coulter, Brea, CA, USA). Cells were passaged twice a week by diluting to  $2.0 \times 10^5$  live cells per mL in fresh medium.

HEK 293A cells (American Type Culture Collection, Manassas, VA, USA) were used for the gene transfer assay (GTA) (Graham et al., 1977). As described previously, they were maintained in a humidified incubator at 5% CO<sub>2</sub> and 37 °C in Dulbecco's Modified Eagle's Medium (DMEM) (Wisent, St-Bruno, QC, Canada), supplemented with 2 mM L Glutamine and 5% Fetal Bovine Serum (FBS) (Corning Inc., Corning, New York, NY, USA) without antibiotics. Cells were passaged twice a week.

## **2.2. Production of conditioned medium containing EV**

Clone 92 cell line was cultivated, and the cell density was measured every day. When the cell density reached  $1 \times 10^6$  cells/mL, the cells were kept in culture for 2 additional days before harvest.

## **2.3. Fractionation of EV and LV/EV samples using iodixanol gradient**

A discontinuous iodixanol gradient was used with concentrations ranging from 6% to 18% in 1.2% steps (a total of 11 steps) in 1 mL fractions (Boker et al., 2017, DeMarino et al., 2019, Steppert et al., 2016).

The following experiment was then performed three times. Three days post-induction flasks and conditioned medium containing EV were harvested, cells were removed by centrifugation, and the supernatant was filtered through a 0.45 or 0.22  $\mu\text{m}$  filter to remove debris and large particles. The filtered supernatant was first concentrated by ultracentrifugation and the pellet containing virions and EV was resuspended in 1 mL of PBS. The obtained samples were then loaded on a 6-18% iodixanol gradient and centrifuged at 250,000 g for 2 hours. Twelve gradient fractions were collected from the top in 1 mL volume. Collected fractions were further analyzed by gene transfer assay (GTA), droplet digital PCR (ddPCR), flow cytometry and p24 ELISA.

#### **2.4. Quantification of functional viral titer by gene transfer assay (GTA)**

A flow cytometry-based GTA was used to determine functional viral titer (Manceur et al., 2017). Briefly, each well of a 24-well plate was seeded with  $1 \times 10^5$  cells of HEK 293A. LV samples were serially diluted in DMEM (Wisent) supplemented with 8  $\mu\text{g}/\text{mL}$  of polybrene (Millipore Sigma) and incubated at 37°C for 30 min following medium removal after cell adherence. 200  $\mu\text{L}$  of diluted LV sample were then added to the cells for transduction and 800  $\mu\text{L}$  of fresh culture medium were added in each well after overnight incubation at 37°C. Three days post-transduction, cells were harvested and analyzed on the Accuri flow cytometer (Becton Dickinson, Franklin Lakes, NJ, USA) to quantify GFP expressing cells. Accepted values ranged between 2-20% fluorescent cells out of total cell count to avoid signal due to super infection.

## **2.5. Quantification of total particles by droplet digital polymerase chain reaction (ddPCR)**

As previously described, RNA was first extracted from LV samples using the High Pure Viral Nucleic Acid Kit (Roche, Mannheim, Germany) according to the manufacturer's instructions. The extracted RNA was then reverse transcribed into cDNA using the iScript™ Select cDNA Synthesis Kit (Bio-Rad Laboratories, Hercules, CA, USA) according to the manufacturer's instructions and using gene-specific primers targeted towards the woodchuck hepatitis virus posttranscriptional regulatory element (WPRE) amplifying a 589-base pair fragment. Primer sequences were: forward primer (5'-GTCCTTTCCATGGCTGCTC-3'), reverse primer (5'-CCGAAGGGACGTAGCAGA-3') (Integrated DNA Technologies, Inc., Coralville, IA, USA). Serial dilutions of cDNA were prepared in nuclease-free water. ddPCR reactions were prepared with the QX200™ ddPCR™ EvaGreen Supermix (Bio-Rad) and the WPRE primer set. PCR mixtures (22 µL) were prepared for the QX200™ Droplet Generator (Bio-Rad, Hercules, California), with final primer concentration of 0.8 µM. After droplet generation, the following PCR program was run: one cycle of 95°C for 10 min; 40 cycles of 95°C for 30s and 60°C for 30s; followed by a final extension at 72°C for 10 min and a 4°C hold. PCR results were analyzed with the Droplet reader and QuantaSoft (Bio-Rad).

## **2.6. Quantification of particles by flow virometry**

For small particle detection, a Cytoflex flow cytometer (Beckman Coulter, Indianapolis, Indiana) with a photomultiplier tube (PMT) for forward scatter detection was used.

Specifications for laser wavelengths and power were as follows: 488 nm–300 mW, 525/40 fluorescent channel. Acquisition was done with CytExpert (Beckman Coulter, Indianapolis, Indiana). Samples, unless otherwise indicated, were acquired at the lowest flow rate 10  $\mu$ l/min. The instrument cleaning procedure prior to acquisition was as follows: 20 min with cleaning solution (Beckman Coulter) or 20 min 0.1% bleach followed by 20 min distilled water.

As described previously (Do Minh et al., 2021), fluorescence was used as the trigger to quantify fluorescent particles.

Samples were double stained to measure different features of EV/LV particles. On one hand, 1:100 anti-VSV-g epitope tag (rabbit) antibody DyLight™ 405 conjugated (Rockland, Limerick, PA, USA) was used to quantify particles bearing the VSV-g at the surface. On the other hand, 100 $\mu$ M SYTO™ 62 Red Fluorescent Nucleic Acid Stain (ThermoFisher Scientific, Waltham, MA, USA) was used for detecting particles with a nucleic acid cargo (Khadijiam et al., 2020).

## **2.7. Titration of p24 viral capsid protein by ELISA**

Physical particle titers were determined by measuring p24 capsid protein by ELISA (HIV1 p24 ELISA Kit ab218268, Abcam, Cambridge, UK). The number of physical particles is calculated from the p24 concentration with the assumption that 1 pg of p24 corresponds to  $1.2 \times 10^4$  lentiviral particles (Delenda and Gaillard, 2005).

### 3. Results

#### 3.1. Iodixanol gradient making

After optimization, a simple way to obtain reproducible gradients was by loading one step and flash-freeze it before loading the next one. It was verified that the method of collecting the fractions after ultracentrifugation did not disturb the gradient. Two conditions, top and bottom collection, were tested and the density of each 1 mL fraction was measured.

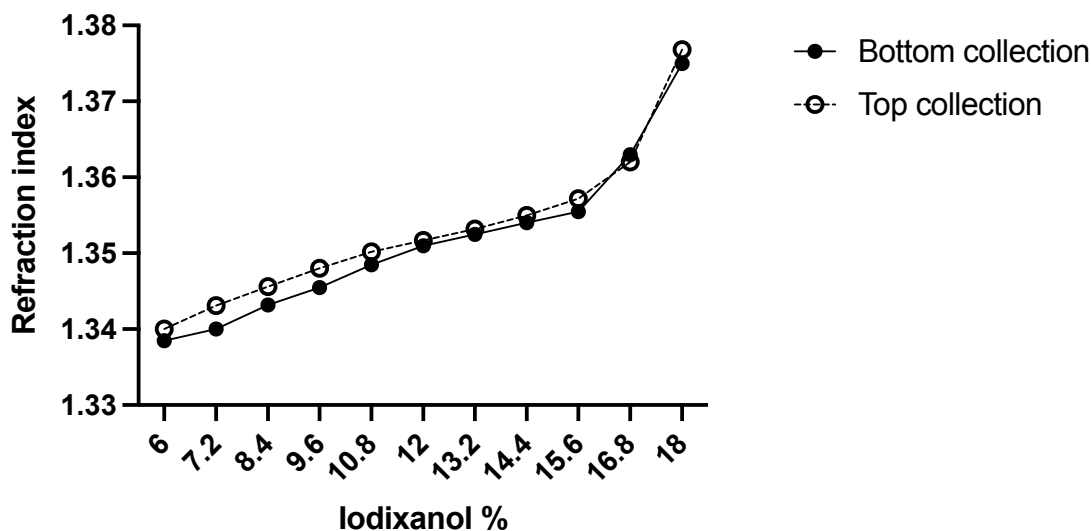


**Figure 13:** Density of iodixanol fractions after 250,000xg centrifugation. Bottom collection was performed by punching a hole at the bottom of the tube while top collection was performed using a pipette.

As seen on Figure 13, both conditions gave similar results with an expected gradient, which is consistent with results found in the literature (Graham, 2002). Collection from the top was applied in subsequent experiments. Fractions were then numbered from 1 to 12, 1 being the top fraction, hence the least dense fraction, and 12 the bottom fraction.

### 3.2. Quantitative characterization of EV to LV spectrum of populations

#### 3.2.1. "Viral genome" quantification

The number of particles carrying the woodchuck hepatitis virus posttranscriptional regulatory element (WPRE) was measured by ddPCR in each fraction (Figure 14).

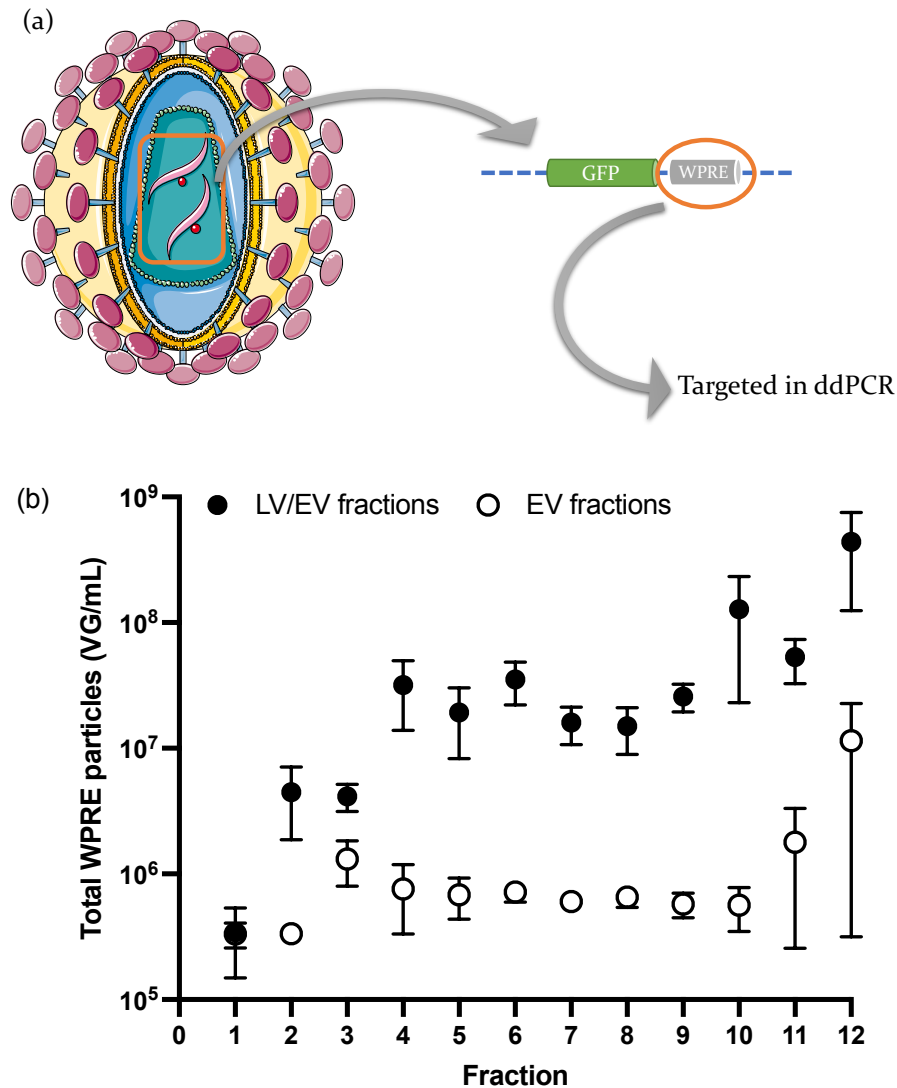
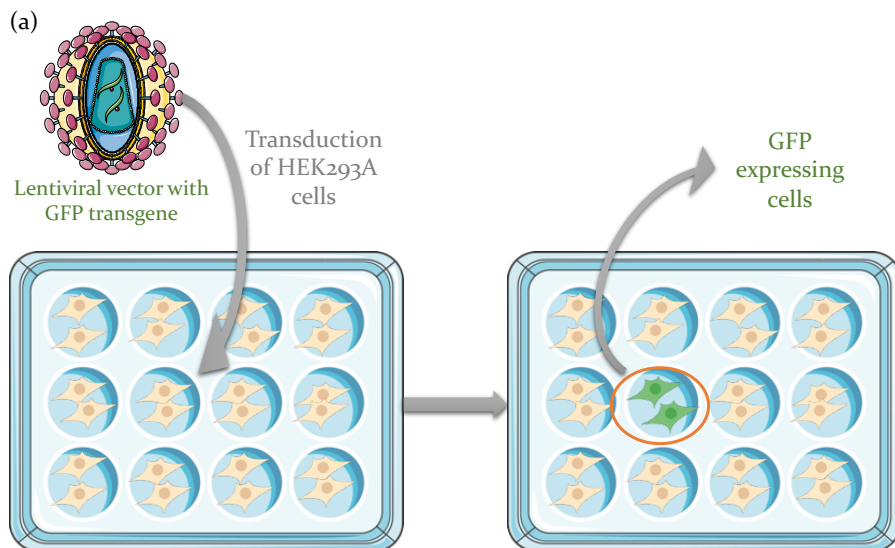


**Figure 14:** WPRE particles quantified by ddPCR in iodixanol fractions. (a) Schematic representation of targeted sequence for the ddPCR assay. Particles which genome contains the WPRE sequence will be detected by ddPCR. (b) WPRE particles titer measured in LV/EV and EV iodixanol fractions. Error bars indicate standard error to the mean (SEM).

All fractions, EV as well as LV/EV rendered a viral genome per mL (VG/mL) titer. In both conditions, the first fraction (top fraction) showed the lowest WPRE titer around  $3.4 \times 10^5$  VG/mL. The titer then increased throughout the fractions, with the bottom fraction showing the highest WPRE titer, reaching  $4.39 \times 10^8$  VG/mL for LV/EV samples and  $1.15 \times 10^7$  VG/mL for EV samples. LV/EV samples showed greater titers than EV fractions, suggesting that part of that titer comes from EV only while the other part comes from LV.

### 3.2.2. Functional titer measurement

Functional particles were quantified by GTA. Results confirmed that only LV/EV fractions have transduction efficiency (Figure 15), while EV fractions did not give a functional titer (data not shown).



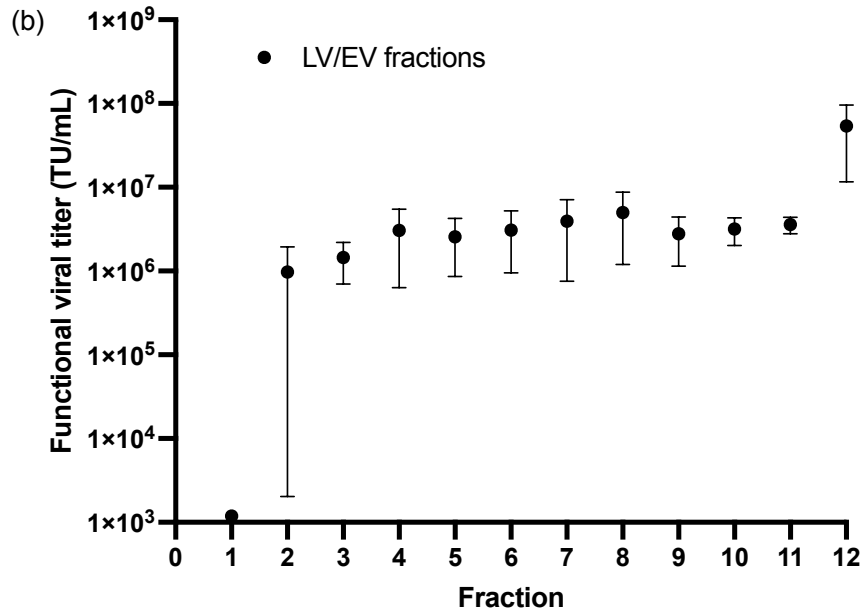


**Figure 15:** Functional viral titer measured by GTA. (a) Schematic representation of GTA: HEK293A cells are transfected with test samples. When transduced with samples containing functional viral particles carrying a GFP reporter gene, GFP positive cells can be measured by flow cytometry 72h after transduction. (b) Functional viral titer measured in LV/EV fractions. Error bars indicate SEM.

Figure 15 also showed that the first fraction contained the lowest functional titer of  $1.19 \times 10^3$  TU/mL. Results suggest improved transduction efficiency in the last fraction with the highest titer of  $5.37 \times 10^7$  TU/mL.

### 3.2.3. Physical particles quantification

Physical particle titer was measured using an ELISA test directed toward the capsid protein (p24). Similar to the GTA results, only LV/EV fractions showed a p24 titer (Figure 16) as EV fractions did not report a p24 titer (data not shown).

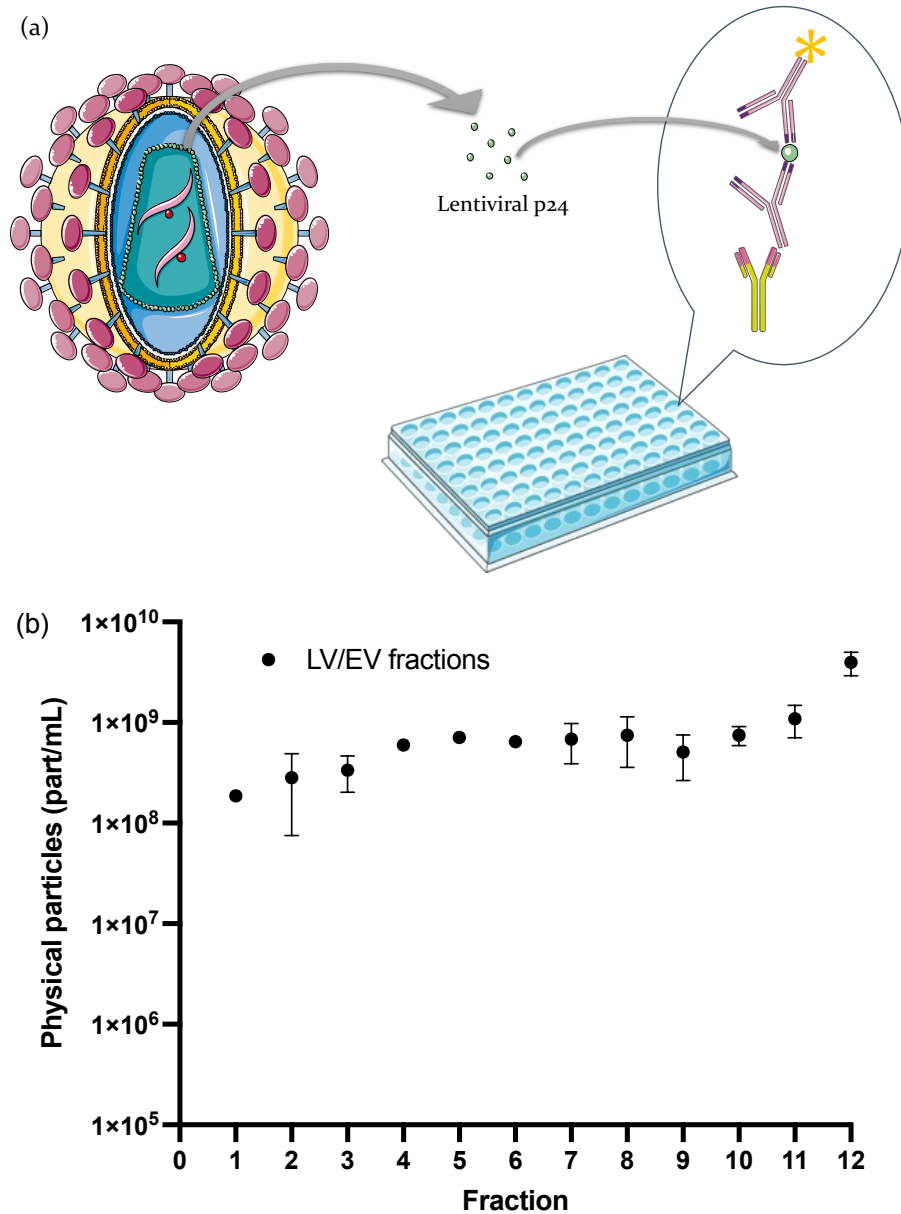


**Figure 16:** Physical particle titer measured by p24 ELISA. (a) Schematic of the p24 ELISA assay (Figure created using Servier Medical Art by Servier): p24 capsid antigen is represented by green spheres. (b) Physical particle titer measured in each LV/EV fraction. Error bars indicate SEM.

Again, the first fraction showed the lowest physical particles. The physical particle titer slightly increases throughout the fractions, with the highest titer of  $3.97 \times 10^9$  pp/mL reached in the last fraction.

### 3.2.4. Fluorescent particles quantification

GFP positive particles as well as VSV-g positive particles were quantified using flow virometry as presented in Figure 17 below. Tagged anti-VSV-g antibody was chosen to avoid crosstalk between conjugated fluorophore DyLight™ 405 and GFP.

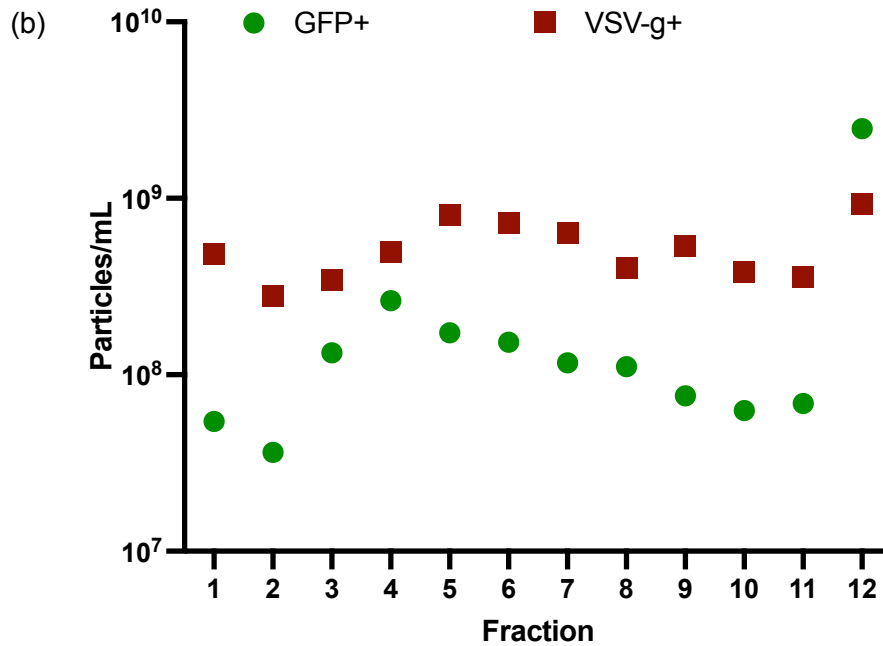
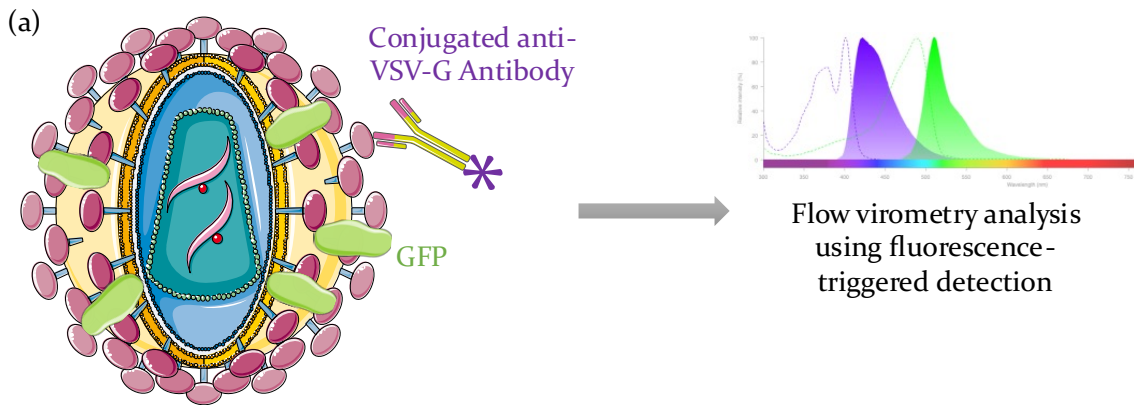


**Figure 17:** Fluorescent particle titer measured by flow virometry. (a) Schematic representation of particle features detected by flow virometry. (b) GFP positive (GFP+) and VSV-g positive (VSV-g+) particle titers measured in EV/LV fractions.

As seen on Figure 17, VSV-g positive particle titer remains stable throughout the fractions, with a slight increase in the last fraction, reaching  $9.26 \times 10^8$  particles/mL.

On the other hand, GFP positive particle titer is lower than VSV-g positive particle titer between  $3.63 \times 10^7$  particles/mL and  $2.63 \times 10^8$  particles/mL in all fractions but the last one, culminating at  $2.48 \times 10^9$  particles/mL.

#### 4. Discussion

Table 8 summarizes each fraction features by categorizing them based on the number of quantified particles.

**Table 8:** Overview of EV/LV fractions landscape. - :  $<10^6$  particle/ml,  $10^6$  particle/ml < + <  $10^8$  particle/ml, ++ >  $10^8$  particle/ml

Fraction #	1	2	3	4	5	6	7	8	9	10	11	12
<b>WPRE particles</b>	-	+	+	+	+	+	+	+	+	++	+	++
<b>Functional particles</b>	-	+	+	+	+	+	+	+	+	+	+	++*
<b>p24 particles</b>	++	++	++	++	++	++	++	++	++	++	++	++
<b>GFP+ particles</b>	+	+	++	++	++	++	++	++	+	+	+	++
<b>VSV-g+ particles</b>	++	++	++	++	++	++	++	++	++	++	++	++

\*Based on biologically significant difference, Fraction 12 was categorized as ++ for Functional particles

Table 8 shows that fraction 12 tends to have the most “complete” particles, with over  $10^8$  particles/mL of each feature, meaning that most particles in fraction 12 will be VSV-g pseudotyped, with the ability to transduce cells, bearing a “viral genome” and the p24 capsid protein. This observation corroborates other studies claiming that HIV viral

particles were isolated in the densest fractions of the iodixanol gradient, when attempting at separating them from EVs (Konadu et al., 2016, Cantin et al., 2008).

Interestingly, the first fraction seems to be depleted in functional particles, also supporting the hypothesis of EV enrichment in the least dense iodixanol fractions.

As previously observed (Do Minh et al., 2021), all particles produced by Clone 92 cells, with or without induction of lentiviral production carry the “viral genome” (Table 14). This is due to the design of the plasmids used to construct the cell line, with the transgene and therefore the WPRE element, under the control of a constitutive promoter.

Moreover, flow virometry results showing a lower GFP positive particle titer than VSVG positive particle titer in all fractions suggest that not all particles bear GFP, unlike previously hypothesized (Do Minh et al., 2021).

In González-Domínguez et al. (González-Domínguez et al., 2020), six biophysical methods have been applied for quantifying virus-like particles (VLPs) and EVs and different concentrations between the methods were observed, highlighting the difficulty for absolute quantification. In the present study however, it is not about differences in quantification, but rather different characteristics measured, leading to different profiles depending on the targeted feature. The quantification methods used in this study present the advantage to be advanced tools for the detection of specific features. For instance, ddPCR is a technique of choice in viral titration that has been proven for its accuracy and specificity (Gélinas et al., 2020). As these methods rely on different technologies, they logically display different method variability, therefore leading to the fact that particles ratios such as functional

particles over total particles will remain at the estimation level. This is highly accepted as the total particle to infectivity (P:I) ratio and is commonly used in the field by using the functional titer measured by GTA versus the total number of particles by p24 ELISA (Perry and Rayat, 2021). As previously stated, highlighting that these quantification methods are based on specific features of the particles, one could question the reliability of the total particles measurement and there is indeed no insurance that all particles bear the p24 capsid protein. Based on the cell line construct, this study confirms that p24 ELISA quantification is the closest to the total particle's quantification, provided that the method is further optimized by ensuring that free p24 proteins not associated with particles are not accounted for to avoid over-quantification (Sena-Esteves and Gao, 2018). Indeed, p24 expression was not detected in any fraction of the non-induced condition, confirming tight regulation of the doxycycline and cumate switches (Broussau et al., 2008). In the light of the presented data, and confirming the switches' regulation, the VSV-g quantification by flow cytometry comes as a promising new total particle quantification method. Indeed, not only do the VSV-g+ titers follow the same trend as the p24 titers, perfectly overlaying on most fractions, but no VSV-g could be observed by mass spectrometry in non-induced condition (data not shown, (Do Minh et al., 2021)) confirming again the tight regulation of the switches.

### **Development perspective**

A way to improve particle ratio accuracy would be to use the same technology to detect the different particles features. In the flow virometry analysis, two features of LV/EV were

targeted, rendering two titers: GFP positive particles initially thought to represent total particles, and VSV-g positive particles, which actually better estimate total particles. The multiplexing capacity of flow virometry could therefore be explored even further. Multiple challenges are foreseen. Indeed, in the scope of the present study, attempts were made to label the p24 capsid protein, thus requiring to permeabilize the viral envelop in the first place to introduce a tagged antibody. Several permeabilization agents such as saponin or FoxP3 buffer (Baxter et al., 2017) and concentrations were investigated but trials turned out to be more challenging than expected when dealing with such fragile particles, coupled with the ambitious goal to introduce a large molecule such as a conjugated antibody. Nucleic acid content could also be targeted with the use of permeable dyes (Khadijiam et al., 2020). This will require careful optimization to avoid crosstalk between fluorophores, with expected washing step for free dye removal that could lead to particle loss (Tang et al., 2017). However, these challenges, when resolved, could open the door to infinite possibilities to characterize LV and EV at a single-particle level.

With the same goal of using the same technology to detect different features, ddPCR multiplexing capacity could be exploited in the same way as flow virometry (Liu et al., 2020). Based on transcriptomic exploratory studies, providing identification of specific markers for EV, relevant sequences could be targeted for designing probes with high specificity. Again, this could lead to a very powerful tool.

Through the fractionation of LV/EV particles, the different quantification methods used in this study highlighted again the diversity of particles generated during lentiviral

production. From fractions enriched with non-functional particles that could be related to a majority of EV, to particles featuring all measured characteristics, intermediate fractions presented most characteristics of functional LV particles to some extent, with variation between the number of GFP positive particles or WPRE particles. Without claiming reaching absolute separation between LV and EV, results of this research converge with other studies suggesting enrichment of fully functional particles in the densest iodixanol fraction.

When it comes to LV production in the context of gene therapy, this finding could lead to an opportunity for downstream processing optimization for enhancing the yield of LV particles able to transduce cells (Logan et al., 2004). Indeed, increasing the ratio of transduction efficient LV particles versus total particles is at the heart of the field progression (Tran and Kamen, 2022).

Another contribution to the field of gene therapy when it comes to regulatory applications is the ability to extensively characterize the proposed product. Yielding less diverse particles by focusing on the densest fraction would lead to an eased extended characterization requested by health authorities. Characterizing even more features than the ones included in the present study using the presented methods or using multiplexing capacity of advanced technologies, combined with the promises of mass spectrometry based multi-attribute method (MAM) (Wu et al., 2022), would help tremendously to monitor critical quality attributes of gene and cell therapy products.

## **Author Contributions**

Conceptualization, A.D.M. and A.A.K.; Methodology, A.D.M. and A.A.K.; Investigation, A.D.M., X.E., Writing – Original Draft, A.D.M.; Writing – Review & Editing, A.A.K.; Funding Acquisition, A.D.M. and A.A.K.; Resources, A.K.; and Supervision, A.A.K.

## **Conflict of Interest**

The authors declare that the research was conducted in the absence of any commercial or financial relationships that could be construed as a potential conflict of interest.

## **Funding / Acknowledgements**

A.D.M. is funded by a Natural Sciences and Engineering Research Council of Canada (NSERC) doctoral scholarship. A.A.K. is a recipient of a Canada Research Chair (CRC/240394) of government of Canada.

## **References**

Ansorge, S., Henry, O. & Kamen, A. 2010. Recent Progress In Lentiviral Vector Mass Production. *Biochemical Engineering Journal*, 48, 362-377.

Barile, L. & Vassalli, G. 2017. Exosomes: Therapy Delivery Tools And Biomarkers Of Diseases. *Pharmacol Ther.*

Baxter, A. E., Niessl, J., Fromentin, R., Richard, J., Porichis, F., Massanella, M., Brassard, N., Alshafi, N., Routy, J. P., Finzi, A., Chomont, N. & Kaufmann, D. E. 2017.

Multiparametric Characterization Of Rare Hiv-Infected Cells Using An RNA-Flow Fish Technique. *Nat Protoc*, 12, 2029-2049.

Boker, K. O., Lemus-Diaz, N., Rinaldi Ferreira, R., Schiller, L., Schneider, S. & Gruber, J. 2017. The Impact Of The Cd9 Tetraspanin On Lentivirus Infectivity And Exosome Secretion. *Mol Ther*.

Broussau, S., Jabbour, N., Lachapelle, G., Durocher, Y., Tom, R., Transfiguracion, J., Gilbert, R. & Massie, B. 2008. Inducible Packaging Cells For Large-Scale Production Of Lentiviral Vectors In Serum-Free Suspension Culture. *Mol Ther*, 16, 500-7.

Cantin, R., Diou, J., Belanger, D., Tremblay, A. M. & Gilbert, C. 2008. Discrimination Between Exosomes And Hiv-1: Purification Of Both Vesicles From Cell-Free Supernatants. *Journal Of Immunological Methods*, 338, 21-30.

Delenda, C. & Gaillard, C. 2005. Real-Time Quantitative Pcr For The Design Of Lentiviral Vector Analytical Assays. *Gene Therapy*, 12, S36-S50.

Demarino, C., Barclay, R. A., Pleet, M. L., Pinto, D. O., Branscome, H., Paul, S., Lepene, B., El-Hage, N. & Kashanchi, F. 2019. Purification Of High Yield Extracellular Vesicle Preparations Away From Virus. *J Vis Exp*.

Do Minh, A. & Kamen, A. A. 2021. Critical Assessment Of Purification And Analytical Technologies For Enveloped Viral Vector And Vaccine Processing And Their Current Limitations In Resolving Co-Expressed Extracellular Vesicles. *Vaccines*, 9, 823.

Do Minh, A., Star, A. T., Stupak, J., Fulton, K. M., Haqqani, A. S., Gélinas, J.-F., Li, J., Twine, S. M. & Kamen, A. A. 2021. Characterization Of Extracellular Vesicles Secreted In Lentiviral Producing Hek293sf Cell Cultures. *Viruses*, 13, 797.

Escors, D. & Breckpot, K. 2010. Lentiviral Vectors In Gene Therapy: Their Current Status And Future Potential. *Arch Immunol Ther Exp (Warsz)*, 58, 107-19.

Gélinas, J. F., Kiesslich, S., Gilbert, R. & Kamen, A. A. 2020. Titration Methods For Rvsv-Based Vaccine Manufacturing. *MethodsX*, 7, 100806.

González-Domínguez, I., Puente-Massaguer, E., Cervera, L. & Gòdia, F. 2020. Quality Assessment Of Virus-Like Particles At Single Particle Level: A Comparative Study. *Viruses*, 12, 223.

Graham, F. L., Smiley, J., Russell, W. C. & Nairn, R. 1977. Characteristics Of A Human Cell Line Transformed By Dna From Human Adenovirus Type 5. *J Gen Virol*, 36, 59-74.

Graham, J. M. 2002. Preparation Of Preformed Iodixanol Gradients. *Scientificworldjournal*, 2, 1351-5.

Heider, S. & Metzner, C. 2014. Quantitative Real-Time Single Particle Analysis Of Virions. *Virology*, 462-463, 199-206.

Khadivjam, B., El Bilali, N. & Lippé, R. 2020. Analysis And Sorting Of Individual Hsv-1 Particles By Flow Virometry. In: Diefenbach, R. J. & Fraefel, C. (Eds.) *Herpes Simplex Virus : Methods And Protocols*. New York, Ny: Springer New York.

Konadu, K. A., Huang, M. B., Roth, W., Armstrong, W., Powell, M., Villinger, F. & Bond, V. 2016. Isolation Of Exosomes From The Plasma Of Hiv-1 Positive Individuals. *J Vis Exp*.

Lippe, R. 2018. Flow Virometry: A Powerful Tool To Functionally Characterize Viruses. *J Virol*, 92.

Liu, X., Feng, J., Zhang, Q., Guo, D., Zhang, L., Suo, T., Hu, W., Guo, M., Wang, X., Huang, Z., Xiong, Y., Chen, G., Chen, Y. & Lan, K. 2020. Analytical Comparisons Of Sars-

Cov-2 Detection By Qrt-Pcr And Ddpcr With Multiple Primer/Probe Sets. *Emerg Microbes Infect*, 9, 1175-1179.

Logan, A. C., Nightingale, S. J., Haas, D. L., Cho, G. J., Pepper, K. A. & Kohn, D. B. 2004. Factors Influencing The Titer And Infectivity Of Lentiviral Vectors. *Hum Gene Ther*, 15, 976-88.

Manceur, A. P., Kim, H., Misic, V., Andreev, N., Dorion-Thibaudeau, J., Lanthier, S., Bernier, A., Tremblay, S., Gelinas, A. M., Broussau, S., Gilbert, R. & Ansorge, S. 2017. Scalable Lentiviral Vector Production Using Stable Hek293sf Producer Cell Lines. *Hum Gene Ther Methods*.

Perry, C. & Rayat, A. 2021. Lentiviral Vector Bioprocessing. *Viruses*, 13.

Sena-Esteves, M. & Gao, G. 2018. Titration Of Lentivirus Vectors. *Cold Spring Harb Protoc*, 2018.

Steppert, P., Burgstaller, D., Klausberger, M., Berger, E., Aguilar, P. P., Schneider, T. A., Kramberger, P., Tover, A., Nöbauer, K., Razzazi-Fazeli, E. & Jungbauer, A. 2016. Purification Of Hiv-1 Gag Virus-Like Particles And Separation Of Other Extracellular Particles. *Journal Of Chromatography A*, 1455, 93-101.

Tang, V. A., Renner, T. M., Fritzsche, A. K., Burger, D. & Langlois, M. A. 2017. Single-Particle Discrimination Of Retroviruses From Extracellular Vesicles By Nanoscale Flow Cytometry. *Sci Rep*, 7, 17769.

Thery, C., Witwer, K. W., Aikawa, E., Alcaraz, M. J., Anderson, J. D., Andriantsitohaina, R., Antoniou, A., Arab, T., Archer, F., Atkin-Smith, G. K., Ayre, D. C., Bach, J. M., Bachurski, D., Baharvand, H., Balaj, L., Baldacchino, S., Bauer, N. N., Baxter, A. A., Bebawy, M.,

Beckham, C., Bedina Zavec, A., Benmoussa, A., Berardi, A. C., Bergese, P., Bielska, E., Blenkiron, C., Bobis-Wozowicz, S., Boilard, E., Boireau, W., Bongiovanni, A., Borrás, F. E., Bosch, S., Boulanger, C. M., Breakefield, X., Breglio, A. M., Brennan, M. A., Brigstock, D. R., Brisson, A., Broekman, M. L., Bromberg, J. F., Bryl-Gorecka, P., Buch, S., Buck, A. H., Burger, D., Busatto, S., Buschmann, D., Bussolati, B., Buzas, E. I., Byrd, J. B., Camussi, G., Carter, D. R., Caruso, S., Chamley, L. W., Chang, Y. T., Chen, C., Chen, S., Cheng, L., Chin, A. R., Clayton, A., Clerici, S. P., Cocks, A., Cocucci, E., Coffey, R. J., Cordeiro-Da-Silva, A., Couch, Y., Coumans, F. A., Coyle, B., Crescitelli, R., Criado, M. F., D'souza-Schorey, C., Das, S., Datta Chaudhuri, A., De Candia, P., De Santana, E. F., De Wever, O., Del Portillo, H. A., Demaret, T., Deville, S., Devitt, A., Dhondt, B., Di Vizio, D., Dieterich, L. C., Dolo, V., Dominguez Rubio, A. P., Dominici, M., Dourado, M. R., Driedonks, T. A., Duarte, F. V., Duncan, H. M., Eichenberger, R. M., Ekstrom, K., El Andaloussi, S., Elie-Caille, C., Erdbrugger, U., Falcon-Perez, J. M., Fatima, F., Fish, J. E., Flores-Bellver, M., Forsonits, A., Frelet-Barrand, A., Et Al. 2018. Minimal Information For Studies Of Extracellular Vesicles 2018 (Misev2018): A Position Statement Of The International Society For Extracellular Vesicles And Update Of The Misev2014 Guidelines. *J Extracell Vesicles*, 7, 1535750.

Tran, M. Y. & Kamen, A. A. 2022. Production Of Lentiviral Vectors Using A Hek-293 Producer Cell Line And Advanced Perfusion Processing. *Front Bioeng Biotechnol*, 10, 887716.

Transfiguracion, J., Tran, M. Y., Lanthier, S., Tremblay, S., Coulombe, N., Acchione, M. & Kamen, A. A. 2020. Rapid In-Process Monitoring Of Lentiviral Vector Particles By High-

Performance Liquid Chromatography. *Molecular Therapy - Methods & Clinical Development*, 18, 803-810.

Wang, Y., Bergelson, S. & Feschenko, M. 2018. Determination Of Lentiviral Infectious Titer By A Novel Droplet Digital Pcr Method. *Hum Gene Ther Methods*, 29, 96-103.

Wu, Z., Wang, H., Tustian, A., Qiu, H. & Li, N. 2022. Development Of A Two-Dimensional Liquid Chromatography-Mass Spectrometry Platform For Simultaneous Multi-Attribute Characterization Of Adeno-Associated Viruses. *Anal Chem*, 94, 3219-3226.

## General Discussion

With the main objective of this work being the characterization of LV, EV and intermediate entities generated during the bioproduction of LV, to help define a better product profile and move towards the acknowledgment of the presence of EV-derived species in the extended characterization of LV products, the work presented in this thesis has contributed to the field of lentiviral vector and extracellular vesicles in the context of cell and gene therapy.

The principle of human gene therapy is to modify or manipulate the expression of a sometimes missing or malfunctioning gene or to change the biological characteristics of living cells for therapeutic purposes. Gene therapy allows to treat or cure disease by changing the patient's DNA. Different mechanisms can be used and include the replacement of a malfunctioning gene with a healthy copy of the gene, the inactivation of the malfunctioning gene, or the introduction of a so-called therapeutic gene to treat a condition (Naldini, 2015). Gene therapy products are being investigated for the treatment of diseases such as infectious diseases, genetic diseases, and cancer.

The landscape of gene therapy is made of a variety of products (Sayed et al., 2022), such as:

- Human gene editing technology with advancement of development of the clustered regularly interspaced short palindromic repeats (CRISPR)-Cas9 system, which goal is to disrupt deleterious genes or repair mutated genes (Torres-Ruiz & Rodriguez-Perales, 2017).

- Plasmid DNA with genetically engineered circular DNA molecules with the ability to carry therapeutic genes into human cells (Schmeer, Buchholz, & Schleef, 2017).
- Bacterial vectors to carry therapeutic genes into human tissues (Celec & Gardlik, 2017).
- Viral vectors: using the natural ability of viruses to deliver genetic material into cells, some gene therapy products are logically derived from viruses to carry therapeutic genes into human cells (Bulcha, Wang, Ma, Tai, & Gao, 2021).
- Patient-derived cellular gene therapy products such as CAR-T cell therapy: patient's cells are genetically modified *ex vivo* (often using a viral vector) and then reinfused into the patient (Sterner & Sterner, 2021).

Diverse viral vectors are currently undergoing late phase clinical trials as well as used in approved therapies, including AAV, adenovirus, retrovirus and lentivirus (Sharon & Kamen, 2018). They are usually produced by cell culture, using mammalian cells such as HEK293 derived cells or insect cells such as Sf9 derived cells. Challenges to overcome for generalizing the use of these viral vectors reside in developing scalable, cost-effective, and robust production platforms reaching high yield of vector required for effective therapy. These high yields must be combined with high purity in a context where patient safety is paramount, therefore extended characterization is expected for all biological products hoping to reach the market.

With the recent interest on EV for their undeniable potential in therapeutic applications, the enveloped virus field can no longer ignore the high probability to retrieve EV derived particles in enveloped virus products, including LV preparations. LV are the

main subject of this work, and the motivation was to extensively characterize LV product, including EV derived particles, to improve current knowledge on such advanced therapies.

In chapter 1 of this thesis, a thorough review of the literature was conducted, detailing commonly used process steps and analytical tools in the enveloped virus production field, and assessing their ability at discriminating EV of similar size and biophysical properties. Setting the scene for this research, the main highlight was that most reviewed techniques were indeed not capable at distinguishing EV from enveloped viruses. On one hand, purification techniques used in enveloped virus production do not guarantee an isolation away from EV. On the other hand, most analytical methods for quantifying and characterizing enveloped viruses do not exclusively target them, except when it comes to infectivity or functionality. Thus, the need for improving analytical tools for better assessing the true part of enveloped viruses and EV in enveloped virus products, and further characterizing their content was underlined.

With regard to the overall objective of this project, the HEK293 derived cell line platform was selected as a model cell line for the production of LV. The specific cell line used in the subsequent studies was developed by the NRC as an inducible LV producer cell line abbreviated Clone 92. It is however evident that HEK293 derived cells are not the only platform used for producing biological products. It is therefore advisable to check if data regarding EV produced by other popular cellular platform exist, such as Vero cells or insect cells, and generate these data if they are missing. Proteomic analyses are facilitated when annotated genomes are available, which is the case for the human genome and therefore

for HEK293 EV. The task at hand for characterizing Vero cell derived EV could be helped by recent advances in genome annotation (Sène et al., 2021).

Following the first chapter, it was crucial to first characterize EV produced in the aforementioned cell line by themselves before comparing them to LV. Recent studies did characterize EV from different body fluids and diverse body related cell types, however characterization of EV secreted by cell lines used as production platform was not covered to the best of our knowledge.

Chapter 2 of this thesis started therefore by developing a scalable process for yielding a high amount of EV necessary to perform selected analyses on the same batch for representativity purpose. This scalable process combining tangential filtration and multimodal chromatography was successful at isolating EV and could be further applied for EV production in therapeutic applications. A multi-omics approach was used as to characterize EV without induction and LV/EV mixture resulting from LV induction. Proteomic and lipidomic analyses shed light on potential markers for EV and LV/EV but also confirmed the similar nature of EV and LV. Transcriptomic on the other hand was only performed on EV samples. Future steps could include a similar comparison between EV and LV/EV on a transcriptomic level. Indeed, while several genes could help further understanding EV functions, miRNA were also identified in EV cargo. The cargo of LV and EV intermediate entities following induction would be interesting to study, as part of the extended characterization expected by health authorities. Additionally, the effect of these cargos on EV uptake should be studied in such a way to determine the effect of EV on model recipient cells such as Jurkat cell to represent patient's T-cells, and to demonstrate that the

lower concentration effect of EV or incomplete LV particles compared to fully functional LV do not have any adverse effect. Although generally not desirable, side effects are not necessarily negative, as immunogenicity can be sought in the case of viral vaccines. Indeed, any demonstrated immunogenicity of EV could be an advantage and serve as natural adjuvants in viral vaccine composition. In that case, the right dosage of EV should of course be carefully evaluated.

As outlined in the first chapter and as suggested by the proteomic and lipidomic findings of the second chapter, LV and EV are not separate entities, but rather a continuum of populations distributed by size due to their biogenesis similarities. In the third chapter, LV, EV and intermediate species were therefore further characterized by fractionating LV/EV samples using iodixanol gradient. Corroborating other studies, the densest iodixanol fraction appeared to be enriched in functional particles. Optimization on the gradient could be a way to refine the fractionation resolution. Applying the same methodology as in the first chapter could also bring additional valuable knowledge by conducting proteomic, lipidomic and transcriptomic analyses on each fraction. Whereas this work was initiated, data recollection could not be completed to be part of the present thesis. Future extensive proteomic and lipidomic analyses of gradient fractions could for instance bring additional knowledge on the biogenesis of each entity, potentially leading to inhibiting or on the contrary facilitating a pathway to enhance LV production.

The work presented in this thesis contributes overall to the advancement of knowledge in the field of LV manufacturing. As outlined throughout this discussion, significant

progress was made, that can have direct and immediate impact within the field of LV, EV, and enveloped virus by extension.

Applicability of the different findings and progress have also been underlined, including the scalable process for EV production, the multiplexing capabilities of ddPCR and flow virometry that could bring to another level the extended characterization of viral products. Capitalizing for instance on the existing Virocyt technology (Americo, Earl, & Moss, 2017) and adding more features to analyze could be a way to go down that road.

## Final Conclusion & Summary

The first objective of this PhD research project was to characterize EV during LV production from a multi-omics perspective. This objective was addressed by the work carried out in the second chapter and extensively characterizing Clone 92 EV on one hand, and the mixture entities called LV/EV resulting from LV induction on the other hand. Several proteins were identified as potential markers and could be further explored, while overall analyses confirmed high similarities between EV and LV.

The second aim of this project was to quantify the different entities from host EV to fully functional particles during LV production. This objective was achieved by the mean of fractionation using iodixanol gradient. While corroborating other findings of enrichment of fully functional particles in the densest iodixanol fractions, middle fractions showed partially complete particles not all harboring each measured feature, thus confirming the hypothesis formulated in the first chapter of a diversity of particles.

Building on the work of this thesis, future research activities, as mentioned in the course of the previous discussion, are necessary to further improve the characterization of such enveloped viral products and associated EV/intermediate entities to increase confidence in the fact that processes are controlled in every way in viral vector manufacturing.

## Literature

Americo, J. L., Earl, P. L., & Moss, B. (2017). Droplet digital PCR for rapid enumeration of viral genomes and particles from cells and animals infected with orthopoxviruses. *Virology*, 511, 19-22. doi:10.1016/j.virol.2017.08.005

Ansorge, S., Lanthier, S., Transfiguracion, J., Durocher, Y., Henry, O., & Kamen, A. (2009). Development of a scalable process for high-yield lentiviral vector production by transient transfection of HEK293 suspension cultures. *Journal of Gene Medicine*, 11(10), 868-876. doi:10.1002/jgm.1370

Bulcha, J. T., Wang, Y., Ma, H., Tai, P. W. L., & Gao, G. (2021). Viral vector platforms within the gene therapy landscape. *Signal Transduct Target Ther*, 6(1), 53. doi:10.1038/s41392-021-00487-6

Celec, P., & Gardlik, R. (2017). Gene therapy using bacterial vectors. *Front Biosci (Landmark Ed)*, 22(1), 81-95. doi:10.2741/4473

Merten, O. W., Hebben, M., & Bovolenta, C. (2016). Production of lentiviral vectors. *Mol Ther Methods Clin Dev*, 3, 16017. doi:10.1038/mtm.2016.17

Naldini, L. (2015). Gene therapy returns to centre stage. *Nature*, 526(7573), 351-360. doi:10.1038/nature15818

Nolte-'t Hoen, E., Cremer, T., Gallo, R. C., & Margolis, L. B. (2016). Extracellular vesicles and viruses: Are they close relatives? *Proc Natl Acad Sci U S A*, 113(33), 9155-9161. doi:10.1073/pnas.1605146113

Sayed, N., Allawadhi, P., Khurana, A., Singh, V., Navik, U., Pasumarthi, S. K., . . . Bharani, K. K. (2022). Gene therapy: Comprehensive overview and therapeutic applications. *Life Sciences*, 294, 120375. doi:10.1016/j.lfs.2022.120375

Schmeer, M., Buchholz, T., & Schleef, M. (2017). Plasmid DNA Manufacturing for Indirect and Direct Clinical Applications. *Hum Gene Ther*, 28(10), 856-861. doi:10.1089/hum.2017.159

Schweizer, M., & Merten, O. W. (2010). Large-scale production means for the manufacturing of lentiviral vectors. *Current Gene Therapy*, 10(6), 474-486.

Sène, M. A., Kiesslich, S., Djambazian, H., Ragoussis, J., Xia, Y., & Kamen, A. A. (2021). Haplotype-resolved de novo assembly of the Vero cell line genome. *NPJ Vaccines*, 6(1), 106. doi:10.1038/s41541-021-00358-9

Sharon, D., & Kamen, A. (2017). Advancements in the design and scalable production of viral gene transfer vectors. *Biotechnol Bioeng*. doi:10.1002/bit.26461

Sharon, D., & Kamen, A. (2018). Advancements in the design and scalable production of viral gene transfer vectors. *Biotechnology and Bioengineering*, 115(1), 25-40. doi:10.1002/bit.26461

Sterner, R. C., & Sterner, R. M. (2021). CAR-T cell therapy: current limitations and potential strategies. *Blood Cancer J*, 11(4), 69. doi:10.1038/s41408-021-00459-7

Torres-Ruiz, R., & Rodriguez-Perales, S. (2017). CRISPR-Cas9 technology: applications and human disease modelling. *Brief Funct Genomics*, 16(1), 4-12. doi:10.1093/bfgp/elw025

Wang, Z., Guo, Y., & Han, W. (2017). Current status and perspectives of chimeric antigen receptor modified T cells for cancer treatment. *Protein Cell*, 8(12), 896-925. doi:10.1007/s13238-017-0400-z

White, M., Whittaker, R., Gandara, C., & Stoll, E. A. (2017). A Guide to Approaching Regulatory Considerations for Lentiviral-Mediated Gene Therapies. *Hum Gene Ther Methods*, 28(4), 163-176. doi:10.1089/hgtb.2017.096